National Library of Canada
Acquisitions and Bibliographic Services Branch
395 Wellington Street
Ottawa, Ontario
K1A 0N4

Bibliothèque nationale du Canada
Direction des acquisitions et des services bibliographiques
395, rue Wellington
Ottawa (Ontario)
K1A 0N4

Your file Votre référence

Our file Notre référence

## NOTICE

The quality of this microform is heavily dependent upon the quality of the original thesis submitted for microfilming. Every effort has been made to ensure the highest quality of reproduction possible.

If pages are missing, contact the university which granted the degree.

Some pages may have indistinct print especially if the original pages were typed with a poor typewriter ribbon or if the university sent us an inferior photocopy.

Reproduction in full or in part of this microform is governed by the Canadian Copyright Act, R.S.C. 1970, c. C-30, and subsequent amendments.

## AVIS

La qualité de cette microforme dépend grandement de la qualité de la thèse soumise au microfilmage. Nous avons tout fait pour assurer une qualité supérieure de reproduction.

S'il manque des pages, veuillez communiquer avec l'université qui a conféré le grade.

La qualité d'impression de certaines pages peut laisser à désirer, surtout si les pages originales ont été dactylographiées à l'aide d'un ruban usé ou si l'université nous a fait parvenir une photocopie de qualité inférieure.

La reproduction, même partielle, de cette microforme est soumise à la Loi canadienne sur le droit d'auteur, SRC 1970, c. C-30, et ses amendements subséquents.

Canada

UNIVERSITY OF ALBERTA

# Finite Amplitude Baroclinic Instability of a Mesoscale Gravity Current in a Channel

BY

**Curtis J. Mooney**

©

A thesis submitted to the Faculty of Graduate Studies and Research in partial fufillment of the requirements for the degree of **Master of Science**

in

**APPLIED MATHEMATICS**

DEPARTMENT OF MATHEMATICAL SCIENCES

EDMONTON, ALBERTA

FALL 1995

National Library
of Canada

Acquisitions and
Bibliographic Services Branch

395 Wellington Street
Ottawa, Ontario
K1A 0N4

Bibliothèque nationale
du Canada

Direction des acquisitions et
des services bibliographiques

395, rue Wellington
Ottawa (Ontario)
K1A 0N4

*Your file Votre référence*

*Our file Notre référence*

THE AUTHOR HAS GRANTED AN IRREVOCABLE NON-EXCLUSIVE LICENCE ALLOWING THE NATIONAL LIBRARY OF CANADA TO REPRODUCE, LOAN, DISTRIBUTE OR SELL COPIES OF HIS/HER THESIS BY ANY MEANS AND IN ANY FORM OR FORMAT, MAKING THIS THESIS AVAILABLE TO INTERESTED PERSONS.

L'AUTEUR A ACCORDE UNE LICENCE IRREVOCABLE ET NON EXCLUSIVE PERMETTANT A LA BIBLIOTHEQUE NATIONALE DU CANADA DE REPRODUIRE, PRETER, DISTRIBUER OU VENDRE DES COPIES DE SA THESE DE QUELQUE MANIERE ET SOUS QUELQUE FORME QUE CE SOIT POUR METTRE DES EXEMPLAIRES DE CETTE THESE A LA DISPOSITION DES PERSONNE INTERESSEES.

THE AUTHOR RETAINS OWNERSHIP OF THE COPYRIGHT IN HIS/HER THESIS. NEITHER THE THESIS NOR SUBSTANTIAL EXTRACTS FROM IT MAY BE PRINTED OR OTHERWISE REPRODUCED WITHOUT HIS/HER PERMISSION.

L'AUTEUR CONSERVE LA PROPRIETE DU DROIT D'AUTEUR QUI PROTEGE SA THESE. NI LA THESE NI DES EXTRAITS SUBSTANTIELS DE CELLE-CI NE DOIVENT ETRE IMPRIMES OU AUTREMENT REPRODUITS SANS SON AUTORISATION.

ISBN 0-612-06511-1

Canada

UNIVERSITY OF ALBERTA

LIBRARY RELEASE FORM

NAME OF AUTHOR: **Curtis J. Mooney**

TITLE OF THESIS: **Finite Amplitude Baroclinic Instability of a Mesoscale Gravity Current in a Channel**

DEGREE: **Master of Science**

YEAR THIS DEGREE GRANTED: **1995**

Permission is hereby granted to the University of Alberta Library to reproduce single copies of this thesis and to lend or sell such copies for private, scholarly, or scientific research purposes only.

The author reserves all other publication and other rights in association with the copyright in the thesis, and except as hereinbefore provided, neither the thesis nor any substantial portion thereof may be printed or otherwise reproduced in any material form whatever without the author's prior written permission.

C Mooney

11410 - 41st Avenue
Edmonton, Alberta, Canada
T6J 0T8

Date: October 5, 1995

UNIVERSITY OF ALBERTA

FACULTY OF GRADUATE STUDIES AND RESEARCH

The undersigned certify that they have read, and recommend to the Faculty of Graduate Studies and Research for acceptance, a thesis entitled **Finite Amplitude Baroclinic Instability of a Mesoscale Gravity Current in a Channel** submitted by **Curtis J. Mooney** in partial fulfilment of the requirements for the degree of Master of Science in Applied Mathematics.

Dr. G.E. Swaters (Supervisor)

Dr. T.B. Moodie

Dr. E.P. Lozowski

Date: September 26, 1995

**Abstract**

A weakly nonlinear theory is developed for the finite-amplitude evolution of marginally unstable modes for a mesoscale gravity current on a sloping bottom. The theory is based on a nonquasigeostrophic, baroclinic model of the convective destabilization of mesoscale gravity currents introduced previously which allows for large-amplitude isopycnal deflections while filtering out shear-based barotropic instabilities. Two calculations are presented. In the first, an amplitude equation is derived for marginally unstable modes not located at the minimum of the marginal stability curve. It is shown that the modes eventually equilibrate with a new finite-amplitude periodic solution formed. In the second, the evolution of a packet of marginally unstable modes located at the bottom of the marginal stability curve is described. The derivation of these two models is dramatically different due to fundamental differences in the mathematical properties of the leading order problems. In particular, it is shown that the nondispersive nature of the leading order problem for the wavepacket analysis leads to an infinity of coupled amplitude equations, each similar in form to those previously obtained for the Phillips model of baroclinic instability. It is shown that if this system is truncated to include only the fundamental harmonic and its accompanying mean flow, there exist steadily-travelling solitary eddy solutions. As well, the sine-Gordon equation is derived from this truncated set, which indicates the existence of multisoliton solutions, among others. Higher order truncations suggest that whenever the closure systematically includes a higher harmonic *and* its accompanying mean flow there exist bounded, periodic solutions. Finally, a solution to the entire infinite set, introduced previously, is adapted to the model used here.

**Acknowledgements**

First, I would like to thank my supervisor, Dr. Gordon Swaters, for all his help related to this thesis. His infectious enthusiasm for geophysical fluid dynamics helped me to see this project through to its conclusion.

I would also like to thank Richard Karsten for some helpful comments which improved Chapters 2 and 3, and David Quick for proofreading the text of the thesis.

Finally, I would like to thank my wife, Debra, who made it possible to do this.

**Table of Contents**


| CHAPTER | | PAGE |
|---|---|---|
| 1. | Introduction | 1 |
| 2. | Derivation of the Governing Equations | 9 |
| | 2.1 The Two Layer Shallow Water Equations | 10 |
| | 2.2 Scales for the Two Layer Equations | 17 |
| | 2.3 Potential Vorticity Formulation of the Two Layer Equations | 23 |
| | 2.4 Derivation of the Governing Equations | 32 |
| 3. | The Hamiltonian Structure of the Governing Equations | 35 |
| | 3.1 A Finite Dimensional Example | 35 |
| | 3.2 The Hamiltonian Formulation for the Channel Model | 38 |
| | 3.2.1 Invariance of the Hamiltonian Functional | 44 |
| | 3.2.2 Governing Equations Derived from the Hamiltonian Formulation | 47 |
| | 3.2.3 Proof of the Algebraic Properties of the Poisson Bracket | 49 |
| | 3.3 The Casimirs | 66 |
| | 3.4 Variational Principle for Steady Solutions | 68 |
| | 3.5 Nonlinear Stability | 77 |
| 4. | The Linear Stability Problem | 86 |
| | 4.1 The Linear Stability Equations | 86 |
| | 4.2 Energetics | 88 |
| | 4.3 Normal Mode Analysis | 90 |
| 5. | Weakly Nonlinear Analysis for Unstable Modes other than $K = 1$ | 97 |
| | 5.1 Derivation of the Amplitude Equation | 98 |
| | 5.2 Solution to the Evolution Equation | 106 |
| | 5.3 Description of the Solutions for the Dnoidal Wave Equation | 109 |
| 6. | Amplitude Equations for the $K = 1$ Mode | 115 |
| | 6.1 Derivation of the Equations | 115 |
| | 6.2 Solitary Wave Solution | 122 |
| | 6.3 Multiple Equation Representation | 136 |
| | 6.4 A Solution to the Complete Multiple Equation Set | 148 |
| 7. | The Sine-Gordon Equation | 160 |
| | 7.1 Derivation of the Sine-Gordon Equation | 161 |
| | 7.2 Cnoidal Wave Solutions to the Sine-Gordon Equation | 164 |
| | 7.3 Single Soliton Solution to the Sine-Gordon Equation | 166 |
| | 7.4 A 2-Soliton Solution | 168 |
| | 7.5 A Kink-Antikink Solution | 178 |
| | 7.6 Breather Solutions | 183 |
| 8. | Summary and Conclusions | 185 |
| | References | 188 |
| | Appendix | 191 |

## List of Figures


| FIGURE | | PAGE |
|---|---|---|
| 1. | Geometry of the channel two-layer model | 8 |
| 2. | Marginal stability curve | 96 |
| 3. | Plot of nondimensional perturbation pressure amplitude $R(T)$ | 112 |
| 4. | Plot of $R_{\max}$ versus $k$ | 113 |
| 5. | Plot of period versus $k$ | 114 |
| 6. | Plot of $V$ and $\kappa$ versus $k$ | 126 |
| 7. | Contour plots of nondimensional perturbation pressure amplitude | |
| | a. $k = 0.2$ | 127 |
| | b. $k = 0.5$ | 128 |
| | c. $k = 0.8$ | 129 |
| 8. | Contour plots of nondimensional perturbation thickness | |
| | a. $k = 0.2$ | 130 |
| | b. $k = 0.5$ | 131 |
| | c. $k = 0.8$ | 132 |
| 9. | Contour plots of nondimensional variable current height | |
| | a. $k = 0.2$ | 133 |
| | b. $k = 0.5$ | 134 |
| | c. $k = 0.8$ | 135 |
| 10. | Plots of temporal solutions for $A(T)$ | |
| | a. 4 equation set | 140 |
| | b. 12 equation set | 141 |
| 11. | Plots of temporal solutions for the 56 equation set | |
| | a. $A(T)$ | 142 |
| | b. $-iB_{1,1}(T)$ | 143 |
| | c. $\alpha_2(T)$ | 144 |
| | d. $B_{8,6}(T)$ | 145 |
| 12. | Plots of temporal solutions for $A(T)$ - 56 equation set | |
| | a. $k = 0.2$ | 146 |
| | b. $k = 0.8$ | 147 |
| 13. | Plot of the 2-soliton solution | |
| | a. arctan solution | 176 |
| | b. "hump" solution | 177 |
| 14. | Plot of the kink-antikink solution | |
| | a. arctan solution | 181 |
| | b. "hump" solution | 182 |
| 15. | Plot of the moving breather solution | 184 |

# Chapter 1

## Introduction

Mesoscale gravity currents are density-driven flows with length and time scales large enough so that the earth's rotation cannot be neglected in modelling their dynamics. These currents appear when dense water is formed or otherwise released in a shallow sea, such as a shelf region, and settles onto the bottom. If the bottom is sloping, then the combined influences of the Coriolis and buoyancy stresses may force the current to be transversely constrained and flow, in the northern hemisphere, with the direction of locally increasing bottom height to its right. Examples include the Denmark Strait overflow (Smith, 1976), Antarctic Bottom Water (Whitehead and Worthington, 1982), deep water formation in the Adriatic Sea (Zoccolotti and Salusti, 1987), and deep water replacement in the Strait of Georgia (Leblond *et al.*, 1991). In particular, it is possible that the formation of coherent cold eddies or domes (e.g. Armi and D'Asaro, 1980; Houghton *et al.*, 1982; Mory *et al.*, 1987; Nof, 1983; Swaters and Flierl, 1991; among others) which propagate along the bottom may be the result of the instability of these currents.

In this thesis, the physical model consists of two layers of fluid in a channel with a gently sloping bottom, where the lower layer is a dense gravity current which extends completely across the bottom of the channel, and the upper layer is less dense with an undulating free surface (Figure 1). Of particular importance in this configuration is the fact that the thickness of the gravity current is much less than the depth of the channel, and so the scale of any deflections of the interface between the upper and lower layers will be small in comparison to the upper layer thickness, but not small in comparison to the gravity current thickness. The ramifications of this will be discussed at length in further sections.

Much of the theoretical work on the stability of benthic gravity currents is based on the study by Griffiths, Killworth, and Stern (1982, hereinafter referred to as GKS). This study presented a long-wavelength perturbation analysis of the ageostrophic (where "geostrophic" is defined to be a dynamical balance between the Coriolis force and pressure gradients in the fluid, such that the isobars act as streamlines for the flow) barotropic instability of a gravity current on a sloping bottom (GKS also studied finite wavenumbers). In order to focus attention on barotropic instability processes (i.e., the release of mean kinetic energy), GKS worked with a reduced-gravity single-layer theory in which the overlying fluid was infinitely deep and motionless. The instability was the result of a coupling of two free lateral boundary streamlines and did not require, as in quasigeostrophic theory (see Pedlosky, 1987, Section 7.14 or Leblond and Mysak, 1978, Section 44), a zero in the cross-shelf potential vorticity gradient (quasigeostrophic theory implies that the leading order dynamics is geostrophic, but the *evolution* of the fields is determined from higher order terms). While the instability was primarily barotropic, the unstable mode described by GKS necessarily had a concomitant release of mean potential energy. In general, the coupled front was found to be quite unstable when the width of the current was of the same scale as the Rossby deformation radius, which is the length scale at which the Coriolis force becomes important.

When GKS compared the predictions of their theory to laboratory simulations of the instability of a buoyant coupled front, substantial differences were found. For example, the unstable modes described by GKS have asymptotically small along-front wavenumbers while the observed instabilities occurred over a range of wavenumbers including those corresponding to finite wavelengths. Another difficulty with the theory was that the observed instability had a dominant

lengthscale independent of the current width in contradiction to the theoretical prediction.

A third aspect of the observations that the theory could not explain was a secondary branch of instabilities which had a dipole-like appearance. This difference was attributed to the existence of another, possibly baroclinic unstable mode (i.e., instabilities which form as a result of the release of available potential energy from the rectification of a situation in which isopycnals and isobars are initially misaligned) outside the range of applicability of the GKS analysis.

To address these issues, Swaters (1991) developed an "intermediate lengthscale" theory for the baroclinic instability of mesoscale gravity currents. This model assumed that the dynamics of the overlying water column (see Figure 1) was quasigeostrophically determined and that the gravity current, while the velocity field was geostrophically determined, was *not* quasigeostrophic because deflections in the current height are on the same order of magnitude as the scale height for the gravity current itself. That is to say (as was mentioned previously), the dynamic deflections associated with the free surface or the interface between the two layers are, roughly speaking, very small in comparison to the mean thickness of the upper layer. However, the dynamic deflections of the interface between the two layers are on the *same* scale as the mean thickness of the lower layer. This balance represents a middle dynamical regime between a full ageostrophic theory in which *all* terms are retained in the governing equations, and the low wavenumber/frequency dynamics of quasigeostrophic theory. This model was derived as a systematic asymptotic reduction of the full two-layer shallow-water equations for a rotating fluid on a sloping bottom and has been used to model aspects of the propagation of cold domes (Swaters and Flierl, 1991) as well as the instability calculation of Swaters (1991).

The instability mechanism modelled by Swaters is the release of the available gravitational potential energy associated with a pool of relatively dense water sitting directly on a sloping bottom surrounded by relatively lighter water. As such, this instability mechanism is phenomenologically completely different than the shear based instability associated with a buoyancy-driven current containing lighter water sitting on top of a finite lower layer (e.g., Paldor and Killworth, 1987). The Swaters theory describes a purely baroclinic instability in that it filters out the shear based instability and exclusively models the convective destabilization of a mesoscale gravity current on a sloping bottom. In addition, the Swaters model does not require a zero in the transverse potential vorticity gradient for instability. By allowing for finite-amplitude deformations in the current height, the Swaters' theory can describe the instability of gravity currents with isopycnals which intersect the bottom.

The intrinsically baroclinic instability of the Swaters model differs from the nonbaroclinic instability identified by GKS associated with the coupling of the two fronts in a mesoscale gravity current (for a discussion comparing these two models see Swaters, 1991). Numerical simulations based on the primitive equations (Kawase, personal communication, 1994) suggest that the convective instability mechanism is two orders of magnitude more important than any other instability mechanism for mesoscale gravity currents.

The most unstable mode (the mode with the fastest growth rate) in the Swaters (1991) calculation was consistent with available observations of propagating cold domes. Moreover, the theory was able to predict the onset of the curious dipole-like branch of instabilities observed in the experiments of GKS.

Notwithstanding the success of the linear instability theory, if this model is to describe the dynamical transition from an unstable gravity current to propa-

gating cold domes, it is necessary to show that the exponentially growing instabilities which are obtained from the linear analysis eventually saturate with a new finite-amplitude configuration formed. That is, if it is found that introducing the nonlinear terms in the governing equations does not lead to an eventual halt to the growth of the instabilities, then we must have serious concerns about the model equations themselves. The principal purpose of this thesis is to develop a finite-amplitude instability theory for the Swaters (1991) model applied to a mesoscale gravity current on a sloping bottom.

The gravity current model examined here will be highly idealized and will *not* include an interface which intersects the bottom in a coupled front configuration. The mathematical difficulties associated with handling the finite-amplitude dynamics of isopycnals which intersect the bottom, while interesting (and ultimately the problem one wants to solve), obscure the essential physics of the problem and are ignored here. After briefly examining the linear stability problem for the model gravity current, two finite-amplitude calculations are presented, in which we employ weakly nonlinear analysis. This procedure allows us to develop equations which follow the evolution of the amplitude of a disturbance associated with a *slightly* unstable (supercritical) mode using the full nonlinear set of governing equations. In the first calculation, we derive a purely *temporal* amplitude equation describing the equilibration of a marginally unstable mode which does not correspond to the mode located at the minimum of the marginal stability curve (which defines the boundary between stability and instability for each horizontal wavenumber versus the variation of the gravity current thickness). In the second, we derive a *wave-packet* amplitude equation for the mode located at the minimum of the marginal stability curve, assuming it is slightly supercritical.

These two models are dramatically different due to the mathematical proper-

ties of the individual leading order linear instability problems. In the first problem, the marginally unstable mode is dispersive (i.e., the frequency is not a linear function of the wavenumber) so that higher order harmonics do not directly produce secularities (terms which result in linear growth over time) in the asymptotic analysis developed here. Our derivation of the temporal amplitude equation for this problem is straightforward and closely follows the classical work of Pedlosky (1970) for quasigeostrophic baroclinic instability modified for our governing equations.

However, the leading order stability problem for a marginally unstable mode located at the minimum of the marginal stability curve is *nondispersive*. This means that *all* higher harmonics necessarily give rise to secularities in the first order perturbation equations in the asymptotic expansion. Consequently, the application of the appropriate solvability conditions will necessarily yield a denumerable infinity of coupled wave-packet equations which are similar in form to those obtained from the revised wave packet analysis presented by Pedlosky (1982b) for the Phillips instability model.

The analysis of these equations is complicated. Nevertheless, we explicitly show that if we retain, on a purely *ad hoc* basis, the principal harmonic and its accompanying mean flow, there exists a steadily-travelling solitary cold eddy solution to the envelope equations. We also examine numerically the purely temporal problem associated with higher order truncations. It appears that whenever the truncation systematically includes a higher harmonic *and* its accompanying mean flow, the evolution equations admit bounded, periodic finite-amplitude solutions. We also briefly describe a technique, introduced by Warn and Gauthier (1989), which allows for the analytical solution of the entire set of equations with respect to the fundamental perturbation pressure harmonic by recasting the solvability conditions into the form of an initial value problem.

The thesis is set out as follows. In Chapter 2, the model is derived, and in Chapter 3, a hamiltonian formulation for the governing equations is introduced and utilized in a linear and nonlinear stability analysis. In Chapter 4, the linear stability problem is reviewed and a marginal stability curve is obtained. Chapter 5 and 6 contain the weakly nonlinear stability analysis for the two cases mentioned above, and in Chapter 7 a sine-Gordon equation is derived from the truncated set of evolution equations which include only the primary modes. Various solutions to this equation are examined. Finally, in Chapter 8, there is a discussion of the results, concluding remarks, and suggestions for further research.

Figure 1. Geometry of the channel two-layer model

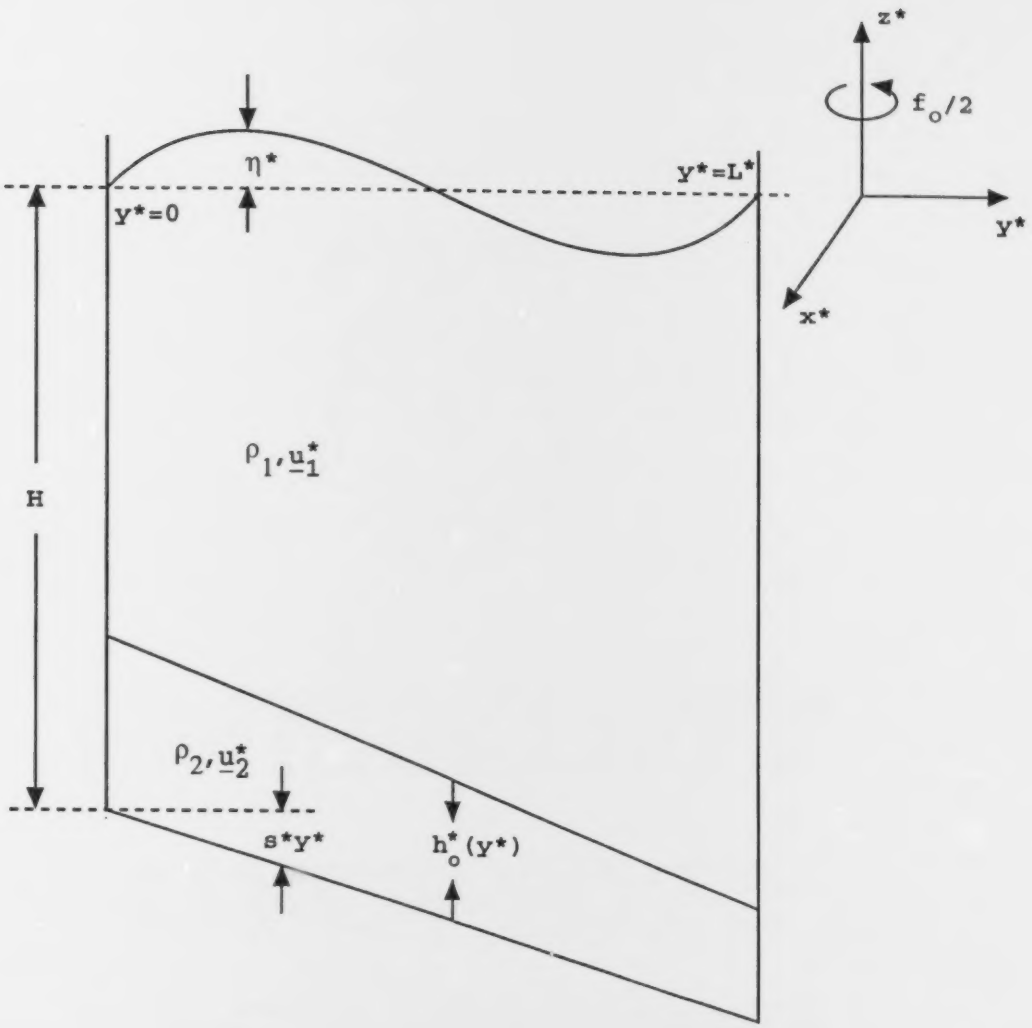

## Chapter 2

## Derivation of the Governing Equations

Geophysical fluids are characterized by a striking difference between the length scale of vertical motion compared to that of horizontal motion. In the atmosphere, for example, vertical movement of air associated with typical weather systems takes place almost entirely in the region between the surface of the earth and the tropopause, a distance of, on average, about 10 kilometers. Coherent horizontal movements occur on a much vaster scale - a typical wavelength for a series of disturbances on a planetary Rossby wave may be one to two thousand kilometers or more. In the ocean, the vertical scale in the mid-ocean is about 5 kilometers, and the horizontal scale is about 100 kilometers. We may take advantage of these scale differences by developing a theory which, to leading order, ignores vertical accelerations compared to horizontal accelerations. The resulting equations are called the *shallow water* equations. In this thesis, we use a two layer rigid-lid model (see Figure 1) in order to address the baroclinic aspect of the problem. In Section 2.1, we derive the shallow water equations for each layer in our model, and we call these the two layer shallow water equations. In Section 2.2, we develop scalings to highlight the dynamics we expect to occur in the specific physical situation studied here, and in Section 2.3, a potential vorticity formulation of the scaled two layer equations is derived. We then apply a straightforward asymptotic expansion in the small slope parameter $s$ to these equations, and from the leading order problem derive, in Section 2.4, the governing equations for our model.

*2.1 The Two Layer Shallow Water Equations*

To derive the shallow water equations in the context of the problem we are studying in this thesis, we start with the inviscid Navier-Stokes equations for a fluid which is incompressible and has constant density (this derivation is adapted from Pedlosky, 1987). Note that these conditions imply that the three dimensional velocity field is divergence free. We take into account the earth's rotation by applying these equations to an $f-$plane, which means the Coriolis parameter is taken to be constant at the value appropriate for the origin of our coordinate system. The equations in vector form are

$$\boldsymbol{u}_t + (\boldsymbol{u}\cdot\nabla)\boldsymbol{u} + f(\hat{e}_3 \times \boldsymbol{u}) = -\frac{1}{\rho}\nabla p - g\,\hat{e}_3, \tag{2.1.1}$$

$$\nabla\cdot\boldsymbol{u} = 0, \tag{2.1.2}$$

where $\boldsymbol{u}(x,y,z,t)$ is the velocity such that $\boldsymbol{u} = (u,v,w)$ where $u, v,$ and $w$ are the along-channel, across-channel, and vertical velocities, respectively, $\rho$ is the density, $p(x,y,z,t)$ is the total pressure, the operator $\nabla = (\partial_x, \partial_y, \partial_z)$, and $f = 2\Omega\sin(\theta_0)$ where $\Omega$ is the magnitude of the earth's rotation vector (i.e., $\Omega = 2\pi$ radians/day) and $\theta_0$ is our reference latitude for the $f-$plane approximation.

We now apply a scaling argument to the above set to arrive at the shallow water equations. The horizontal lengthscale is much larger than the vertical lengthscale, as mentioned before, and this ansatz is quantified in the following relation

$$A_R = H/L \ll 1, \tag{2.1.3}$$

where $(H, L)$ are the horizontal and vertical length scales, respectively, and

$A_R$ is called the *aspect ratio.* We now apply (2.1.3) to (2.1.1) and (2.1.2) using the symbols $(U, V)$ for along and across channel velocity scales and $W$ for the vertical velocity scale. The continuity equation (2.1.2) is, with scales beneath,

$$u_x + v_y + w_z = 0. \tag{2.1.4}$$
$$\frac{U}{L} \quad \frac{U}{L} \quad \frac{W}{H}$$

This implies that $W = \mathrm{O}(UH/L) = \mathrm{O}(A_R U)$, if all terms in (2.1.4) are to be of the same order of magnitude.

Now we write down (2.1.1) in component form with scales underneath

$$u_t + uu_x + vu_y + wu_z - fv = -\frac{1}{\rho}p_x, \tag{2.1.5}$$
$$\frac{U}{T} \quad \frac{UU}{L} \quad \frac{UU}{L} \quad \frac{UW}{H} \quad fU$$
$$v_t + uv_x + vv_y + wv_z + fu = -\frac{1}{\rho}p_y, \tag{2.1.6}$$
$$\frac{U}{T} \quad \frac{UU}{L} \quad \frac{UU}{L} \quad \frac{UW}{H} \quad fU$$
$$w_t + uw_x + vw_y + ww_z = -\frac{1}{\rho}p_z - g. \tag{2.1.7}$$
$$\frac{W}{T} \quad \frac{UW}{L} \quad \frac{UW}{L} \quad \frac{WW}{H}$$

First we examine the vertical momentum equation. We see that (assuming an advective timescale $T = L/U$) that, in terms of the scales, (2.1.7) suggests

$$\mathrm{O}\left(\frac{A_R U^2}{L}\right) = -\frac{1}{\rho}p_z - g. \tag{2.1.8}$$

Now, for the sake of argument, suppose we use typical mid-ocean scales to determine the left hand side, i.e, let $A_R = 10^{-2}, U = 10^{-1}\,\mathrm{m/s}, \quad L = 10^5\,\mathrm{m}$. We

then find

$$\frac{1}{\rho}p_z = -g + \mathrm{O}(10^{-9}\mathrm{m/s}^2), \tag{2.1.9}$$

which means that the hydrostatic approximation is an excellent estimate under these circumstances, and we shall assume it to hold from here on in.

We now integrate the relation (2.1.9), neglecting the non-hydrostatic terms, with respect to $z$ to get

$$p(x,y,z,t) = -\rho g z + \tilde{p}(x,y,t), \tag{2.1.10}$$

where $\tilde{p}$ is the dynamic pressure. Since $\tilde{p}$ is independent of $z$, it follows from (2.1.10) that the horizontal pressure gradients in (2.1.5) and (2.1.6) will also be independent of $z$, which in turn means that $u_z = v_z = 0$ if they are initially independent of $z$. This is known in geophysical fluid dynamics as the Taylor-Proudman Theorem, and its basic assertion is that in classical shallow water theory the motion is strictly two dimensional (Pedlosky, 1987). It can be shown that if $u_z = v_z = 0$ at $t = 0$, then $u$ and $v$ are independent of $z$ for all time $t \geq 0$. We will assume that this is the case here.

The relationship between the dynamic pressure and the other dynamical variables depends on the specific layer. In the upper layer, which has density $\rho_1$ (see Figure 1), (2.1.10) takes the form

$$p_1(x,y,z,t) = -\rho_1 g z + \tilde{p}_1(x,y,t), \tag{2.1.11}$$

where the subscripts refer to the specific layer.

We assume that the undulations of the free surface do not change the stresses acting on the atmosphere, because, compared to the size of the deflection of the

free surface, which we denote by $\eta(x,y,t)$, the atmosphere may be considered to be infinitely deep. This allows us to assume the atmospheric pressure at the free surface to be constant, which we then scale by setting it to zero. We now apply this to (2.1.11) and we obtain

$$0 = -\rho_1 g\eta(x,y,t) + \tilde{p}_1(x,y,t), \tag{2.1.12}$$

which means that

$$p_1(x,y,z,t) = -\rho_1 g(z-\eta). \tag{2.1.13}$$

In the lower layer, which has density $\rho_2 > \rho_1$ (stable stratification is assumed), it is convenient to write (2.1.10) in the form

$$p_2(x,y,z,t) = \rho_1 gH - \rho_2 g(z+H) + \tilde{p}_2(x,y,t). \tag{2.1.14}$$

We determine $\tilde{p}_2$ by imposing the *dynamic* boundary condition that the *total* pressure must be continuous across the interface between the two layers. Referring to Figure 1, the position of the interface is given by $z = -H - sy + h$ where $H$ is the mean thickness of layer 1, $h(x,y,t)$ is the thickness of the lower layer, and the $sy$ depth term is associated with the sloping bottom. Thus the dynamic boundary condition is

$$p_1(x,y,-H-sy+h,t) = p_2(x,y,-H-sy+h,t). \tag{2.1.15}$$

Applying (2.1.13) and (2.1.14) to the equation (2.1.15) gives

$$\rho_1 g(\eta + H + sy - h) = \rho_1 gH - \rho_2 g(-H - sy + h + H) + \tilde{p}_2. \tag{2.1.16}$$

Rearranging, we find that

$$\begin{aligned}\tilde{p}_2 &= \rho_1 g(\eta + sy - h) - \rho_2 g(sy - h) \\ &= \rho_1 g\eta + (\rho_2 - \rho_1) g(h - sy) \\ &= \rho_1 g\eta + \rho_2 g'(h - sy), \end{aligned} \tag{2.1.17}$$

where $g' = g(\rho_2 - \rho_1)/\rho_2 > 0$ is the reduced gravity. Therefore the total pressure in the lower layer is given by

$$p_2 = \rho_1 g(H + \eta) - \rho_2(z + H) + \rho_2 g'(h - sy). \tag{2.1.18}$$

We now develop a mass conservation equation for the upper layer. In order to do this, we will need to apply kinematic boundary conditions at the interface between this layer and the gravity current, and at the surface. We require that if a fluid parcel is on either of these boundaries initially, it remains there for all time. This condition prevents "cavitation" at these interfaces and ensures that the boundaries between the fluids share the same shape on either side. These requirements are stated mathematically by

$$w_1 = \frac{D}{Dt}(-H - sy + h) \qquad \text{on} \quad z = -H - sy + h, \tag{2.1.19}$$

for the condition on the interface between the gravity current and the ambient fluid, and

$$w_1 = \frac{D\eta}{Dt} \qquad \text{on} \quad z = \eta, \tag{2.1.20}$$

for the condition on the surface (see Figure 1 for the description of the boundaries for $z$). The operator $D/Dt = \partial/\partial t + \boldsymbol{u}_1 \cdot \nabla$ represents the *total* derivative,

or the derivative following the motion, in layer 1. Note that $\nabla = (\partial_x, \partial_y)$, the horizontal gradient operator, here and from now on.

Because $u$ and $v$ are independent of $z$, we may integrate the continuity equation (2.1.4) over the entire layer 1 thickness given by the interval $-H - sy + h < z < \eta$. The result is

$$w_1(x,y,\eta,t) - w_1(x,y,-H-sy+h,t) = -(\eta + H + sy - h)(u_{1x} + v_{1y}). \quad (2.1.21)$$

If (2.1.19) and (2.1.20) are substituted into (2.1.21), we obtain

$$\frac{D\eta}{Dt} + \frac{D(H+sy-h)}{Dt} + (\eta + H + sy - h)(u_{1x} + v_{1y}) = 0, \quad (2.1.22)$$

which may be expanded in vector form as

$$(\eta + H + sy - h)_t + \mathbf{u}_1 \cdot \nabla(\eta + H + sy - h) + (\eta + H + sy - h)\nabla \cdot \mathbf{u}_1. \quad (2.1.23)$$

Equation (2.1.23) may be written more compactly by using the vector identity $\nabla \cdot (\mathbf{a}\phi) = \phi \nabla \cdot \mathbf{a} + \mathbf{a} \cdot \nabla\phi$ for an arbitrary vector $\mathbf{a}$ and an arbitrary scalar $\phi$. The result is

$$(\eta - h)_t + \nabla \cdot [\mathbf{u}_1(\eta + H + sy - h)] = 0. \quad (2.1.24)$$

The mass conservation equation for the gravity current (layer 2) is found in much the same way. The boundary conditions are

$$w_2 = \frac{D}{Dt}(-H - sy + h) \qquad \text{on} \quad z = -H - sy + h, \quad (2.1.25)$$

on the interface, where $D/Dt = \partial/\partial_t + \mathbf{u}_2 \cdot \nabla$, and

$$w_2 = u_2(-H - sy)_x + v_2(-H - sy)_y \qquad \text{on} \quad z = -H - sy, \quad (2.1.26)$$

which arises from the requirement that there be no component of the flow normal to the bottom of the channel (i.e. $\mathbf{u}_2 \cdot \hat{n} = 0$ on $z = -H - sy$). Note that (2.1.26) implies that we have the simple relation $w_2 = -sv_2$ on the channel bottom.

We integrate the continuity equation (2.1.4) over the thickness of the gravity current, an interval defined by $-H - sy < z < -H - sy + h$, and obtain

$$w_2(x, y, -H - sy + h, t) - w_2(x, y, -H - sy, t) + (u_{2x} + v_{2y})h = 0. \quad (2.1.27)$$

We substitute (2.1.25) and (2.1.26) into (2.1.27) to get

$$\frac{D}{Dt}(-H - sy + h) - u_2(-H - sy)_x - v_2(-H - sy)_y + (u_{2x} + v_{2y})h = 0, \quad (2.1.28)$$

or

$$\frac{Dh}{Dt} + (u_{2x} + v_{2y})h = 0, \quad (2.1.29)$$

which may be rewritten in conservation form, with the same procedure as was used to derive the layer 1 mass conservation equation, as

$$h_t + \nabla \cdot (\mathbf{u}_2 h) = 0. \quad (2.1.30)$$

The set of equations for the two layers are listed below. We introduce asterisks to emphasize the fact that the variables are *dimensional*. For the overlying fluid we have

$$\mathbf{u}_{1t}^* + (\mathbf{u}_1^* \cdot \nabla^*)\mathbf{u}_1^* + f(\hat{e}_3 \times \mathbf{u}_1^*) + g\nabla^*\eta^* = \mathbf{0}, \quad (2.1.31)$$

$$(\eta^* - h^*)_{t^*} + \nabla^* \cdot [\mathbf{u}_1^*(\eta^* + H + s^*y^* - h^*)] = 0, \quad (2.1.32)$$

where $p_1$ has been replaced by (2.1.13), and the gravity current equations are

$$\boldsymbol{u}_{2t^*}^* + (\boldsymbol{u}_2^* \cdot \nabla^*)\boldsymbol{u}_2^* + f(\hat{e}_3 \times \boldsymbol{u}_2^*) + \frac{1}{\rho_2}\nabla^* p_2^* = \boldsymbol{0}, \tag{2.1.33}$$

$$h_{t^*}^* + \nabla^* \cdot [\boldsymbol{u}_2^* h^*] = 0. \tag{2.1.34}$$

The set (2.1.31)-(2.1.34) is closed with the pressure continuity condition, given by

$$p_2^* = \rho_1 g \eta^* + \rho_2 g'(h^* - s^* y^*), \tag{2.1.35}$$

where $p_2$ is the dynamic pressure in the lower layer (the tilde in equation (2.1.17) has been dropped).

*2.2 Scales for the Two Layer Equations*

Now we must scale the two layer equations according to parameters which are specific to the physics of the problem (see Swaters and Flierl (1991)). The scaling for horizontal length is

$$(x^*, y^*) = L^*(x, y) = [(g'H)^{\frac{1}{2}}/f](x, y), \tag{2.2.1}$$

so that $L^*$ represents the internal radius of deformation, and where, henceforth, all variables *without* an asterisk are dimensionless. This scaling implies that we look for motions which are of a magnitude where the effects of rotation are at least as important as buoyancy effects. Note that $(g'H)^{\frac{1}{2}}$ is the phase speed of an internal gravity wave unaffected by rotation (Pedlosky, 1987).

The timescale will be given by

$$t^* = (fL^*/g's^*)t, \tag{2.2.2}$$

where $g's^*/f$ is the *Nof* speed, which is the theoretical speed at which an isolated cold eddy travels along a bottom which slopes in the zonal direction if there is no interaction with the surrounding fluid (Nof, 1983). The Nof speed is a logical choice for this problem because if there are instabilities in the gravity current, the possibility exists that it may break up into isolated travelling eddies. Note that this is an *advective* time scale, because it consists of a lengthscale divided by a speed.

The thickness of the gravity current will be scaled according to

$$h^* = h_0 h, \tag{2.2.3}$$

where $h_0$ is the maximum thickness of the undisturbed current, and we let $\delta = h_0/H \ll 1$.

The layer 1 velocity $\mathbf{u}_1^*$ and the free surface deformation $\eta^*$ are scaled as

$$\mathbf{u}_1^* = \delta f L^* \mathbf{u}_1 = (h_0/H)(g'H)^{\frac{1}{2}}\mathbf{u}_1, \tag{2.2.4}$$

$$\eta^* = [\delta(fL^*)^2\eta/g] = (h_0 g'/g)\eta. \tag{2.2.5}$$

We scale $\mathbf{u}_1^*$ by dividing the deformation radius by the inertial timescale $(1/f)$ and multiplying by the ratio of $h_0/H$. The purpose of this scaling is to ensure that changes in the relative vorticity (i.e. $\nabla \times \mathbf{u}_1^*$) in the upper layer are a result of vortex tube stretching/contraction caused by the movement of the gravity current underneath. Note that if $h_0$ is small compared to $H$ then $\mathbf{u}_1^*$ (and therefore the upper layer relative vorticity) is also small. The scaling for $\eta^*$ is constructed so that $\mathbf{u}_1^*$ and $\eta^*$ are in geostrophic balance to leading order. The geostrophic scaling simply implies that the upper layer velocity is scaled so

that it is proportional to the dynamic pressure gradient to leading order.

For the gravity current, we scale $\boldsymbol{u}_2^*$ with the Nof speed, and then scale $p_2^*$ geostrophically, so that

$$\boldsymbol{u}_2^* = g' s^* \boldsymbol{u}_2 / f, \tag{2.2.6}$$

$$p_2^* = \rho_2 L^* g' s^* p_2. \tag{2.2.7}$$

The slope of the channel is scaled by

$$s^* = (H/L)s = (g'H)^{\frac{1}{2}} s/(g'/f), \tag{2.2.8}$$

which, if rearranged, may be written as

$$s = (s^* g'/f)/(g'H)^{\frac{1}{2}}, \tag{2.2.9}$$

which allows interpretation of the scaling as the ratio of the Nof speed to the speed of long baroclinic gravity waves. A small $s$ acts as a filter to remove these long waves from the upper layer and so focus attention on the vorticity generated waves (Swaters and Flierl, 1991).

To arrive at the *non-dimensional* equations for the upper layer, we apply the scales above to (2.1.31) and (2.1.32). The momentum equations become

$$\frac{\delta (g'H)^{\frac{1}{2}}}{\frac{(g'H)^{\frac{1}{2}}}{g'} \cdot \frac{g'}{(g'H)^{\frac{1}{2}} fs}} \boldsymbol{u}_{1_t} + \delta (g'H)^{\frac{1}{2}} \frac{f}{(g'H)^{\frac{1}{2}}} (\boldsymbol{u}_1 \cdot \nabla) \delta (g'H)^{\frac{1}{2}} \boldsymbol{u}_1$$

$$+ f(\hat{e}_3 \times (g'H)^{\frac{1}{2}} \delta \boldsymbol{u}_1) + \frac{gf}{(g'H)^{\frac{1}{2}}} \nabla \frac{h_0 g'}{g} \eta = \boldsymbol{0}, \tag{2.2.10}$$

where $\delta = h_0/H$ has been used wherever applicable. Simplifying each term

leads to

$$\delta(g'H)^{\frac{1}{2}} f s \boldsymbol{u}_{1_t} + \delta^2 (g'H)^{\frac{1}{2}} f(\boldsymbol{u}_1 \cdot \nabla)\boldsymbol{u}_1 + f(g'H)^{\frac{1}{2}} \delta(\hat{\epsilon}_3 \times \boldsymbol{u}_1) + \frac{f h_0 g'}{(g'H)^{\frac{1}{2}}} \nabla\eta = \mathbf{0}. \tag{2.2.11}$$

Dividing (2.2.11) through by $\delta(g'H)^{\frac{1}{2}} f$ and simplifying the last term on the left hand side provides the end result, which is

$$s\boldsymbol{u}_{1_t} + \delta(\boldsymbol{u}_1 \cdot \nabla)\boldsymbol{u}_1 + \hat{\epsilon}_3 \times \boldsymbol{u}_1 + \nabla\eta = \mathbf{0}. \tag{2.2.12}$$

The mass continuity equation for the upper layer is handled in a similar fashion. We obtain

$$\frac{\left(\frac{h_0 g'}{g}\eta - h_0 h\right)_t}{\frac{(g'H)^{\frac{1}{2}}}{g'} \cdot \frac{g'}{(g'H)^{\frac{1}{2}} f s}} + \frac{f}{(g'H)^{\frac{1}{2}}} \nabla \cdot \left[\delta(g'H)^{\frac{1}{2}} \boldsymbol{u}_1 \left(\frac{h_0 g'}{g}\eta + H + \frac{(g'H)^{\frac{1}{2}} s f}{g'} \cdot \frac{(g'H)^{\frac{1}{2}}}{f} s y - h_0 h\right)\right] = 0. \tag{2.2.13}$$

Simplifying each term in (2.2.13) leads to

$$f s \left(\frac{h_0 g'}{g}\eta - h_0 h\right)_t + \delta f \nabla \cdot \left[\boldsymbol{u}_1 \left(\frac{h_0 g'}{g}\eta + H + H s y - h_0 h\right)\right] = 0. \tag{2.2.14}$$

We drop terms in (2.2.14) which are multiplied by $g'/g = (\rho_2 - \rho_1)/\rho_2$, because we assume that the difference in the densities of the two layers is small, which means that $(\rho_2 - \rho_1) \ll \rho_2$. This approximation is equivalent to assuming that the upper surface in layer 1 is rigid, and that $\eta(x, y, t)$ may be interpreted as the *dynamic* pressure in that layer. This also eliminates long surface gravity waves (i.e., Poincare waves) from the model (Swaters and Flierl, 1991). This leaves

$$-h_0 f s h_t + \delta f \nabla \cdot [\boldsymbol{u}_1 (H + H s y - h_0 h)] = 0. \tag{2.2.15}$$

Dividing by $-h_0 f$ and using $\delta = h_0/H$ to simplify the second term on the left hand side of (2.2.15) leads to

$$sh_t + \nabla \cdot [\boldsymbol{u}_1(\delta h - sy - 1)] = 0, \tag{2.2.16}$$

which is the nondimensional upper layer mass continuity equation.

The nondimensional equations for the lower layer (or gravity current) are obtained in exactly an analogous manner to the upper layer equations, and the result is

$$s\boldsymbol{u}_{2_t} + s(\boldsymbol{u}_2 \cdot \nabla)\boldsymbol{u}_2 + \hat{e}_3 \times \boldsymbol{u}_2 + \nabla p_2 = \boldsymbol{0}, \tag{2.2.17}$$

$$h_t + \nabla \cdot (h\boldsymbol{u}_2) = 0. \tag{2.2.18}$$

Application of the scales to the equation for the dynamic pressure in the lower layer (2.1.35) gives

$$\frac{\rho_2 (g'H)^{\frac{1}{2}} g' (g'H)^{\frac{1}{2}} fs}{fg'} p_2 = \rho_2 g' \left( h_0 h - \frac{(g'H)^{\frac{1}{2}} f}{g'} \cdot \frac{(g'H)^{\frac{1}{2}}}{f} sy \right) + \frac{\rho_1 g h_0 g'}{g} \eta. \tag{2.2.19}$$

Algebraic simplification of (2.2.19) leaves

$$\rho_2 g' H s p_2 = \rho_2 g' (h_0 h - Hsy) + \rho_1 h_0 g' \eta. \tag{2.2.20}$$

Dividing through by $g'H$ and using $\delta = h_0/H$ gives

$$\rho_2 s p_2 = \rho_2 (\delta h - sy) + \rho_1 \delta \eta. \tag{2.2.21}$$

Now we use the fact that $\rho_1$ and $\rho_2$ are of a similar magnitude to eliminate the densities in (2.2.21) (this assumption is precisely the same as assuming, as we

did in (2.2.14), that $g'/g$ is small enough to ignore terms multiplied by it). The end result is

$$sp_2 = \delta(\eta + h) - sy. \tag{2.2.22}$$

The boundary conditions on the channel walls are very simple; there can be no flux of fluid through the walls, which implies that the velocity component normal to the walls must be zero. In mathematical terms, we have

$$v_{1,2}(x, 0, t) = v_{1,2}(x, L, t) = 0, \tag{2.2.23}$$

where $y = 0$ and $y = L$ are the nondimensional location of the walls.

Typical values for the dimensional parameters appropriate for a continental shelf are (e.g., Houghton *et al.* (1982)) $s^* \approx 1.2$m/km, $h^* \approx 40$m, and $H \approx 250$m, which suggest $s \approx 7 \times 10^{-2}$, $\delta \approx 1.6 \times 10^{-1}$, $L^* \approx 15$km and an *advective* timescale of $t^* = fL^*/(g's^*) \approx 7$ days. Note that $s$ and $\delta$ are both $O(10^{-1})$. These scalings imply that a new parameter, denoted $\mu$, may be introduced, such that

$$\delta = \mu s, \tag{2.2.24}$$

where $\mu \approx O(1)$; for the above scalings, $\mu \approx 2$. We call $\mu$ the *interaction parameter* (after Swaters and Flierl (1991)), and it physically measures the ratio of the destabilizing influence of baroclinic vortex tube stretching/compression in the nonfrontal area to the stabilizing influence of the sloping bottom, which acts like a topographic $\beta$-plane.

Substituting (2.2.24) into (2.2.12) and (2.2.16)-(2.2.18) yields the two layer

equations

$$\hat{e}_3 \times \boldsymbol{u}_1 + \nabla\eta = -s\boldsymbol{u}_{1_t} - s\mu(\boldsymbol{u}_1 \cdot \nabla)\boldsymbol{u}_1, \tag{2.2.25}$$

$$\nabla \cdot \boldsymbol{u}_1 = sh_t - s\nabla \cdot (y\boldsymbol{u}_1) + s\mu\nabla \cdot (h\boldsymbol{u}_1), \tag{2.2.26}$$

$$\hat{e}_3 \times \boldsymbol{u}_2 - \hat{e}_2 + \mu\nabla(h+\eta) = -s\boldsymbol{u}_{2_t} - s(\boldsymbol{u}_2 \cdot \nabla)\boldsymbol{u}_2, \tag{2.2.27}$$

$$h_t + \nabla \cdot (h\boldsymbol{u}_2) = 0, \tag{2.2.28}$$

where we have separated terms multiplied by the small parameter $s$ from those which are not. We have also substituted (2.2.22) into (2.2.17) to arrive at (2.2.27). The pressure continuity equation becomes

$$p_2 = -y + \mu(\eta + h). \tag{2.2.29}$$

Note that the location of the small parameter $s$ in the above equations produces the effect suggested in words earlier, which is that the channel water will follow quasigeostrophic dynamics but the frontal interior will be geostrophic, but *not* quasigeostrophic. Specifically, this is manifested in the retention, to leading order, of mass flux terms in the gravity current continuity equation, whereas the velocity field is divergence free to leading order in the upper layer.

### *2.3 Potential Vorticity Formulation of the Two Layer Equations*

We will convert the two layer equations into a single potential vorticity equation for each layer. In the next section, we will then use this formulation to derive the governing equations, which are the ones studied throughout the rest of the thesis.

Casting the equations in terms of potential vorticity implies that the curl of the momentum equations is taken to arrive at the vorticity equation, and from this

we look for a quantity, called the potential vorticity, which is conserved following the motion of a fluid parcel. Of course, taking the curl means that certain information is lost, and we will see that we must refer back to the momentum equations to determine the velocity fields which are inherent in the relative vorticity.

We first work with the upper layer equations. The curl of equation (2.2.25) is taken by first forming $\partial/\partial_y[\hat{e}_1 \cdot (2.2.25)]$ and $\partial/\partial_x[\hat{e}_2 \cdot (2.2.25)]$, which yields, respectively,

$$-v_{1y} + \eta_{1xy} = -su_{1ty} - s\mu(u_{1y}u_{1x} + u_1u_{1xy} + v_{1y}u_{1y} + v_1u_{1yy}), \tag{2.3.1}$$

$$u_{1x} + \eta_{1yx} = -sv_{1tx} - s\mu(u_{1x}v_{1x} + u_1v_{1xx} + v_{1x}v_{1y} + v_1v_{1yx}). \tag{2.3.2}$$

Then, subtracting (2.3.2) from (2.3.1) gives

$$-(u_{1x} + v_{1y}) = s\zeta_{1t} + s\mu[u_1\zeta_{1x} + v_1\zeta_{1y} + (u_{1x} + v_{1y})\zeta_1], \tag{2.3.3}$$

where $\zeta_1 = v_{1x} - u_{1y}$ is the relative vorticity in the upper layer. This may be rewritten as

$$-(u_{1x} + v_{1y}) = s\frac{D\zeta}{Dt}_1 + s\mu(u_{1x} + v_{1y})\zeta_1, \tag{2.3.4}$$

where we have used the scaled material (total) derivative, written as

$$\frac{D}{Dt} = \frac{\partial}{\partial t} + \mu\left[u_1\frac{\partial}{\partial x} + v_1\frac{\partial}{\partial y}\right]. \tag{2.3.5}$$

We expand (2.2.16) after applying (2.2.24) to obtain

$$sh_t + (\mu sh - sy - 1)\nabla \cdot \mathbf{u}_1 + \mathbf{u}_1 \cdot \nabla(\mu sh - sy - 1) = 0. \tag{2.3.6}$$

Solving for the divergence in (2.3.6) leads to

$$\nabla \cdot \boldsymbol{u}_1 = -\frac{sh_t + \boldsymbol{u}_1 \cdot \nabla(\mu sh - sy - 1)}{\mu sh - sy - 1}$$

$$= -\frac{D/Dt(\mu sh - sy - 1)}{\mu(\mu sh - sy - 1)}. \tag{2.3.7}$$

Now substitute this into (2.3.4) to get

$$s\frac{D\zeta_1}{Dt} - (1 + s\mu\zeta_1)\left[\frac{D/Dt(\mu sh - sy - 1)}{\mu(\mu sh - sy - 1)}\right] = 0, \tag{2.3.8}$$

or

$$\frac{D}{Dt}(1 + s\mu\zeta_1) - \frac{(1 + s\mu\zeta_1)}{(\mu sh - sy - 1)}\frac{D}{Dt}(\mu sh - sy - 1) = 0. \tag{2.3.9}$$

This may be rewritten as

$$\frac{D}{Dt}\left[\frac{1 + s\mu\zeta_1}{\mu sh - sy - 1}\right] = 0, \tag{2.3.10}$$

which is the potential vorticity equation for the upper layer. The potential vorticity is the quantity in the square brackets, and it is conserved following the motion.

It is of some interest to note that the equation (2.3.10) may be derived in another way. Shallow water theory dictates that, in general, the potential vorticity equation for an inviscid, incompressible layer of fluid which feels the earth's rotation will take the form (Pedlosky, 1987)

$$\frac{D}{Dt^*}\left[\frac{\text{relative + planetary vorticity}}{\text{depth of layer}}\right] = 0. \tag{2.3.11}$$

For the upper layer in our model, equation (2.3.11) is equivalent to

$$\frac{D}{Dt^*}\left[\frac{\zeta_1^* + f}{H + s^*y^* - h^*}\right] = 0. \tag{2.3.12}$$

When the scales from Section 2.2 are applied to equation (2.3.12), the result is equation (2.3.10).

In order to derive the governing equations for the upper layer, we exploit the fact that $0 < s \ll 1$ to derive a leading order potential vorticity equation for the upper layer. Our procedure will be to rewrite the dependent variables in a series, where each succeeding term is asymptotically smaller than the last. For example, suppose we have an ordinary differential equation given by

$$r''(x) + 2\epsilon \sin(x) r'(x) + r(x) = 0, \tag{2.3.13}$$

where the prime denotes differentiation with respect to $x$, and $\epsilon$ is a small parameter. We then expand $r$ in a series in terms of $\epsilon$, so that

$$r(x) \sim r^{(0)} + \epsilon r^{(1)}(x) + \epsilon^2 r^{(2)}(x) + \ldots = p^{(0)} + p^{(1)} + p^{(2)} + \ldots, \tag{2.3.14}$$

where the $p^{(i)}$ represent the terms in the asymptotic series. This series is then substituted into (2.3.13) and terms collected to form equations at each order of $\epsilon$. The *leading order* problem (i.e., the O(1) problem) for $r(x)$ is simply

$$r^{(0)''} + r^{(0)} = 0. \tag{2.3.15}$$

The next order (the $O(\epsilon)$ problem), is

$$r^{(1)''} + 2\sin(x) r^{(0)'} + r^{(1)} = 0, \tag{2.3.16}$$

and so on, to all orders of $\epsilon$.

We proceed by solving the leading order problem, subject to the initial conditions, then substitute the solution into (2.3.16) and solve the $O(\epsilon)$ problem. If

more terms in the series are required, this procedure is continued at higher orders. The advantage of this method is that the problems at each order are generally easier to solve than the original equation, especially the leading order problem (see (2.3.15) compared to (2.3.13)). As well, if $\epsilon$ is small enough, very good accuracy may be obtained by retaining only one or two of the terms in the series. We shall see why by looking at the definition of such series.

The term "asymptotic series" is defined mathematically by stating that each term in the series must meet the requirement that (Bender and Orszag, 1979)

$$\lim_{\epsilon \to 0} \frac{r - \sum_{i=0}^{n} p^{(i)}}{p^{(n)}} = 0 \quad \text{for all} \quad n = 0, 1, 2, \ldots . \tag{2.3.17}$$

where the $p^{(i)}$ represent terms in the series, as in (2.3.14). Equation (2.3.17) states that the remainder left, after subtracting an $n$ term asymptotic series from the function $r(x)$, is asymptotically smaller than the $n$th term in that series. We see that (2.3.14) meets this requirement, as long as the $r^{(i)}$ are O(1) quantities. Also, if $n = 0$ in (2.3.17), as $\epsilon \to 0$, the term $p^{(0)} \to r$, and thus $p^{(0)}$ may be an accurate reflection of the behavior of $r$ under these circumstances, if $\epsilon$ is small enough.

From a physical point of view, we want to *segregate* the dynamics of a system into distinct orders, so that the leading order dynamics are unencumbered by the effects of terms asymptotically smaller than those retained in the leading order problem. This allows a determination of the dominant dynamical balance in the problem, which will be perturbed only slightly by the higher order effects. That is not to say that these effects are not important; in fact, it will be seen that in quasigeostrophic theory, the evolution in time of the velocity fields, balanced to leading order with pressure gradients, is determined by appeal to second order

dynamics.

With the above discussion in mind, we construct a straightforward asymptotic expansion in the small parameter $s$ of the form

$$(\eta, \boldsymbol{u}_1, h) \sim (\eta, \boldsymbol{u}_1, h)^{(0)} + s(\eta, \boldsymbol{u}_1, h)^{(1)} + \dots . \tag{2.3.18}$$

The first step is to expand the potential vorticity equation (2.3.10) by carrying out the material differentiation with respect to time, so that

$$(\mu sh - sy - 1)\frac{D}{Dt}(s\mu\zeta_1) - (1 + s\mu\zeta_1)\frac{D}{Dt}(\mu sh - sy) = 0, \tag{2.3.19}$$

where all $D(1)/Dt$ terms have been ignored, and where a division through by $s$ was done.

The leading order problem is obtained by gathering all the terms which are in the lowest order of the small parameter $s$, after application of the asymptotic expansion (2.3.18) to (2.3.19), and this leads to

$$-\frac{D^{(0)}}{Dt}(\mu\zeta_1^{(0)}) - \frac{D^{(0)}}{Dt}(\mu h^{(0)} - y) = 0, \tag{2.3.20}$$

where $D^{(0)}/Dt = \partial_t + \mu\boldsymbol{u}_1^{(0)} \cdot \nabla$. Dividing (2.3.20) through by $-\mu$ and combining the two terms on the left hand side gives

$$\frac{D^{(0)}}{Dt}\left[\zeta_1^{(0)} + h^{(0)} - \frac{y}{\mu}\right] = 0. \tag{2.3.21}$$

To eliminate the velocity terms which make up $\zeta_1^{(0)}$, we utilize the asymptotic expansion (2.3.18) in the upper layer momentum equations (2.2.25). We immediately see that the leading order terms form the equation

$$\hat{e}_3 \times \boldsymbol{u}_1^{(0)} + \nabla\eta^{(0)} = 0. \tag{2.3.22}$$

We may solve for $\boldsymbol{u}_1^{(0)}$ by applying $\hat{e}_3 \times$ to each term in equation (2.3.22). The result is

$$\boldsymbol{u}_1^{(0)} = \hat{e}_3 \times \nabla \eta^{(0)} = (-\eta_y^{(0)}, \eta_x^{(0)}). \tag{2.3.23}$$

This is known as the *geostrophic relation*, for reasons we will soon discuss. Substituting (2.3.23) into (2.3.21) gives

$$\frac{D^{(0)}}{Dt}\left[\Delta \eta^{(0)} + h^{(0)} - \frac{y}{\mu}\right] = 0, \tag{2.3.24}$$

where $\Delta = \partial_{xx} + \partial_{yy}$. We may refer to equation (2.3.24) as the quasigeostrophic potential vorticity equation for the upper layer, where the quasigeostrophic potential vorticity is the quantity inside the brackets, and it is conserved following the flow.

The geostrophic relation (2.3.23) may be obtained in another way. In quasigeostrophic shallow water theory, the velocity fields are determined geostrophically, which means that the isobars are the streamlines for the flow. However, the geostrophic relations are degenerate in the sense that *any* pressure field is a solution (i.e., creates a velocity field). To find the time evolution of the pressure fields, it is necessary to consider the $O(s)$ dynamics, while still requiring the geostrophic determination of the velocity fields. This is the essense of quasigeostrophic shallow water theory.

The geostrophic relations, in general, for a shallow, inviscid, incompressible layer of fluid which feels the effect of the earth's rotation are simply

$$\begin{aligned} -fu^* &= -\frac{1}{\rho} p_{x^*}^* \\ fv^* &= -\frac{1}{\rho} p_{y^*}^*, \end{aligned} \tag{2.3.25}$$

in component form, or in vector form

$$f(\hat{e}_3 \times \boldsymbol{u}^*) = -\frac{1}{\rho}\nabla p^*. \tag{2.3.26}$$

But for the upper layer, $p_1^*$ is given by equation (2.1.13), so that the dimensional geostrophic relation becomes

$$f(\hat{e}_3 \times \boldsymbol{u}_1^*) = g\nabla\eta^*. \tag{2.3.27}$$

When this equation is scaled using the scalings set out in Section 2.2, we arrive at (2.3.23).

The situation is quite different for the lower layer (i.e., the gravity current), because, as has been indicated previously, the dynamics here are not quasigeostrophic. The divergence of the velocity field does not vanish to leading order, which is a requirement in quasigeostrophic theory. We begin the derivation of the governing equations for the gravity current by taking the curl of equation (2.2.27), following the same procedure as that used to find the curl of (2.2.25), and the result is

$$u_{2x} + v_{2y} = -s\left[\frac{D\zeta_2}{Dt} + (u_{2x} + v_{2y})\zeta_2\right], \tag{2.3.28}$$

where $\zeta_2 = v_{2x} - u_{2y}$, and $D/Dt = \partial_t + \boldsymbol{u}_2 \cdot \nabla$ is the scaled material derivative for the lower layer.

If we then rewrite (2.2.28) so that

$$-\frac{1}{h}\frac{Dh}{Dt} = \nabla \cdot \boldsymbol{u}_2 = u_{2x} + v_{2y}, \tag{2.3.29}$$

we may substitute (2.3.29) into (2.3.28) to obtain

$$-\frac{1}{h}\frac{Dh}{Dt} = -s\left[\frac{D\zeta_2}{Dt} - \frac{1}{h}\frac{Dh}{Dt}\zeta_2\right], \tag{2.3.30}$$

or, after multiplying by $1/h$ and rearranging

$$\frac{s}{h}\frac{D\zeta_2}{Dt} - \frac{1+s\zeta_2}{h^2}\frac{Dh}{Dt} = 0. \tag{2.3.31}$$

Equation (2.3.31) may then be rewritten as

$$\frac{D}{Dt}\left[\frac{1+s\zeta_2}{h}\right] = 0, \tag{2.3.32}$$

which is the potential vorticity form of the governing equations.

As was the case for the upper layer, the equation (2.3.32) could also have been obtained by scaling the dimensional shallow water potential vorticity equation (2.3.11), as it relates to the lower layer,

$$\frac{D}{Dt^*}\left[\frac{\zeta_2^* + f}{h^*}\right] = 0. \tag{2.3.33}$$

As was done for the upper layer equations, an asymptotic expansion in the small parameter $s$ of the form

$$(\eta, \boldsymbol{u}_2, h) \sim (\eta, \boldsymbol{u}_2, h)^{(0)} + s(\eta, \boldsymbol{u}_2, h)^{(1)} + \ldots . \tag{2.3.34}$$

is applied to equation (2.3.32) to get the leading order potential vorticity equation for the gravity current

$$\frac{D^{(0)}}{Dt}\left[\frac{1}{h^{(0)}}\right] = 0, \tag{2.3.35}$$

where $D^{(0)}/Dt = \partial_t + \boldsymbol{u}_2^{(0)}\nabla\cdot$.

The velocity terms which are implicit in the material derivative operator may be replaced by a geostrophic relation which is obtained in precisely the same fashion as for the upper layer. We apply the asymptotic expansion (2.3.33) to the gravity current momentum equations (2.2.27) and collect the lowest order terms in the small parameter $s$. These terms form the equation

$$\hat{e}_3 \times \boldsymbol{u}_2 - \hat{e}_2 + \mu\nabla(h+\eta) = 0, \tag{2.3.36}$$

or solving for $\boldsymbol{u}_2$ by applying $\hat{e}_3 \times \cdot$ to all terms in (2.3.36), we find

$$\boldsymbol{u}_2 = \hat{e}_1 + \mu\hat{e}_3 \times \nabla(\eta + h). \tag{2.3.37}$$

Note that this equation could also have been derived by substituting the dynamic gravity current pressure equation (2.1.35) into the general geostrophic relations (2.3.25), and then scaling the result.

*2.4 Derivation of the Governing Equations*

In this section, the leading order potential vorticity formulation developed in Section 2.3 is used to derive the governing equations for the model. We start by rewriting the expression (2.3.35). We have

$$\frac{D^{(0)}}{Dt}\left[\frac{1}{h^{(0)}}\right] = -\frac{D^{(0)}(h^{(0)})}{Dt}\frac{1}{(h^{(0)})^2} = 0 \Longrightarrow \frac{D^{(0)}(h^{(0)})}{Dt} = 0. \tag{2.4.1}$$

We may utilize (2.4.1) by writing it in component form (where we drop the "(0)" superscripts)

$$h_t + u_2 h_x + v_2 h_y = 0. \tag{2.4.2}$$

Using (2.3.37) to substitute for the velocity fields gives

$$h_t + [1 - \mu(h_y + \eta_y)]h_x + \mu(h_x + \eta_x)h_y = 0, \tag{2.4.3}$$

and this may be rewritten as

$$h_t + h_x + \mu J(\eta, h) = 0, \tag{2.4.4}$$

where $J(A, B) = A_x B_y - A_y B_x$ is the Jacobian operator.

Now we return to the upper layer equations, and expand equation (2.3.21) to get

$$(\Delta\eta + h)_t + \mu u_1(\Delta\eta + h)_x + \mu v_1(\Delta\eta + h)_y - v = 0, \tag{2.4.5}$$

where we again have dropped the "(0)" superscripts. If we now use the geostrophic relation (2.3.23) to substitute for the velocity fields in (2.4.5), we obtain, after some rearrangement

$$(\Delta\partial_t - \partial_x)\eta + h_t + \mu J(\eta, \Delta\eta) + \mu J(\eta, h) = 0. \tag{2.4.6}$$

Equation (2.4.4) is then used to eliminate two terms in favor of $h_x$ to give

$$(\Delta\partial_t - \partial_x)\eta - h_x + \mu J(\eta, \Delta\eta) = 0. \tag{2.4.7}$$

We may now write down the complete set of governing equations as they will be used in this thesis. We have

$$(\Delta\partial_t - \partial_x)\eta - h_x + \mu J(\eta, \Delta\eta) = 0, \tag{2.4.8}$$

$$h_t + h_x + \mu J(\eta, h) = 0, \tag{2.4.9}$$

with the leading order "auxiliary" relations

$$\boldsymbol{u}_1 = \hat{\epsilon}_3 \times \nabla\eta, \tag{2.4.10a}$$

$$\boldsymbol{u}_2 = \hat{\epsilon}_1 + \mu\hat{\epsilon}_3 \times \nabla(\eta + h), \tag{2.4.10b}$$

$$p = -y + \mu(\eta + h), \tag{2.4.10c}$$

where we have dropped the subscript "2" in (2.2.29), and where (2.4.10a) is taken from (2.3.23) and (2.4.10b) is taken from (2.3.37).

The boundary condition on the channel walls (2.2.23) now takes the form, after applying (2.4.10a) and (2.4.10b),

$$\left.\begin{array}{l} \eta_x = 0 \\ h_x = 0 \end{array}\right\} \quad \text{on} \quad y = 0, L. \tag{2.4.11}$$

The model (2.4.8) - (2.4.11) has an exact *steady* nonlinear along-channel solution given by

$$\left.\begin{array}{l} \eta = \eta_0(y) = -\int_0^y U_0(\xi)d\xi \\ h = h_0(y) \end{array}\right\} \quad \text{for} \quad 0 < y < L, \tag{2.4.12}$$

where we assume $h_0(y)$ is everywhere non-negative. It may easily be verified that (2.4.12) is a solution by direct substitution into (2.4.8) and (2.4.9). Equation (2.4.12) is the general form of the steady solution whose stability characteristics we will study throughout the remainder of this thesis.

## Chapter 3

## The Hamiltonian Structure of the Governing Equations

The model equations for the channel may be recast into a hamiltonian formulation. The chief advantage of this is that more general and sweeping statements may be made about the stability, in particular the nonlinear stability, of steady solutions to the governing equations. Swaters (1993) did an extensive examination of these same equations applied to an arbitrarily-shaped gravity current on a continental shelf, and this investigation is adapted here to the channel model, which, with its simple gravity current profile, allows some specific conclusions to be drawn. We make one simplifying assumption here. In the governing equations derived in Chapter 2, the Jacobian terms are multiplied by the O(1) quantity $\mu$. For the purposes of this analysis we take $\mu = 1$ so that all the calculations in this chapter do not carry this coefficient. It turns out, as will be seen later, that $\mu$ determines the nature of the instability if there is instability, but it does not appear in the criteria which set the boundaries between stability and instability, outside of the requirement that $\mu > 0$ (i.e., there must be a sloping bottom). This is not to say that a hamiltonian formulation cannot be found with this coefficient included; we are simply stating that it complicates the calculations but in the end has no effect on the stability convexity estimates and so it is excluded in favor of a simpler presentation. Setting $\mu = 1$ in the governing equations is equivalent to introducing the transformation $\eta = \tilde{\eta}/\mu$ and $h = \tilde{h}/\mu$ in equations (2.4.8) and (2.4.9).

### *3.1 A Finite Dimensional Example*

The hamiltonian formulation for a system of partial differential equations is

essentially an extension of the classical canonical hamiltonian formulation of finite dimensional conservative systems. The equations of motion for such systems are (Goldstein (1980); Shepherd (1990))

$$\frac{dq_i}{dt} = \frac{\partial H}{\partial p_i}; \qquad \frac{dp_i}{dt} = -\frac{\partial H}{\partial q_i}, \tag{3.1.1}$$

where $q_i$ and $p_i$ are the generalized coordinates and momenta, respectively, in the phase space denoted by $[q_i, p_i]$ where $i = 1, 2, \cdots, N$, and where $H = H(q_i, p_i)$ is the hamiltonian, which is generally an expression of the total energy of the system. These equations may be written in *symplectic* form as well (Shepherd, 1990), such that

$$\frac{d\mathbf{q}}{dt} = \mathbf{M}\frac{\partial H}{\partial \mathbf{q}}, \tag{3.1.2}$$

where $\mathbf{M}$ is a skew-symmetric matrix given by

$$\mathbf{M} = \begin{bmatrix} 0 & I \\ -I & 0 \end{bmatrix}, \tag{3.1.3}$$

and $\mathbf{q}$ is a column vector with $2N$ components. Note that this matrix is invertible; this makes the formulation *canonical.*

We look at a simple two dimensional example to fix these ideas. Suppose we have a massless spring with a spring constant $k$ fixed at one end to a frictionless table, with a mass $m$ attached at the other end. The equation of motion for this system is given by Hooke's Law for ideal springs combined with Newton's 2nd Law, so that

$$m\frac{d^2x}{dt^2} = -kx, \tag{3.1.4}$$

where $x$ is the spatial coordinate along which the mass-spring system moves,

and $t$ is time. If we scale $t$ such that $\sqrt{k/m}\,t = \tilde{t}$, then, after dropping the tildes,

$$x_{tt} + x = 0, \tag{3.1.5}$$

where the subscript denotes differentiation. We see that the motion is decribed by a simple harmonic oscillation.

We wish to form an energy equation, so equation (3.1.5) is multiplied by $x_t$ and then rearranged to give

$$\frac{1}{2}(x_t)_t^2 + \frac{1}{2}(x^2)_t = 0, \tag{3.1.6}$$

and then integrating (3.1.6) with respect to $t$, we find

$$\frac{1}{2}(x_t)^2 + \frac{1}{2}x^2 = E. \tag{3.1.7}$$

We see that the expression on the left hand side of (3.1.7) is simply the total energy (a constant which is denoted by $E$) where $\frac{1}{2}(x_t)^2$ is the kinetic energy, and $\frac{1}{2}x^2$ is the potential energy. We call this the *hamiltonian* and rewrite it as

$$H(q,p) = \frac{1}{2}p^2 + \frac{1}{2}q^2, \tag{3.1.8}$$

because $p = x_t$ is the scaled momentum, and $q = x$ is the coordinate for the motion. It is easy to see that the equations (3.1.1) applied to (3.1.8) lead to

$$H_q = q = -p_t, \tag{3.1.9}$$

$$H_p = p = q_t, \tag{3.1.10}$$

and if (3.1.10) is differentiated with respect to $t$ and the result substituted into (3.1.9), then we obtain (3.1.5).

Note also that $H(q,p)$ is invariant with respect to time, since

$$\frac{dH}{dt} = p\frac{dp}{dt} + q\frac{dq}{dt} = -pq + qp = 0. \tag{3.1.11}$$

This result is not surprising, since the hamiltonian represents the total energy of this system, which is conserved. The symplectic form of (3.1.9) and (3.1.10) is simply

$$\begin{bmatrix} q \\ p \end{bmatrix}_t = \begin{bmatrix} 0 & 1 \\ -1 & 0 \end{bmatrix} \begin{bmatrix} H_q \\ H_p \end{bmatrix}. \tag{3.1.12}$$

We apply the formulation developed here to a simple problem to illustrate its utility. We look for a *steady* solution (a solution independent of time) to the governing equation, which we call $\mathbf{q}_0 = (q_0, p_0)$. Then the equations (3.1.9) and (3.1.10) give

$$H_q(q_0, p_0) = q_0 = -p_{0_t} = 0, \tag{3.1.13}$$

$$H_p(q_0, p_0) = p_0 = q_{0_t} = 0. \tag{3.1.14}$$

This implies that, as we would expect, the only steady solution for this system is $x = x_t = 0$, i.e., the system is at rest (which means $E \equiv 0$ for the steady state).

### *3.2 The Hamiltonian Formulation for the Channel Model*

In the case of partial differential equations, the independent variables $\mathbf{q} = \mathbf{q}(\mathbf{x}, t)$ are functions of both space and time, and so functions of $\mathbf{q}$ become *functionals* (Shepherd (1990)), and we will need to take variational derivatives rather than partial derivatives. With this in mind, we say that a system of partial differential equations is hamiltonian (Olver (1982); Benjamin (1984)) if there exists

a *conserved* functional $H(\mathbf{q})$ such that

$$\mathbf{q}_t = \mathbf{M}\frac{\delta H}{\delta \mathbf{q}}, \tag{3.2.1}$$

where $\mathbf{q} = (q_1, \ldots, q_n)^T$ is a column vector of $n$ independent variables, $\mathbf{M}$ is a matrix for which the associated Poisson bracket must satisfy the five properties of self-commutation, skew-symmetry, distributive property, associative property, and, finally, the Jacobi identity. We will carefully describe the Poisson bracket and these algebraic properties later in this section. It should be noted that such a system has an infinite dimensional phase space, in contrast to the finite dimensional, canonical hamiltonian systems governed by ordinary differential equations with time as the independent variable (the harmonic oscillator in Section 3.1 is an example). The infinite number of dimensions is a result of the fact that the $p(t)$ and $q(t)$ analogues may be represented by an infinite Fourier series in a spatial basis function.

The domain, for the purposes of the hamiltonian analysis, is given by $y = (0, L)$ in the cross-channel direction. In the along-channel direction, we specify a periodic domain $x = (-\lambda, \lambda)$ such that $\eta$ and $h$ are smoothly periodic at $x = \pm\lambda$. This "periodicity boundary condition," as we will refer to it, implies that at every point $0 \leq y \leq L$, and at any time $t$, $\eta$, and $h$, and all their derivatives, have the same value on the boundaries $x = \pm\lambda$. Therefore the domain is

$$\Omega = \{(x, y) | -\lambda < x < \lambda, 0 < y < L\}. \tag{3.2.2}$$

The boundary of the domain, $\partial\Omega$, is simply the piecewise continuous curve

bounding the open set $\Omega$. This may be represented as

$$\partial\Omega = \{[-\lambda, \lambda] \times [0, L]\} - \{(-\lambda, \lambda) \times (0, L)\}. \tag{3.2.3}$$

The boundary conditions on the channel walls are, from equation (2.4.11),

$$\eta_x = h_x = 0 \quad \text{on} \quad y = 0, L. \tag{3.2.4}$$

This implies directly that $\eta$ and $h$ must be independent of $x$ on the channel walls. Therefore, we conclude that $\eta$ and $h$ are constant on $y = 0, L$ (not necessarily the same constant). For our purposes here, we shall assume that $\eta = 0$ on the channel walls (i.e., the constants are set to zero), which implies that there will be no net along-channel flux in the upper layer. Also, as alluded to above, the "periodicity boundary condition" on the boundaries $x = \pm\lambda$ implies that at every point $y$, and at any time $t$, $\eta$ (and $h$) has the same value on the boundaries $x = \pm\lambda$.

The above discussion is consistent with the analysis we intend to carry out in this thesis. We will set $U_0 = 0$ in (2.4.12) (and therefore $\eta_0 = 0$) in order to confine our work to baroclinic phenomena, and we will look for wave-like solutions for the perturbations with along-channel structure $\exp[ik(x-ct)]$ +c.c., where $k$ is the along-channel wavenumber and $c$ is the phase speed. Both of these conditions imply that if $\eta_x = 0$ then $\eta = 0$, i.e., the amplitude of the perturbation fields must be zero, on the channel walls. Therefore, the boundary

conditions may be stated as

$$\begin{aligned} &\eta = 0 \quad \text{on} \quad y = 0, L, \\ &h = \text{constant} \quad \text{on} \quad y = 0, L, \\ &[\eta, h](-\lambda, y, t) = [\eta, h](\lambda, y, t). \end{aligned} \tag{3.2.5}$$

We also require, as indicated above, that all *derivatives* of $\eta$ and $h$ meet the periodicity boundary condition (e.g., $\eta_x(x = -\lambda) = \eta_x(x = \lambda)$, $\eta_y(x = -\lambda) = \eta_y(x = \lambda)$ and so on), just as would be expected from an along-channel travelling wave solution.

We also need to define the boundary conditions for *perturbations* on $\eta$ and $h$, which will be denoted $\delta\eta$ and $\delta h$. Recall the boundary conditions set out in (3.2.5), and suppose we have steady solutions $\eta_0$ and $h_0$ which depend on $y$ only. We must have

$$\begin{aligned} \eta_0(y) + \delta\eta(x, y, t) &= 0 \quad \text{on} \quad y = 0, L, \\ h_0(y) + \delta h(x, y, t) &= \text{constant} \quad \text{on} \quad y = 0, L, \\ [\eta_0, h_0](y) + \delta[\eta, h](-\lambda, y, t) &= [\eta_0, h_0](y) + \delta[\eta, h](\lambda, y, t). \end{aligned} \tag{3.2.6}$$

But the steady solutions themselves must meet the boundary conditions (3.2.5), so this fact, combined with (3.2.6) leads to the boundary conditions for the perturbations

$$\begin{aligned} \delta[\eta, h] &= 0 \quad \text{on} \quad y = 0, L, \\ \delta[\eta, h](x = -\lambda) &= \delta[\eta, h](x = \lambda), \end{aligned} \tag{3.2.7}$$

where it is understood that the constant in the boundary condition for $h$ as

written in (3.2.5) is, in fact, the value of $h_0$ on $y = 0, L$, respectively. We see that the boundary conditions on the perturbations are essentially the same as those set out in (3.2.5), and we also note that any higher variations taken on $\eta$ or $h$ will meet the same conditions as well (i.e., $\delta^2\eta$) for the same reasons. As well, as previously described for the general boundary conditions above, any spatial derivative of $\delta\eta$ or $\delta h$ also meets the periodicity boundary conditions. For example, this implies that $[\Delta\delta\eta]_{x=-\lambda} = [\Delta\delta\eta]_{x=\lambda}$, and so on.

Swaters (1993) has shown that for the governing equations (2.4.8) and (2.4.9) (setting $\mu = 1$), a hamiltonian formulation may be found, and that it takes the form

$$H(\mathbf{q}) = \frac{1}{2}\int\int_{\Omega} \nabla\eta \cdot \nabla\eta + [(h-y)^2 - y^2]dxdy, \tag{3.2.8}$$

where $\mathbf{M}$ is the two by two matrix

$$\mathbf{M} = \begin{bmatrix} -J(q_1 - y, \cdot) & 0 \\ 0 & J(q_2, \cdot) \end{bmatrix}, \tag{3.2.9}$$

and where

$$q_1 = \Delta\eta + h, \tag{3.2.10}$$

$$q_2 = h. \tag{3.2.11}$$

Here $J$ is the Jacobian operator, as it was defined in the previous chapter. Note that if $\mu$ was included in this analysis, $J(q_1 - y)$ would be given by $J(q_1 - y/\mu)$ (see equation (2.3.24)).

For (3.2.8)-(3.2.11) to be considered as a Hamiltonian formulation for the governing equations, three requirements must be met.

(1) The functional $H(\mathbf{q})$ must be invariant with respect to time.

(2) The formulation must be equivalent to the governing equations.

(3) The associated Poisson bracket of the $\mathbf{M}$ matrix must satisfy five algebraic properties. In Poisson bracket form, these are

(a) Self-commutation

$$[F, F] = 0, \tag{3.2.12}$$

(b) Skew-symmetry

$$[F, G] = -[G, F], \tag{3.2.13}$$

(c) Distributive property

$$[\alpha F + \beta G, Q] = \alpha[F, Q] + \beta[G, Q], \tag{3.2.14}$$

(d) Associative property

$$[FG, Q] = F[G, Q] + [F, Q]G, \tag{3.2.15}$$

(e) Jacobi identity

$$[F, [G, H]] + [G, [H, F]] + [H, [F, G]] = 0, \tag{3.2.16}$$

where $[*, *]$ is the Poisson bracket, which may be rewritten as (Shepherd (1990))

$$[F, G] = \left\langle \frac{\delta F}{\delta \mathbf{q}}, \mathbf{M} \frac{\delta G}{\delta \mathbf{q}} \right\rangle, \tag{3.2.17}$$

where

$$\langle *_1, *_2 \rangle = \iint_{\Omega} (*_1 *_2^T)\, dxdy, \tag{3.2.18}$$

and where $F, G,$ and $Q$ are arbitrary *allowable* functionals (the concept of allowable functionals will be discussed in more detail later).

### 3.2.1 Invariance of the Hamiltonian Functional

We begin the analysis by proving that the system (3.2.8)-(3.2.11) is, in fact, a hamiltonian representation of the governing equations. We first show that $H(\mathbf{q})$ is invariant in time. The first derivative of $H$ with respect to time is

$$\begin{aligned}\frac{dH}{dt} &= \iint_{\Omega} \{\nabla\eta \cdot \nabla\eta_t + (h-y)h_t\} dx dy \\ &= \oint_{\partial\Omega} \eta(\mathbf{n} \cdot \nabla\eta_t)\, dS - \iint_{\Omega} \{\eta\Delta\eta_t + (h-y)h_t\} dx dy,\end{aligned} \tag{3.2.19}$$

where Green's first identity has been used. Here $\mathbf{n}$ is the unit outward-pointing normal and $dS$ is the differential arclength. We may rewrite this boundary integral as

$$\begin{aligned}&\oint_{\partial\Omega} \eta(\mathbf{n} \cdot \nabla\eta_t)\, dS \\ &\qquad = -\int_0^L [\eta\eta_{xt}]_{x=-\lambda}\, dy + \int_{-\lambda}^{\lambda} [\eta\eta_{yt}]_{y=L}\, dx \\ &\qquad + \int_0^L [\eta\eta_{xt}]_{x=\lambda}\, dy - \int_{-\lambda}^{\lambda} [\eta\eta_{yt}]_{y=0}\, dx \\ &\qquad = 0.\end{aligned} \tag{3.2.20}$$

The second and fourth terms in the first line of (3.2.20) are zero because $\eta = 0$ on $y = 0, L$. The first and third terms add to zero because the integrands are equal, due to the periodicity boundary condition, but the signs of the integrals are opposite.

This means that the boundary integral on the right hand side of (3.2.19)

contributes nothing, so that

$$\frac{dH}{dt} = -\iint_{\Omega} \{\eta \Delta\eta_t + (h-y)h_t\} dxdy. \tag{3.2.21}$$

Now the governing equations (2.4.8) and (2.4.9) are utilized to replace $\Delta\eta_t$ and $h_t$ to obtain

$$\begin{aligned}\frac{dH}{dt} =& -\iint_{\Omega} \{\eta[\eta_x + h_x - J(\eta, \Delta\eta)] + (h-y)[-h_x - J(\eta, h)]\} dxdy \\ =& \frac{1}{2}\iint_{\Omega} \{-(\eta^2)_x - 2\eta h_x - J(\eta^2, \Delta\eta) - (h^2)_x \\ & - J(\eta, h^2) + 2yh_x + 2yJ(\eta, h)\} dxdy. \end{aligned} \tag{3.2.22}$$

An $x-$integration of the first, fourth, and sixth terms in (3.2.22) and the use of the periodicity boundary condition shows that these terms contribute nothing. This gives

$$\frac{dH}{dt} = \frac{1}{2}\iint_{\Omega} \{-2\eta h_x - 2\eta_x h - J(\eta^2, \Delta\eta) - J(\eta, h^2) + 2J(\eta, hy)\} dxdy, \tag{3.2.23}$$

where we have rewritten the last term in (3.2.22). The integrals involving the Jacobian terms in (3.2.23) may be evaluated by using the following property, for arbitrary scalars $A$ and $B$,

$$J(A, B) = \nabla \cdot [B\hat{e}_3 \times \nabla A] = -\nabla \cdot [A\hat{e}_3 \times \nabla B], \tag{3.2.24}$$

which can be easily proved by writing both sides of (3.2.24) in component form.

First we look at the third term in (3.2.23). We have

$$\begin{aligned}\iint_{\Omega} J(\eta^2, \Delta\eta) &= \iint_{\Omega} \nabla \cdot [\Delta\eta \hat{e}_3 \times \nabla\eta^2]\, dxdy \\ &= \oint_{\partial\Omega} \mathbf{n} \cdot (\hat{e}_3 \times \nabla\eta^2) \Delta\eta\, dS, \end{aligned} \tag{3.2.25}$$

where $\mathbf{n}$ is again the unit outward pointing normal vector and where we have used the divergence theorem. To evaluate the integral (3.2.25), we break it up, as we did in (3.2.20), in such a way as to integrate separately along each of the lines forming the piecewise continuous boundary, so that

$$\begin{aligned}\oint_{\partial\Omega} \mathbf{n}\cdot(\hat{e}_3\times\nabla\eta^2)\Delta\eta\,dS &= -\int_0^L [-(\eta^2)_y\Delta\eta]_{x=-\lambda}\,dy + \int_{-\lambda}^{\lambda}[(\eta^2)_x\Delta\eta]_{y=L}\,dx \\ &\quad + \int_0^L [-(\eta^2)_y\Delta\eta]_{x=\lambda}\,dy - \int_{-\lambda}^{\lambda}[(\eta^2)_x\Delta\eta]_{y=0}\,dx \\ &=0, \end{aligned} \tag{3.2.26}$$

where the first and third terms on the right hand side of (3.2.26) cancel because of the periodicity of $\eta$ and its derivatives on $x=\pm\lambda$, and the second and fourth terms are each zero because $(\eta^2)_x = 2\eta\eta_x$ and $\eta,\eta_x = 0$ on $y=0,L$.

We integrate the fourth term in (3.2.23) in an analogous fashion, so that

$$\begin{aligned}\iint_\Omega J(\eta,h^2)\,dxdy &= \iint_\Omega \nabla\cdot[h^2\hat{e}_3\times\nabla\eta]\,dxdy = \oint_{\partial\Omega}\mathbf{n}\cdot(\hat{e}_3\times\nabla\eta)h^2\,dxdy \\ &= -\int_0^L [-\eta_y h^2]_{x=-\lambda}\,dy + \int_{-\lambda}^{\lambda}[\eta_x h^2]_{y=L}\,dx \\ &\quad + \int_0^L [-\eta_y h^2]_{x=\lambda}\,dy - \int_{-\lambda}^{\lambda}[\eta_x h^2]_{y=0}\,dx \\ &=0, \end{aligned} \tag{3.2.27}$$

because of the periodicity boundary condition on derivatives of $\eta$, and because $\eta_x = 0$ on $y=0,L$.

Finally, the last term in (3.2.23) is evaluated as

$$\begin{aligned} 2\iint_\Omega J(\eta, hy)\,dxdy =& 2\iint_\Omega \nabla\cdot[hy\hat{e}_3\times\nabla\eta]\,dxdy = 2\oint_{\partial\Omega}\mathbf{n}\cdot(\hat{e}_3\times\nabla\eta)hy\,dxdy \\ =& -2\int_0^L[-\eta_y hy]_{x=-\lambda}\,dy + 2\int_{-\lambda}^{\lambda}[\eta_x hy]_{y=L}\,dx \\ &+2\int_0^L[-\eta_y hy]_{x=\lambda}\,dy - 2\int_{-\lambda}^{\lambda}[\eta_x hy]_{y=0}\,dx \\ =& 0, \end{aligned} \tag{3.2.28}$$

for exactly the same reasons as (3.2.27).

The results of (3.2.26)-(3.2.28) imply that (3.2.23) may be rewritten as

$$\frac{dH}{dt} = \iint_\Omega(-\eta h_x - \eta_x h)dxdy = \iint_\Omega(\eta h)_x\,dxdy = 0, \tag{3.2.29}$$

upon integration with respect to $x$ and the application of the periodic boundary conditions, and thus we have shown that $H(\mathbf{q})$ is invariant with respect to time.

### 3.2.2 Governing Equations Derived from the Hamiltonian Formulation

We now show that the components of the Hamiltonian formulation do indeed represent the governing equations. First, we calculate the first variation of the

Hamiltonian functional, which is

$$\begin{aligned}
\delta H &= \iint_\Omega \{\nabla\eta\cdot\nabla\delta\eta + (h-y)\delta h\}dxdy \\
&= \oint_{\partial\Omega} \eta(\mathbf{n}\cdot\nabla\delta\eta)\,dS + \iint_\Omega \{-\eta\Delta\delta\eta + (h-y)\delta h\}dxdy \\
&= -\int_0^L [\eta(\delta\eta)_x]_{x=-\lambda}\,dy + \int_{-\lambda}^{\lambda} [\eta(\delta\eta)_y]_{y=L}\,dx \\
&\quad + \int_0^L [\eta(\delta\eta)_x]_{x=\lambda}\,dy - \int_{-\lambda}^{\lambda} [\eta(\delta\eta)_y]_{y=0}\,dx \\
&\quad + \iint_\Omega \{-\eta\Delta\delta\eta + (h-y)\delta h + \eta\delta h - \eta\delta h\}dxdy \\
&= \iint_\Omega \{-\eta(\Delta\delta\eta + \delta h) + (h+\eta-y)\delta h\}dxdy \\
&= \iint_\Omega \{-\eta\delta q_1 + (h+\eta-y)\delta q_2\}dxdy, \qquad (3.2.30)
\end{aligned}$$

where the components of the boundary integral contribute nothing because of the periodicity condition on $\eta$ and $\delta\eta$ at $x = \pm\lambda$, and because $\eta = 0$ on $y = 0, L$. Equation (3.2.30) implies that $\delta H/\delta q_1 = -\eta$ and $\delta H/\delta q_2 = h + \eta - y$. Therefore, we may write

$$\mathbf{q}_t = \mathbf{M}\frac{\delta H}{\delta \mathbf{q}}, \qquad (3.2.31)$$

as

$$\begin{bmatrix} \Delta\eta + h \\ h \end{bmatrix}_t = \begin{bmatrix} -J(\Delta\eta + h - y, \cdot) & 0 \\ 0 & J(h,\cdot) \end{bmatrix} \begin{bmatrix} -\eta \\ h + \eta - y \end{bmatrix}. \qquad (3.2.32)$$

Expanding the first row in the matrix, we obtain

$$\begin{aligned}
\Delta\eta_t + h_t &= -J(\Delta\eta + h - y, -\eta) = -J(\eta, \Delta\eta) - J(\eta, h) - J(y, \eta) \\
&= -J(\eta, \Delta\eta) - J(\eta, h) + \eta_x, \qquad (3.2.33)
\end{aligned}$$

and expanding the second row of the matrix

$$\begin{aligned} h_t &= J(h, h+\eta-y) \\ &= J(h,\eta) - J(h,y) \\ &= -J(\eta,h) - h_x, \end{aligned} \tag{3.2.34}$$

which is precisely equation (2.4.9). Now we insert (3.2.34) into (3.2.33) to get

$$\Delta\eta_t - J(\eta,h) - h_x = -J(\eta,\Delta\eta) - J(\eta,h) + \eta_x, \tag{3.2.35}$$

or

$$\Delta\eta_t - \eta_x - h_x + J(\eta,\Delta\eta) = 0, \tag{3.2.36}$$

which is exactly equation (2.4.8). Therefore the Hamiltonian formulation is equivalent to the governing equations as required.

### 3.2.3 Proof of the Algebraic Properties of the Poisson Bracket

We must now show that the Poisson bracket associated with the $\mathbf{M}$ matrix satisfies the required five algebraic properties, as set out in (3.2.12)-(3.2.16). Before we begin, it is necessary to point out that because of boundary integrals which appear in the course of the proofs, we are restricted to the use of arbitrary *allowable* functionals only. An allowable functional is a functional $R(\mathbf{q})$ which meets either of the following requirements (Shepherd, 1990; McIntyre and Shepherd, 1987):

1) $[F,R] = 0$ for any arbitrary functional $F$ (these are known as *Casimir* functionals - see section 3.3)

2) On the channel walls $y = 0, L$, $R(\mathbf{q})$ satisfies

$$\frac{\partial}{\partial S}\left[\frac{\delta R}{\delta q_i}\right] = 0, \tag{3.2.37}$$

where $i = 1, 2$. The second requirement implies that $[\delta R/\delta q_i]$ is identically constant on $y = 0, L$, and therefore that

$$\frac{\delta^2 R}{\delta q_i \delta q_j} = 0, \tag{3.2.38}$$

on $y = 0, L$. This restriction on the functionals, as we shall see, ensures that the boundary integrals which arise contribute nothing, and that the algebraic properties are met.

There are physical reasons for the use of allowable functionals as well. In a finite dimensional system, a *function of state* is a function which depends only on the state of a system, that is, on the variables which describe its state. For such systems, position and velocity (momentum) of particles are enough to completely describe the state. However, in an infinite dimensional system, such as a fluid flow, individual parcels are indistinguishable (i.e., they may be interchanged) and so a function or functional of state must depend only on the velocity (McIntyre and Shepherd, 1987). It would then be expected that boundary conditions on the functional of state would, in some way, be related to the boundary conditions on the velocity, which are

$$\frac{\partial \psi}{\partial S} = 0 \quad \text{on} \quad y = 0, L, \tag{3.2.39}$$

where $\psi$ is the streamfunction. In accordance with the discussion above, we ask that the variational derivative with respect to $\mathbf{q}$ of a functional of state for the system meets the same criterion (McIntyre and Shepherd, 1987), which leads

to (3.2.37).

It follows from (3.2.37) that

$$\frac{\partial}{\partial x}\left[\frac{\delta R}{\delta q_i}\right] = 0, \tag{3.2.40}$$

for $i = 1, 2$ on $y = 0, L$, or equivalently, that

$$\frac{\delta R}{\delta q_i} = \text{constant}, \tag{3.2.41}$$

on $y = 0, L$, respectively, if $R$ is not a Casimir.

At $x = -\lambda, \lambda$ we demand that $\delta R/\delta q_i$ be smoothly periodic, i.e.,

$$\left[\frac{\delta R}{\delta q_i}\right]_{x=-\lambda} = \left[\frac{\delta R}{\delta q_i}\right]_{x=\lambda}, \tag{3.2.42}$$

as well as all the derivatives of $\delta R/\delta q_i$.

The above conditions on the first variation of an allowable functional lead directly to conditions on the *second* variation, based on (3.2.38), which are

$$\left[\frac{\delta^2 R}{\delta q_i \delta q_j}\right]_{y=0,L} = 0,$$

$$\left[\frac{\delta^2 R}{\delta q_i \delta q_j}\right]_{x=-\lambda} = \left[\frac{\delta^2 R}{\delta q_i \delta q_j}\right]_{x=\lambda}. \tag{3.2.43}$$

Let us fix these ideas by applying them to the hamiltonian itself, which is given by equation (3.2.8). We found in (3.2.30) that $\delta H/\delta q_1 = -\eta$ and $\delta H/\delta q_2 = \eta + h - y$. We have

$$\left[\left(\frac{\delta H}{\delta q_i}\right)_x\right]_{y=0,L} = (-\eta_x, \eta_x + h_x)_{y=0,L} = 0, \tag{3.2.44}$$

by application of the boundary conditions (3.2.4). Also

$$\left[\frac{\delta H}{\delta q_i}\right]_{x=\pm\lambda} = (-\eta, \eta + h - y)_{x=\pm\lambda}, \tag{3.2.45}$$

which satisfies by hypothesis the periodicity boundary condition at $x = \pm\lambda$.

We now have the prerequisites in place for the proof of the five algebraic identities. We start with the skew-symmetry property, where we must show that

$$[F, G] = -[G, F], \tag{3.2.46}$$

where $F$ and $G$ are any allowable functionals. We have

$$\begin{aligned}[F, G] &= \left\langle \frac{\delta F}{\delta q_1}, M_1 \frac{\delta G}{\delta q_1} \right\rangle + \left\langle \frac{\delta F}{\delta q_2}, M_2 \frac{\delta G}{\delta q_2} \right\rangle \\ &= -\iint_\Omega \frac{\delta F}{\delta q_1} J\left(q_1 - y, \frac{\delta G}{\delta q_1}\right) dxdy + \iint_\Omega \frac{\delta F}{\delta q_2} J\left(q_2, \frac{\delta G}{\delta q_2}\right) dxdy,\end{aligned} \tag{3.2.47}$$

where we have let $M_1 = -J(q_1 - y, *)$ and $M_2 = J(q_2, *)$ be the two non-zero diagonal components of the $\mathbf{M}$ matrix.

We now rewrite the first term on the right hand side of (3.2.47) using the identity (3.2.24) for Jacobians

$$-\iint_\Omega \frac{\delta F}{\delta q_1} J\left(q_1 - y, \frac{\delta G}{\delta q_1}\right) dxdy = -\iint_\Omega \frac{\delta F}{\delta q_1} \nabla \cdot \left[\frac{\delta G}{\delta q_1} \hat{e}_3 \times \nabla(q_1 - y)\right] dxdy. \tag{3.2.48}$$

We may make use of the vector identity (twice)

$$\nabla \cdot (\phi \mathbf{a}) = \phi \nabla \cdot \mathbf{a} + \mathbf{a} \cdot \nabla \phi, \tag{3.2.49}$$

for an arbitrary vector $\mathbf{a}$ and an arbitrary scalar $\phi$, to rewrite this equation

as

$$
\begin{aligned}
&-\iint_\Omega \frac{\delta F}{\delta q_1}\nabla\cdot\left[\frac{\delta G}{\delta q_1}\hat{e}_3\times\nabla(q_1-y)\right]dxdy\\
&=-\iint_\Omega \nabla\cdot\left[\frac{\delta F}{\delta q_1}\frac{\delta G}{\delta q_1}\hat{e}_3\times\nabla(q_1-y)\right]dxdy\\
&\quad+\iint_\Omega \frac{\delta G}{\delta q_1}[\hat{e}_3\times\nabla(q_1-y)]\cdot\nabla\left(\frac{\delta F}{\delta q_1}\right)dxdy\\
&=-\oint_{\partial\Omega}\frac{\delta F}{\delta q_1}\frac{\delta G}{\delta q_1}\mathbf{n}\cdot[\hat{e}_3\times\nabla(q_1-y)]\,dxdy\\
&\quad+\iint_\Omega \frac{\delta G}{\delta q_1}\nabla\cdot\left[\frac{\delta F}{\delta q_1}\hat{e}_3\times\nabla(q_1-y)\right]dxdy\\
&\quad-\iint_\Omega \frac{\delta G}{\delta q_1}\frac{\delta F}{\delta q_1}\nabla\cdot[\hat{e}_3\times\nabla(q_1-y)]\,dxdy. \qquad (3.2.50)
\end{aligned}
$$

But we may rewrite the divergence of the quantity in the square brackets in the last term in (3.2.50) using the following vector identity

$$\nabla\cdot(\mathbf{a}\times\mathbf{b})=\mathbf{b}\cdot(\nabla\times\mathbf{a})-\mathbf{a}\cdot(\nabla\times\mathbf{b}), \qquad (3.2.51)$$

for arbitrary vectors $\mathbf{a}$ and $\mathbf{b}$, so that we may write, in general, that

$$
\begin{aligned}
\nabla\cdot[\hat{e}_3\times\nabla\phi]&=\nabla\phi\cdot(\nabla\times\hat{e}_3)-\hat{e}_3\cdot[\nabla\times\nabla\phi]\\
&=0, \qquad (3.2.52)
\end{aligned}
$$

for any arbitrary scalar $\phi$. It is easy to see that both terms on the right hand side of (3.2.52) are zero, and therefore that the last term in (3.2.50) is also zero.

We now break up the boundary integral in (3.2.50) into four integrals, each

representing a side of the domain, so that

$$
\begin{aligned}
-\oint_{\partial\Omega} \frac{\delta F}{\delta q_1}\frac{\delta G}{\delta q_1}\mathbf{n}\cdot[\hat{e}_3\times\nabla(q_1-y)]\,dS &= \int_0^L \left[-\frac{\delta F}{\delta q_1}\frac{\delta G}{\delta q_1}(q_1-y)_y\right]_{x=-\lambda} dy \\
&\quad - \int_{-\lambda}^{\lambda} [f_L(q_1)(q_1-y)_x]_{y=L}\,dx - \int_0^L \left[-\frac{\delta F}{\delta q_1}\frac{\delta G}{\delta q_1}(q_1-y)_y\right]_{x=\lambda} dy \\
&\quad + \int_{-\lambda}^{\lambda} [f_0(q_1)(q_1-y)_x]_{y=0}\,dx \\
&= 0,
\end{aligned}
\tag{3.2.53}
$$

where we make use of the fact that $F$ and $G$ are allowable functionals by defining $f_{0,L}(q_1)$ to be

$$
f_{0,L}(q_1) = \left[\frac{\delta F}{\delta q_1}\frac{\delta G}{\delta q_1}\right]_{y=0,L}. \tag{3.2.54}
$$

The first and third terms (3.2.53) cancel because of the periodicity boundary conditions in $x$.

We note that if *both* $F$ and $G$ are *not* Casimirs, then $f_{0,L}$ are simply constants. If either $F$ or $G$ *are* Casimirs, then $f_{0,L}$ may explicitly depend only on $q_1 - y$ (see Section 3.3). Regardless, the second and fourth terms in (3.2.53) integrate to zero, since

$$
\begin{aligned}
\int_{-\lambda}^{\lambda} [f_{0,L}(q_1-y)(q_1-y)_x]_{y=0,L}\,dx &= \int_{-\lambda}^{\lambda} [f_{0,L}(q_1-y)q_{1x}]_{y=0,L}\,dx \\
&= \int_{-\lambda}^{\lambda} \left[\frac{\partial}{\partial x}\int_{-y}^{q_1-y} f_{0,L}(\xi)\,d\xi\right]_{y=0,L} dx \\
&= 0,
\end{aligned}
\tag{3.2.55}
$$

due to periodicity at $x = \pm\lambda$.

The second term in (3.2.47) is evaluated in an analogous way, so that

$$\begin{aligned}\iint_\Omega \frac{\delta F}{\delta q_2} J\left(q_2, \frac{\delta G}{\delta q_2}\right) dxdy &= \iint_\Omega \frac{\delta F}{\delta q_2} \nabla \cdot \left[\frac{\delta G}{\delta q_2} \hat{e}_3 \times \nabla q_2\right] dxdy \\ &= \oint_{\partial\Omega} \frac{\delta F}{\delta q_2}\frac{\delta G}{\delta q_2} \mathbf{n} \cdot [\hat{e}_3 \times \nabla q_2]\, dS \\ &\quad - \iint_\Omega \frac{\delta G}{\delta q_2} \nabla \cdot \left[\frac{\delta F}{\delta q_2} \hat{e}_3 \times \nabla q_2\right] dxdy \\ &\quad + \iint_\Omega \frac{\delta F}{\delta q_2}\frac{\delta G}{\delta q_2} \nabla \cdot [\hat{e}_3 \times \nabla q_2]\, dxdy. \end{aligned} \tag{3.2.56}$$

The third term is zero from a similar argument to that shown for (3.2.52), and the first term becomes

$$\begin{aligned}&\oint_{\partial\Omega} \frac{\delta F}{\delta q_2}\frac{\delta G}{\delta q_2} \mathbf{n} \cdot [\hat{e}_3 \times \nabla q_2]\, dS = \\ &\qquad - \int_0^L \left[\frac{\delta F}{\delta q_2}\frac{\delta G}{\delta q_2}(-q_{2y})\right]_{x=-\lambda} dy + \int_{-\lambda}^{\lambda} [g_L(q_2) q_{2x}]_{y=L}\, dx \\ &\qquad + \int_0^L \left[\frac{\delta F}{\delta q_2}\frac{\delta G}{\delta q_2}(-q_{2y})\right]_{x=\lambda} dy - \int_{-\lambda}^{\lambda} [g_0(q_2) q_{2x}]_{y=0}\, dx \\ &\quad = \quad 0, \end{aligned} \tag{3.2.57}$$

where $g_{0,L}(q_2)$ is defined to be

$$g_{0,L}(q_2) = \left[\frac{\delta F}{\delta q_2}\frac{\delta G}{\delta q_2}\right]_{y=0,L}. \tag{3.2.58}$$

The first and third terms in equation (3.2.57) sum to zero due to the periodic boundary conditions in $x$, and the second and fourth terms are zero individually because $q_{2x} = h_x = 0$ on $y = 0, L$.

We are left with the second terms on the right hand side of (3.2.50) and

(3.2.56), which gives

$$\begin{aligned}[F,G] &= \iint_\Omega \frac{\delta G}{\delta q_1} \nabla \cdot \left[ \frac{\delta F}{\delta q_1} \hat{e}_3 \times \nabla (q_1 - y) \right] dxdy \\ &\quad - \iint_\Omega \frac{\delta G}{\delta q_2} \nabla \cdot \left[ \frac{\delta F}{\delta q_2} \hat{e}_3 \times \nabla q_2 \right] dxdy \\ &= -[G,F]. \end{aligned} \tag{3.2.59}$$

We see immediately that (3.2.59) implies that the Poisson bracket must self-commute, that is, since $[F,F] = -[F,F]$ by skew-symmetry, we must have that $[F,F] = 0$ for an arbitrary allowable functional $F$. Also, the above proof implies that *each* term in (3.2.47) is individually skew-symmetric, which will be a useful result in later derivations.

We now prove the distributive property for the Poisson bracket. For any constants $\alpha$ and $\beta$, we have

$$\begin{aligned}[\alpha F + \beta G, Q] &= -\iint_\Omega \frac{\delta(\alpha F + \beta G)}{\delta q_1} J\left(q_1 - y, \frac{\delta Q}{\delta q_1}\right) dxdy \\ &\quad + \iint_\Omega \frac{\delta(\alpha F + \beta G)}{\delta q_2} J\left(q_2, \frac{\delta Q}{\delta q_2}\right) dxdy \\ &= -\alpha \iint_\Omega \frac{\delta F}{\delta q_1} J\left(q_1 - y, \frac{\delta Q}{\delta q_1}\right) dxdy + \alpha \iint_\Omega \frac{\delta F}{\delta q_2} J\left(q_2, \frac{\delta Q}{\delta q_2}\right) dxdy \\ &\quad - \beta \iint_\Omega \frac{\delta G}{\delta q_1} J\left(q_1 - y, \frac{\delta Q}{\delta q_1}\right) dxdy + \beta \iint_\Omega \frac{\delta G}{\delta q_2} J\left(q_2, \frac{\delta Q}{\delta q_2}\right) dxdy \\ &= \alpha[F,Q] + \beta[G,Q]. \end{aligned} \tag{3.2.60}$$

The associative property of the Poisson bracket is proved as follows

$$
\begin{aligned}
[FG,Q] =& -\iint_\Omega \frac{\delta(FG)}{\delta q_1} J\left(q_1 - y, \frac{\delta Q}{\delta q_1}\right) dxdy + \iint_\Omega \frac{\delta(FG)}{\delta q_2} J\left(q_2, \frac{\delta Q}{\delta q_2}\right) dxdy \\
=& -\iint_\Omega \left(G\frac{\delta F}{\delta q_1} + F\frac{\delta G}{\delta q_1}\right) J\left(q_1 - y, \frac{\delta Q}{\delta q_1}\right) dxdy \\
&+ \iint_\Omega \left(G\frac{\delta F}{\delta q_2} + F\frac{\delta G}{\delta q_2}\right) J\left(q_2, \frac{\delta Q}{\delta q_2}\right) dxdy \\
=& -F\left\{\iint_\Omega \frac{\delta G}{\delta q_1} J\left(q_1 - y, \frac{\delta Q}{\delta q_1}\right) dxdy - \iint_\Omega \frac{\delta G}{\delta q_2} J\left(q_2, \frac{\delta Q}{\delta q_2}\right) dxdy\right\} \\
&- G\left\{\iint_\Omega \frac{\delta F}{\delta q_1} J\left(q_1 - y, \frac{\delta Q}{\delta q_1}\right) dxdy - \iint_\Omega \frac{\delta G}{\delta q_2} J\left(q_2, \frac{\delta Q}{\delta q_2}\right) dxdy\right\} \\
=& F[G,Q] + [F,Q]G,
\end{aligned}
\tag{3.2.61}
$$

where the functionals $F$ and $G$ may be pulled outside the integrals because they are independent of the spatial integration (i.e., dependent on time only).

Finally we must show that the Poisson bracket satisfies the Jacobi identity. Before we proceed, note that if any one of the allowable functionals $F, G,$ or $Q$ in (3.2.16) is a Casimir (i.e., the first requirement for allowable functionals), the Jacobi identity is trivially satisfied, since the Poisson bracket of a Casimir with any functional is zero. We therefore assume that the allowable functionals all meet the second requirement (3.2.37). We have (the following proof is based on the one

given by Scinocca and Shepherd, 1992)

$$
\begin{aligned}
[F,[G,Q]]+[G,[Q,F]]+[Q,[F,G]] &= -[[G,Q],F]-[[Q,F],G]-[[F,G],Q] \\
&= -\left\langle \frac{\delta}{\delta q_1}\left\{\left\langle \frac{\delta G}{\delta q_1}, M_1\frac{\delta Q}{\delta q_1}\right\rangle + \left\langle \frac{\delta G}{\delta q_2}, M_2\frac{\delta Q}{\delta q_2}\right\rangle\right\}, M_1\frac{\delta F}{\delta q_1}\right\rangle \\
&\quad -\left\langle \frac{\delta}{\delta q_2}\left\{\left\langle \frac{\delta G}{\delta q_1}, M_1\frac{\delta Q}{\delta q_1}\right\rangle + \left\langle \frac{\delta G}{\delta q_2}, M_2\frac{\delta Q}{\delta q_2}\right\rangle\right\}, M_2\frac{\delta F}{\delta q_2}\right\rangle \\
&\quad -\left\langle \frac{\delta}{\delta q_1}\left\{\left\langle \frac{\delta Q}{\delta q_1}, M_1\frac{\delta F}{\delta q_1}\right\rangle + \left\langle \frac{\delta Q}{\delta q_2}, M_2\frac{\delta F}{\delta q_2}\right\rangle\right\}, M_1\frac{\delta G}{\delta q_1}\right\rangle \\
&\quad -\left\langle \frac{\delta}{\delta q_2}\left\{\left\langle \frac{\delta Q}{\delta q_1}, M_1\frac{\delta F}{\delta q_1}\right\rangle + \left\langle \frac{\delta Q}{\delta q_2}, M_2\frac{\delta F}{\delta q_2}\right\rangle\right\}, M_2\frac{\delta G}{\delta q_2}\right\rangle \\
&\quad -\left\langle \frac{\delta}{\delta q_1}\left\{\left\langle \frac{\delta F}{\delta q_1}, M_1\frac{\delta G}{\delta q_1}\right\rangle + \left\langle \frac{\delta F}{\delta q_2}, M_2\frac{\delta G}{\delta q_2}\right\rangle\right\}, M_1\frac{\delta Q}{\delta q_1}\right\rangle \\
&\quad -\left\langle \frac{\delta}{\delta q_2}\left\{\left\langle \frac{\delta F}{\delta q_1}, M_1\frac{\delta G}{\delta q_1}\right\rangle + \left\langle \frac{\delta F}{\delta q_2}, M_2\frac{\delta G}{\delta q_2}\right\rangle\right\}, M_2\frac{\delta Q}{\delta q_2}\right\rangle .
\end{aligned}
\tag{3.2.62}
$$

The first step in this procedure is to calculate the variational derivatives inside the outer Poisson bracket, which are quantities of the form

$$
\frac{\delta}{\delta q_i}\left\langle \frac{\delta G}{\delta q_1}, M_1\frac{\delta Q}{\delta q_1}\right\rangle , \tag{3.2.63}
$$

where we have taken as an example the first and second lines in (3.2.62). To calculate this variational derivative, we first integrate the Poisson bracket in (3.2.63) by parts as follows

$$
\begin{aligned}
\left\langle \frac{\delta G}{\delta q_1}, M_1\frac{\delta Q}{\delta q_1}\right\rangle &= -\iint_\Omega \frac{\delta G}{\delta q_1} J\left(q_1-y, \frac{\delta Q}{\delta q_1}\right) dxdy \\
&= +\iint_\Omega \frac{\delta G}{\delta q_1}\nabla\cdot\left[(q_1-y)\hat{e}_3\times\nabla\left(\frac{\delta Q}{\delta q_1}\right)\right] dxdy \\
&= \iint_\Omega \nabla\cdot\left[\frac{\delta G}{\delta q_1}(q_1-y)\hat{e}_3\times\nabla\left(\frac{\delta Q}{\delta q_1}\right)\right] dxdy \\
&\quad -\iint_\Omega (q_1-y)\left[\hat{e}_3\times\nabla\left(\frac{\delta Q}{\delta q_1}\right)\right]\cdot\nabla\left(\frac{\delta G}{\delta q_1}\right) dxdy.
\end{aligned}
\tag{3.2.64}
$$

We proceed by applying the divergence theorem to the first term on the right hand side in (3.2.64), and by using the vector identity (3.2.49) to rewrite the second term, so that

$$\begin{aligned}\left\langle \frac{\delta G}{\delta q_1}, M_1 \frac{\delta Q}{\delta q_1} \right\rangle &= \oint_{\partial\Omega} \frac{\delta G}{\delta q_1}(q_1 - y)\mathbf{n} \cdot \left[\hat{e}_3 \times \nabla \left(\frac{\delta Q}{\delta q_1}\right)\right] dS \\ &\quad - \iint_{\Omega} (q_1 - y)\nabla \cdot \left[\frac{\delta G}{\delta q_1}\hat{e}_3 \times \nabla \left(\frac{\delta Q}{\delta q_1}\right)\right] dxdy \\ &\quad + \iint_{\Omega} (q_1 - y)\frac{\delta G}{\delta q_1}\nabla \cdot \left[\hat{e}_3 \times \nabla \left(\frac{\delta Q}{\delta q_1}\right)\right] dxdy \\ &= \oint_{\partial\Omega} \frac{\delta G}{\delta q_1}(q_1 - y)\mathbf{n} \cdot \left[\hat{e}_3 \times \nabla \left(\frac{\delta Q}{\delta q_1}\right)\right] dS \\ &\quad + \iint_{\Omega} (q_1 - y) J\left(\frac{\delta G}{\delta q_1}, \frac{\delta Q}{\delta q_1}\right) dxdy, \end{aligned} \tag{3.2.65}$$

where the integral on the third last line of (3.2.65) is zero because of (3.2.52), and where we have used the identity (3.2.24). The boundary integral in (3.2.65) is evaluated as follows

$$\begin{aligned}\oint_{\partial\Omega} \frac{\delta G}{\delta q_1}(q_1 - y)\mathbf{n} \cdot \left[\hat{e}_3 \times \nabla \left(\frac{\delta Q}{\delta q_1}\right)\right] dS &= -\int_0^L \left[\frac{\delta G}{\delta q_1}(q_1 - y)\left(-\frac{\delta Q}{\delta q_1}\right)_y\right]_{x=-\lambda} dy \\ &\quad + \int_{-\lambda}^{\lambda} \left[\frac{\delta G}{\delta q_1}(q_1 - y)\left(\frac{\delta Q}{\delta q_1}\right)_x\right]_{y=L} dx + \int_0^L \left[\frac{\delta G}{\delta q_1}(q_1 - y)\left(-\frac{\delta Q}{\delta q_1}\right)_y\right]_{x=\lambda} dy \\ &\quad - \int_{-\lambda}^{\lambda} \left[\frac{\delta G}{\delta q_1}(q_1 - y)\left(\frac{\delta Q}{\delta q_1}\right)_x\right]_{y=0} dx \\ &= 0, \end{aligned} \tag{3.2.66}$$

since the first and third terms in (3.2.66) sum to zero by the periodicity boundary condition. The second and fourth terms are zero because $[(\delta Q/\delta q_i)_x]_{y=0,L} = 0$ by the definition of allowable functionals. Therefore the boundary integral in

(3.2.65) contributes nothing. Thus we have found that

$$\left\langle \frac{\delta G}{\delta q_1}, M_1 \frac{\delta Q}{\delta q_1} \right\rangle = \left\langle q_1 - y, J\left(\frac{\delta G}{\delta q_1}, \frac{\delta Q}{\delta q_1}\right) \right\rangle. \tag{3.2.67}$$

To proceed, we take the variational derivative of (3.2.67) to obtain

$$\begin{aligned}
&\delta \left\langle q_1 - y, J\left(\frac{\delta G}{\delta q_1}, \frac{\delta Q}{\delta q_1}\right) \right\rangle = \\
&= \iint_\Omega J\left(\frac{\delta G}{\delta q_1}, \frac{\delta Q}{\delta q_1}\right) \delta q_1 \, dxdy + \iint_\Omega (q_1 - y) J\left(\frac{\delta^2 G}{\delta q_1^2}\delta q_1, \frac{\delta Q}{\delta q_1}\right) dxdy \\
&+ \iint_\Omega (q_1 - y) J\left(\frac{\delta G}{\delta q_1}, \frac{\delta^2 Q}{\delta q_1^2}\delta q_1\right) dxdy + \iint_\Omega (q_1 - y) J\left(\frac{\delta^2 G}{\delta q_1 \delta q_2}\delta q_2, \frac{\delta Q}{\delta q_1}\right) dxdy \\
&+ \iint_\Omega (q_1 - y) J\left(\frac{\delta G}{\delta q_1}, \frac{\delta^2 Q}{\delta q_1 \delta q_2}\delta q_2\right) dxdy.
\end{aligned} \tag{3.2.68}$$

Now we evaluate the second integral in (3.2.68) to obtain

$$\begin{aligned}
&\iint_\Omega (q_1 - y) J\left(\frac{\delta^2 G}{\delta q_1^2}\delta q_1, \frac{\delta Q}{\delta q_1}\right) dxdy \\
&= -\iint_\Omega (q_1 - y) \nabla \cdot \left[\frac{\delta^2 G}{\delta q_1^2}\delta q_1 \hat{e}_3 \times \nabla\left(\frac{\delta Q}{\delta q_1}\right)\right] dxdy \\
&= -\iint_\Omega \nabla \cdot \left[(q_1 - y)\frac{\delta^2 G}{\delta q_1^2}\delta q_1 \hat{e}_3 \times \nabla\left(\frac{\delta Q}{\delta q_1}\right)\right] dxdy \\
&\quad + \iint_\Omega \left[\frac{\delta^2 G}{\delta q_1^2}\delta q_1 \hat{e}_3 \times \left(\frac{\delta Q}{\delta q_1}\right) \cdot \nabla(q_1 - y)\right] dxdy \\
&= -\oint_{\partial\Omega} (q_1 - y)\frac{\delta^2 G}{\delta q_1^2}\delta q_1 \mathbf{n} \cdot \left[\hat{e}_3 \times \nabla\left(\frac{\delta Q}{\delta q_1}\right)\right] dS \\
&\quad + \iint_\Omega \frac{\delta^2 G}{\delta q_1^2}\delta q_1 \nabla \cdot \left[(q_1 - y)\hat{e}_3 \times \nabla\left(\frac{\delta Q}{\delta q_1}\right)\right] dxdy \\
&\quad - \iint_\Omega \frac{\delta^2 G}{\delta q_1^2}\delta q_1 (q_1 - y) \nabla \cdot \left[\hat{e}_3 \times \nabla\left(\frac{\delta Q}{\delta q_1}\right)\right] dxdy \\
&= -\iint_\Omega \frac{\delta^2 G}{\delta q_1^2}\delta q_1 J\left(q_1 - y, \frac{\delta Q}{\delta q_1}\right) dxdy,
\end{aligned} \tag{3.2.69}$$

where we have integrated by parts in exactly an analogous manner as was done in

(3.2.66). The boundary integral in (3.2.69) contributes nothing, because

$$\begin{aligned}\oint_{\partial\Omega}(q_1-y)\frac{\delta^2 G}{\delta q_1^2}\delta q_1\,\mathbf{n}\cdot\left[\hat{e}_3\times\nabla\left(\frac{\delta Q}{\delta q_1}\right)\right]dS = \\ -\int_0^L\left[(q_1-y)\frac{\delta^2 G}{\delta q_1^2}\delta q_1\left(-\frac{\delta Q}{\delta q_1}\right)_y\right]_{x=-\lambda}dy \\ +\int_{-\lambda}^{\lambda}\left[(q_1-y)\frac{\delta^2 G}{\delta q_1^2}\delta q_1\left(\frac{\delta Q}{\delta q_1}\right)_x\right]_{y=L}dx \\ +\int_0^L\left[(q_1-y)\frac{\delta^2 G}{\delta q_1^2}\delta q_1\left(-\frac{\delta Q}{\delta q_1}\right)_y\right]_{x=\lambda}dy \\ -\int_{-\lambda}^{\lambda}\left[(q_1-y)\frac{\delta^2 G}{\delta q_1^2}\delta q_1\left(\frac{\delta Q}{\delta q_1}\right)_x\right]_{y=0}dx \\ =0. \qquad (3.2.70)\end{aligned}$$

The first and third terms of (3.2.70) are zero by the periodicity boundary conditions, and the second and fourth terms are zero because of (3.2.43).

The last three integrals in (3.2.68) are evaluated in the same fashion as was the integral in (3.2.69), which means we may write (3.2.68) as

$$\begin{aligned}&\delta\left\langle q_1-y, J\left(\frac{\delta G}{\delta q_1},\frac{\delta Q}{\delta q_1}\right)\right\rangle \\ &=\iint_\Omega\Big[\left\{-\frac{\delta^2 G}{\delta q_1^2}J\left(q_1-y,\frac{\delta Q}{\delta q_1}\right)+J\left(\frac{\delta G}{\delta q_1},\frac{\delta Q}{\delta q_1}\right)+\frac{\delta^2 Q}{\delta q_1^2}J\left(q_1-y,\frac{\delta G}{\delta q_1}\right)\right\}\delta q_1 \\ &+\left\{-\frac{\delta^2 G}{\delta q_1\delta q_2}J\left(q_1-y,\frac{\delta Q}{\delta q_1}\right)+\frac{\delta^2 Q}{\delta q_1\delta q_2}J\left(q_1-y,\frac{\delta G}{\delta q_1}\right)\right\}\delta q_2\Big]\,dxdy. \qquad (3.2.71)\end{aligned}$$

We now introduce a shortform notation to simplify the lengthy derivations which will follow. Subscripts 1 and 2 appended to the allowable functionals $F, G$, and $Q$ will denote variational differentiation with respect to $q_1$ and $q_2$, respectively. As an example

$$G_{12}=\frac{\delta^2 G}{\delta q_1\delta q_2}. \qquad (3.2.72)$$

Using this notation, it follows from (3.2.63), (3.2.67) and (3.2.68) that (using inner product notation)

$$\frac{\delta}{\delta q_1}\langle G_1, M_1 Q_1\rangle = G_{11} M_1 Q_1 + J(G_1, Q_1) - Q_{11} M_1 G_1,$$
$$\frac{\delta}{\delta q_2}\langle G_1, M_1 Q_1\rangle = G_{12} M_1 Q_1 - Q_{12} M_1 G_1. \tag{3.2.73}$$

We may generalize this result by stating that

$$\frac{\delta}{\delta q_j}\langle G_i, M_i Q_i\rangle = G_{ij} M_i Q_i + J(G_i, Q_i)\delta_{ij} - Q_{ij} M_i G_i, \tag{3.2.74}$$

where $i = j = 1, 2$, $\delta_{ij}$ is the Kroneker delta and no summation is implied. We may now write (3.2.62) as

$$[F,[G,Q]] + [G,[Q,F]] + [Q,[F,G]] =$$
$$-\{\langle G_{11} M_1 Q_1, M_1 F_1\rangle + \langle J(G_1, Q_1), M_1 F_1\rangle - \langle Q_{11} M_1 G_1, M_1 F_1\rangle\}$$
$$-\{\langle G_{21} M_2 Q_2, M_1 F_1\rangle - \langle Q_{21} M_2 G_2, M_1 F_1\rangle\}$$
$$-\{\langle G_{22} M_2 Q_2, M_2 F_2\rangle + \langle J(G_2, Q_2), M_2 F_2\rangle - \langle Q_{22} M_2 G_2, M_2 F_2\rangle\}$$
$$-\{\langle G_{12} M_1 Q_1, M_2 F_2\rangle - \langle Q_{12} M_1 G_1, M_2 F_2\rangle\}$$
$$-\{\langle Q_{11} M_1 F_1, M_1 G_1\rangle + \langle J(Q_1, F_1), M_1 G_1\rangle - \langle F_{11} M_1 Q_1, M_1 G_1\rangle\}$$
$$-\{\langle Q_{21} M_2 F_2, M_1 G_1\rangle - \langle F_{21} M_2 Q_2, M_1 G_1\rangle\}$$
$$-\{\langle Q_{22} M_2 F_2, M_2 G_2\rangle + \langle J(Q_2, F_2), M_2 G_2\rangle - \langle F_{22} M_2 Q_2, M_2 G_2\rangle\}$$
$$-\{\langle Q_{12} M_1 F_1, M_2 G_2\rangle - \langle F_{12} M_1 Q_1, M_2 G_2\rangle\}$$
$$-\{\langle F_{11} M_1 G_1, M_1 Q_1\rangle + \langle J(F_1, G_1), M_1 Q_1\rangle - \langle G_{11} M_1 F_1, M_1 Q_1\rangle\}$$
$$-\{\langle F_{21} M_2 G_2, M_1 Q_1\rangle - \langle G_{21} M_2 F_2, M_1 Q_1\rangle\}$$
$$-\{\langle F_{22} M_2 G_2, M_2 Q_2\rangle + \langle J(F_2, G_2), M_2 Q_2\rangle - \langle G_{22} M_2 F_2, M_2 Q_2\rangle\}$$

$$-\{\langle F_{12}M_1G_1, M_2Q_2\rangle - \langle G_{12}M_1F_1, M_2Q_2\rangle\} \tag{3.2.75}$$

Using the fact that for the inner product we may write $\langle A, BC\rangle = \langle AB, C\rangle$ for arbitrary scalars $A, B,$ and $C,$ and that (McIntyre and Shepherd, 1987)

$$\frac{\delta^2 R}{\delta q_i \delta q_j} = \frac{\delta^2 R}{\delta q_j \delta q_i}, \tag{3.2.76}$$

for any arbitrary functional $R,$ we see that all the terms in (3.2.75) sum to zero except for

$$\begin{aligned}[F,[G,Q]] + [G,[Q,F]] + [Q,[F,G]] = \\ - \langle J(G_1,Q_1), M_1F_1\rangle - \langle J(G_2,Q_2), M_2F_2\rangle - \langle J(Q_1,F_1), M_1G_1\rangle \\ - \langle J(Q_2,F_2), M_2G_2\rangle - \langle J(F_1,G_1), M_1Q_1\rangle - \langle J(F_2,G_2), M_2Q_2\rangle .\end{aligned} \tag{3.2.77}$$

The Jacobian terms may be rewritten as (taking the first term in (3.2.77) as an example)

$$\begin{aligned}\langle J(G_1,Q_1), M_1F_1\rangle &= -\langle J(G_1,Q_1), J(q_1 - y, F_1)\rangle \\ &= \iint_\Omega J(G_1,Q_1)\nabla\cdot[(q_1-y)\hat{e}_3 \times \nabla F_1]\,dxdy \\ &= \iint_\Omega \nabla\cdot[J(G_1,Q_1)(q_1-y)\hat{e}_3 \times \nabla F_1]\,dxdy \\ &\quad - \iint_\Omega [(q_1-y)\hat{e}_3 \times \nabla F_1]\cdot\nabla(J(G_1,Q_1))\,dxdy \\ &= \oint_{\partial\Omega} (q_1-y)J(G_1,Q_1)\mathbf{n}\cdot[\hat{e}_3 \times \nabla F_1]\,dS \\ &\quad - \iint_\Omega (q_1-y)[\hat{e}_3 \times \nabla F_1\cdot\nabla(J(G_1,Q_1))]\,dxdy \\ &= -\iint_\Omega (q_1-y)\nabla\cdot[J(G_1,Q_1)\hat{e}_3 \times \nabla F_1]\,dxdy \\ &\quad + \iint_\Omega (q_1-y)J(G_1,Q_1)\nabla\cdot[\hat{e}_3 \times \nabla F_1]\,dxdy\end{aligned}$$

$$= \iint_{\Omega} (q_1 - y) J(J(G_1, Q_1), F_1)\, dxdy. \tag{3.2.78}$$

The boundary integral contributes nothing by virtue of

$$\begin{aligned}
&\oint_{\partial\Omega} (q_1 - y) J(G_1, Q_1) \mathbf{n} \cdot [\hat{e}_3 \times \nabla F_1]\, dS = \\
&\quad - \int_0^L [(q_1 - y) J(G_1, Q_1)(-F_{1y})]_{x=-\lambda}\, dy \\
&\quad + \int_{-\lambda}^{\lambda} [(q_1 - y) J(G_1, Q_1)(F_{1x})]_{y=L}\, dx \\
&\quad + \int_0^L [(q_1 - y) J(G_1, Q_1)(-F_{1y})]_{x=\lambda}\, dy \\
&\quad - \int_{-\lambda}^{\lambda} [(q_1 - y) J(G_1, Q_1)(F_{1x})]_{y=0}\, dx \\
&\quad = 0,
\end{aligned} \tag{3.2.79}$$

where the first and third integrals sum to zero by the periodicity boundary condition, and the second and fourth integrals are each zero because $F_1 =$ constant on $y = 0, L$, and so $F_{1x} = 0$ there (see (3.2.40)).

The other Jacobian terms in (3.2.77) evaluate the same way, and when they are added to (3.2.78), we get

$$\begin{aligned}
&[F,[G,Q]] + [G,[Q,F]] + [Q,[F,G]] \\
&= \iint_{\Omega} (q_1 - y)\{J(J(G_1, Q_1), F_1) + J(J(F_1, G_1), Q_1) + J(J(Q_1, F_1), G_1)\}\, dxdy \\
&\quad - \iint_{\Omega} q_2\{J(J(G_2, Q_2), F_2) + J(J(F_2, G_2), Q_2) + J(J(Q_2, F_2), G_2)\}\, dxdy.
\end{aligned} \tag{3.2.80}$$

To complete the proof, we use the Jacobi identity for Jacobians, which states that for arbitrary scalars $A, B,$ and $C,$ the following holds

$$J(J(A,B),C) + J(J(C,A),B) + J(J(B,C),A) = 0. \tag{3.2.81}$$

This identity may easily be proved by writing (3.2.81) in component form. We see that this immediately allows us to state that

$$[F,[G,Q]]+[G,[Q,F]]+[Q,[F,G]]=0, \tag{3.2.82}$$

so that we have proven the Jacobi identity holds for the Poisson brackets associated with the $\mathbf{M}$ matrix.

Therefore (3.2.8)-(3.2.11) is a hamiltonian formulation of the problem. It should be noted that with the skew symmetry property of the Poisson bracket, the invariance of the hamiltonian with respect to time may be proved in a much more succinct manner than was done in Subsection 3.2.1. We have (Shepherd, 1990)

$$\frac{dH}{dt}=\left\langle \frac{\delta H}{\delta \mathbf{q}},\mathbf{q}_t\right\rangle=\left\langle \frac{\delta H}{\delta \mathbf{q}},\mathbf{M}\frac{\delta H}{\delta \mathbf{q}}\right\rangle=0, \tag{3.2.83}$$

by skew symmetry (self-commutation).

The five algebraic properties (3.2.12)-(3.2.16), which we have proved above, in particular skew symmetry and the Jacobi identity, are essential to the proper formulation of the hamiltonian structure. From (3.2.83), we see that skew symmetry guarantees the invariance of the hamiltonian with respect to time, if the governing equations can be cast in the hamiltonian form (3.2.8)-(3.2.11). The Jacobi identity is the *closure condition* which must be met on an associated symplectic formulation if the $\mathbf{M}$ matrix has explicit dependence on $\mathbf{q}$ (Olver, 1982). This requirement (as well as skew symmetry), originally derives from connections this method has with Lie algebras, and has much in common with, for example, quantum mechanical Poisson brackets (McIntyre and Shepherd, 1987).

It is possible, in many cases, to find alternative "hamiltonian" formulations

which meet all requirements except the Jacobi identity. This could lead to serious deficiencies in the resulting analysis, however. Benjamin (1984) gives an example of just such a case, and it was found that the Casimirs were incorrectly determined by the formulation (Shepherd, 1990).

*3.3 The Casimirs*

There are two kinds of invariants associated with hamiltonian dynamics. One type relates to the hamiltonian's own symmetry properties, and if these symmetries are continuous (such as translations in space or time), then connections between these symmetries and conservation laws are given by Noether's theorem (Shepherd, (1990)).

The other type of invariant are called the Casimirs, which are functionals $C(\mathbf{q})$ that satisfy the requirement

$$[F, C] = \left\langle \frac{\delta F}{\delta \mathbf{q}}, \mathbf{M} \frac{\delta C}{\delta \mathbf{q}} \right\rangle = \mathbf{0}, \tag{3.3.1}$$

for any arbitrary functional $F(\mathbf{q})$. If (3.3.1) holds, then we must have

$$\mathbf{M} \frac{\delta C}{\delta \mathbf{q}} = \mathbf{0}, \tag{3.3.2}$$

since $F(\mathbf{q})$ is arbitrary. Note that the Casimirs will not be trivial if the matrix $\mathbf{M}$ is not invertible. Equation (3.3.2) may be rewritten as follows

$$\begin{bmatrix} -J(q_1 - y, \cdot) & 0 \\ 0 & J(q_2, \cdot) \end{bmatrix} \begin{bmatrix} \delta C/\delta q_1 \\ \delta C/\delta q_2 \end{bmatrix} = \mathbf{0}, \tag{3.3.3}$$

which leads to the equations

$$J(q_1 - y, \delta C/\delta q_1) = 0, \tag{3.3.4}$$

$$J(q_2, \delta C/\delta q_2) = 0. \tag{3.3.5}$$

We are able to integrate (3.3.4) and (3.3.5) by taking advantage of a property of the Jacobian. Suppose we have

$$J(A, B) = 0, \tag{3.3.6}$$

for arbitrary scalars $A$ and $B$. Then we may write

$$A = \Phi(B), \tag{3.3.7}$$

or

$$B = \Psi(A) = \Phi^{-1}(A), \tag{3.3.8}$$

for arbitrary functions $\Phi$ and $\Psi$. We prove this by rewriting (3.3.6) in another form, which is

$$J(A, B) = \hat{e}_3 \cdot [\nabla A \times \nabla B] = 0, \tag{3.3.9}$$

which may easily be verified by writing the right hand side of (3.3.9) in component form. Since the normal vectors to the surfaces $A$ and $B$ are given by $\frac{\nabla A}{|\nabla A|}$ and $\frac{\nabla B}{|\nabla B|}$, respectively, these vectors must coincide everywhere, since the cross-product $\nabla A \times \nabla B$ is zero. This implies that the two surfaces must have the same slope at every point $(x, y)$ (but not necessarily the same value) which allows us to write $A$ as a function of $B$ or vice versa.

Using the above property of the Jacobian, we may integrate the equations (3.3.4) and (3.3.5) once to find

$$\frac{\delta C}{\delta q_1} = \Phi_1'(q_1 - y) = \frac{d\Phi_1(q_1 - y)}{d(q_1 - y)}, \tag{3.3.10}$$

$$\frac{\delta C}{\delta q_2} = \Phi_2'(q_2) = \frac{d\Phi_2(q_2)}{d(q_2)}, \tag{3.3.11}$$

where $\Phi_1'$ and $\Phi_2'$ are arbitrary functions.

From this we may construct $C(\mathbf{q})$ as

$$\begin{aligned} C(\mathbf{q}) &= \iint_\Omega \{\Phi_1(q_1 - y) + \Phi_2(q_2)\}\, dxdy, \\ &= \iint_\Omega \{\Phi_1(\Delta\eta + h - y) + \Phi_2(h)\} dxdy. \end{aligned} \tag{3.3.12}$$

We call the functions $\Phi_1$ and $\Phi_2$ the Casimir densities.

*3.4 Variational Principle for Steady Solutions*

Our treatment will closely follow Swaters (1993). Steady solutions of the governing equations have no dependence on time, and so they may be written in the form

$$\mathbf{M}\frac{\delta H}{\delta \mathbf{q}} = \mathbf{0}. \tag{3.4.1}$$

We have calculated the first variation of $H$ in the previous subsection, and found there that (see equation (3.2.30))

$$\frac{\delta H}{\delta q_1} = -\eta; \qquad \frac{\delta H}{\delta q_2} = h + \eta - y. \tag{3.4.2}$$

We denote a general steady solution of the governing equations by $\eta = \eta_0(x, y)$ and $h = h_0(x, y)$. We note that we will still assume that $\eta_0(x, y = 0, L) = 0$.

It is possible to generalize the boundary conditions, but it would involve including additional circulation integrals in the hamiltonian which are not relevant in the analysis described here.

Using this solution and equations (3.4.1) and (3.4.2) we write the Hamiltonian formulation for the steady solution as

$$\begin{bmatrix} -J(\Delta\eta_0 + h_0 - y, \cdot) & 0 \\ 0 & J(h_0, \cdot) \end{bmatrix} \begin{bmatrix} -\eta_0 \\ h_0 + \eta_0 - y \end{bmatrix} = \mathbf{0}, \tag{3.4.3}$$

or

$$J(\Delta\eta_0 + h_0 - y, \eta_0) = 0, \tag{3.4.4}$$

$$J(h_0, h_0 + \eta_0 - y) = 0. \tag{3.4.5}$$

We now integrate (3.4.4) and (3.4.5) once, using the property of the Jacobian as set out after (3.3.5), to obtain

$$\eta_0 = F_1(\Delta\eta_0 + h_0 - y), \tag{3.4.6}$$

$$\eta_0 - y = F_2(h_0), \tag{3.4.7}$$

where $F_1$ and $F_2$ are arbitrary functions, and where we have used the fact that $J(h_0, h_0) = 0$ to arrive at (3.4.7).

In finite dimensional, canonical, non-dissipative systems, it is easy to see that the hamiltonian is extremized by a steady solution, since (Goldstein, 1980; Shepherd, 1990)

$$\mathbf{q}_t = 0 = \mathbf{M}\frac{\partial H}{\partial \mathbf{q}} \Longrightarrow \frac{\partial H}{\partial \mathbf{q}} = \mathbf{0}, \tag{3.4.8}$$

since $\mathbf{M}$ is invertible in such cases. However, this property does not necessarily hold in the infinite dimensional case. For example, in our case, if $\delta\mathcal{H}(\eta_0, h_0) = 0$, then from (3.4.2) we have $\eta_0 = 0$ and $h_0 = y$ which, as will be seen, does not represent all possible steady solutions. This means that we cannot use the hamiltonian alone as a functional for a variational principle describing arbitrary steady solutions.

However, it is possible to find a functional which does behave in this fashion by making use of the Casimir functional determined earlier. Consider the following *constrained* hamiltonian

$$\mathcal{H} = H + C, \tag{3.4.9}$$

which, when written out, is

$$\mathcal{H}(\eta, h) = \frac{1}{2}\int\int_{\Omega}\{\nabla\eta\cdot\nabla\eta + [(h-y)^2 - y^2] + 2\Phi_1 + 2\Phi_2\}dxdy. \tag{3.4.10}$$

We take the first variation of $\mathcal{H}$, so that

$$\begin{aligned}
\delta\mathcal{H}(\eta, h) &= \int\int_{\Omega}\{\nabla\eta\cdot\nabla\delta\eta + (h-y)\delta h + \Phi_1'\delta q_1 + \Phi_2'\delta q_2\}dxdy \\
&= \oint_{\partial\Omega}\eta(\mathbf{n}\cdot\nabla\delta\eta)\,dS + \int\int_{\Omega}\{-\eta\Delta\delta\eta + (h-y)\delta h + \Phi_1'\delta q_1 + \Phi_2'\delta q_2\}dxdy \\
&= \int\int_{\Omega}\{-\eta(\Delta\delta\eta + \delta h) + (h - y + \eta)\delta h + \Phi_1'\delta q_1 + \Phi_2'\delta q_2\}dxdy \\
&= \int\int_{\Omega}\{(\Phi_1' - \eta)\delta q_1 + (\Phi_2' + h + \eta - y)\delta q_2\}dxdy,
\end{aligned} \tag{3.4.11}$$

where the boundary integral in (3.4.11) contributes nothing because

$$\oint_{\partial\Omega} \eta(\mathbf{n}\cdot\nabla\delta\eta)\,dS = -\int_0^L [\eta\delta\eta_x]_{x=-\lambda}\,dy + \int_{-\lambda}^{\lambda} [\eta\delta\eta_y]_{y=L}\,dx + \int_0^L [\eta\delta\eta_x]_{x=\lambda}\,dy - \int_{-\lambda}^{\lambda} [\eta\delta\eta_y]_{y=0}\,dx = 0. \tag{3.4.12}$$

The first and third integrals on the right hand side of (3.4.12) sum to zero because of the periodicity boundary condition, and the second and fourth terms are zero because $\eta = 0$ on $y = 0, L$.

It is easy to see that the steady solutions will lead to $\delta\mathcal{H}(\eta_0, h_0) = 0$, (i.e., the first order necessary conditions for extremizing $\mathcal{H}$) if

$$\Phi'_{10} - \eta_0 = 0, \tag{3.4.13}$$

$$\Phi'_{20} + h_0 + \eta_0 - y = 0, \tag{3.4.14}$$

where $\Phi'_{10}$ and $\Phi'_{20}$ represent $\Phi'_1$ and $\Phi'_2$ evaluated at the steady solution. We may develop expressions for $\Phi_1$ and $\Phi_2$ in terms of $F_1$ and $F_2$ which encompass (3.4.6), (3.4.7), (3.4.13) and (3.4.14) if we simply set

$$\begin{aligned} \Phi'_1(q_1 - y) &= F_1(q_1 - y), \\ \Phi'_2(q_2) &= -F_2(q_2) - h = -F_2 - q_2, \end{aligned} \tag{3.4.15}$$

which become, after integrating

$$\Phi_1(q_1 - y) = \int_{-y}^{q_1 - y} F_1(\xi)d\xi, \tag{3.4.16}$$

$$\Phi_2(q_2) = -\int_0^{q_2} F_2(\xi)d\xi - \frac{1}{2}(q_2)^2. \tag{3.4.17}$$

In order to see if the steady solution is stable or unstable to small perturbations, we first, in an analogous manner to what would be done in finite dimensional canonical systems, find the second variation of the constrained hamiltonian. If the second variation evaluated at the steady solution is definite, then we have proved that the system is *formally* stable as defined by Holm *et al.* (1985). Formal stability does not necessarily imply nonlinear stability in the sense of Liapunov, however, as it would in the finite dimensional case.

To prove linear stability in the sense of Liapunov, we must show that for every $\epsilon > 0$ there exists a $\delta > 0$ such that (Drazin and Reid, 1981)

$$||\delta \mathbf{q}|| < \delta \quad \text{at} \quad t = 0 \Longrightarrow ||\delta \mathbf{q}|| < \epsilon \quad \text{for all} \quad t \tag{3.4.18}$$

where $\delta \mathbf{q}$ is a small perturbation, and $\epsilon$ and $\delta$ are arbitrary small numbers.

In order to prove this, we must first *choose* a norm which serves as a measure of the size of the perturbations, because in infinite dimensional vector spaces, norms are not necessarily equivalent. The next step is to find criteria which bound the second variation of the constrained hamiltonian evaluated at the steady solution with respect to this disturbance norm. If the system meets these criteria, it is then possible to prove that we have stability in the sense of Liapunov.

We proceed by taking the second variation of the constrained hamiltonian. The first variation is

$$\delta \mathcal{H}(\eta, h) = \int\int_{\Omega} \{\nabla \eta \cdot \nabla \delta \eta + \delta h(h - y) + \Phi_1' \delta q_1 + \Phi_2' \delta q_2\} dx dy. \tag{3.4.19}$$

which means that the second variation is

$$\begin{aligned}\delta^2\mathcal{H}(\eta,h) &= \iint_\Omega \{\nabla\delta\eta\cdot\nabla\delta\eta + \nabla\eta\cdot\nabla\delta^2\eta + \delta^2 h(h-y) + (\delta h)^2 \\ &\quad + \Phi_1''(\delta q_1)^2 + \Phi_2''(\delta q_2)^2 + \Phi_1'\delta^2 q_1 + \Phi_2'\delta^2 q_2\}dxdy \\ &= \oint_{\partial\Omega} \eta(\mathbf{n}\cdot\nabla\delta^2\eta)\,dS \\ &\quad + \iint_\Omega \{\nabla\delta\eta\cdot\nabla\delta\eta - \eta\Delta\delta^2\eta + \delta^2 h(h-y) + \eta\delta^2 h - \eta\delta^2 h + (\delta h)^2 \\ &\quad + \Phi_1''(\Delta\delta\eta+\delta h)^2 + \Phi_2''(\delta h)^2 + \Phi_1'\delta^2 q_1 + \Phi_2'\delta^2 q_2\}dxdy,\end{aligned} \tag{3.4.20}$$

where Green's first identity has been used. The boundary integral is evaluated as

$$\begin{aligned}\oint_{\partial\Omega} \eta(\mathbf{n}\cdot\nabla\delta^2\eta)\,dS &= -\int_0^L [\eta(\delta^2\eta)_x]_{x=-\lambda}\,dy + \int_{-\lambda}^{\lambda}[\eta(\delta^2\eta)_y]_{y=L}\,dx \\ &\quad + \int_0^L [\eta(\delta^2\eta)_x]_{x=\lambda}\,dy - \int_{-\lambda}^{\lambda}[\eta(\delta^2\eta)_y]_{y=0}\,dx, \\ &= 0,\end{aligned} \tag{3.4.21}$$

where the first and third integrals sum to zero due to the periodicity boundary conditions on $\eta$ and the perturbation $\delta\eta$. The second and fourth terms are zero because $\eta = 0$ on $y = 0, L$.

We are left with

$$\begin{aligned}\delta^2\mathcal{H}(\eta,h) &= \iint_\Omega \{\nabla\delta\eta\cdot\nabla\delta\eta + \Phi_1''(\Delta\delta\eta+\delta h)^2 + (\Phi_2''+1)(\delta h)^2\}dxdy \\ &\quad + \iint_\Omega \{(\Phi_1'-\eta)(\Delta\delta^2\eta+\delta^2 h) + (\Phi_2'+h+\eta-y)\delta^2 h\}dxdy.\end{aligned} \tag{3.4.22}$$

But for steady solutions, the second integral is zero by using (3.4.13) and (3.4.14), and therefore we have

$$\delta^2\mathcal{H}(\eta_0,h_0) = \iint_\Omega \{\nabla\delta\eta\cdot\nabla\delta\eta + \Phi_{10}''(\Delta\delta\eta+\delta h)^2 + (\Phi_{20}''+1)(\delta h)^2\}dxdy. \tag{3.4.23}$$

We may substitute for $\Phi''_{10}$ and $\Phi''_{20}$ into (3.4.23) directly by differentiating equations (3.4.15) and by using the steady solution (see equation (2.4.12), setting $U_0 = 0$) whose stability characteristics will be studied throughout this thesis. This solution is given by

$$\begin{aligned} \eta_0(x,y) &= 0, \\ h_0(x,y) &= 1 - \gamma y, \end{aligned} \tag{3.4.24}$$

where $\gamma$ is a real constant. This steady state corresponds to a calm upper layer with the gravity current having a linearly decreasing thickness in the cross-channel direction. We may now solve for $F_1$ and $F_2$ using the above solution along with equations (3.4.6) and (3.4.7) to find

$$\begin{aligned} F_1(q_{10} - y) &= 0, \\ F_2(q_{20}) &= -y. \end{aligned} \tag{3.4.25}$$

We may recast $F_2$ in terms of $h_0$ by using equation (3.4.24). This gives

$$F_2(q_{20}) = F_2(h_0) = \frac{h_0 - 1}{\gamma}. \tag{3.4.26}$$

We now obtain $\Phi''_{10}$ and $\Phi''_{20}$ by differentiating $F_1$ and $F_2$ once with respect to $q_1 - y$ and $q_2$, respectively, and utilizing equations (3.4.15). This gives

$$\begin{aligned} \Phi''_{10} &= 0, \\ \Phi''_{20} &= -\frac{1}{\gamma} - 1. \end{aligned} \tag{3.4.27}$$

Substituting this into equation (3.4.23) gives

$$\delta^2\mathcal{H}(\eta_0, h_0) = \iint_\Omega \{\nabla\delta\eta \cdot \nabla\delta\eta - (\delta h)^2/\gamma\} dxdy. \tag{3.4.28}$$

Before we discuss this equation in the context of linear stability, we must first show that $\delta^2\mathcal{H}(\eta_0, h_0)$ is invariant in time with respect to small perturbations. This is needed to ensure that if the constrained hamiltonian is definite at some time, say $t = 0$, then it is definite for all time $t$. We define these perturbations as follows

$$\begin{aligned} \eta &= \eta_0 + \delta\eta = \delta\eta, \\ h &= h_0 + \delta h = 1 - \gamma y + \delta h, \end{aligned} \tag{3.4.29}$$

where the steady solutions (3.4.24) have been substituted, and where $\delta\eta$ and $\delta h$ represent the perturbations. We now insert (3.4.29) into the governing equations (2.4.8) and (2.4.9) to obtain the linear stability equations

$$\begin{aligned} \Delta\delta\eta_t - \delta\eta_x - \delta h_x &= 0, \\ \delta h_t + \delta h_x - \gamma\delta\eta_x &= 0, \end{aligned} \tag{3.4.30}$$

where we have excluded all terms which are quadratic in the perturbations.

We now take the derivative of the second variation of the constrained hamil-

tonian (3.4.28) with respect to time, which gives

$$\begin{aligned}\frac{\partial(\delta^2\mathcal{H})}{\partial t}(\eta_0,h_0) &= \iint_\Omega \{2\nabla\delta\eta\cdot\nabla\delta\eta_t-(2\delta h\delta h_t)/\gamma\}dxdy\\ &= \oint_{\partial\Omega} 2\delta\eta(\mathbf{n}\cdot\nabla\delta\eta_t)\,dS-\iint_\Omega\{2\delta\eta\Delta\delta\eta_t+(2\delta h\delta h_t)/\gamma\}dxdy\\ &= -\iint_\Omega\{2\delta\eta(\delta\eta_x+\delta h_x)+2\delta h(\gamma\delta\eta_x-\delta h_x)/\gamma\}dxdy\\ &= -\iint_\Omega\{[(\delta\eta)^2]_x+2\delta\eta\delta h_x+2\delta h\delta\eta_x-2[(\delta h)^2]_x/\gamma\}dxdy,\end{aligned} \tag{3.4.31}$$

where we have substituted the linear stability equations (3.4.30) for $\Delta\delta\eta_t$ and $\delta h_t$. The boundary integral is zero because

$$\begin{aligned}\oint_{\partial\Omega} 2\delta\eta(\mathbf{n}\cdot\nabla\delta\eta_t)\,dS &= -\int_0^L 2[\delta\eta\delta\eta_{tx}]_{x=-\lambda}\,dy+\int_{-\lambda}^{\lambda}2[\delta\eta\delta\eta_{ty}]_{y=L}\,dx\\ &\quad+\int_0^L 2[\delta\eta\delta\eta_{tx}]_{x=\lambda}\,dy-\int_{-\lambda}^{\lambda}2[\delta\eta\delta\eta_{ty}]_{y=L}\,dx\\ &=0,\end{aligned} \tag{3.4.32}$$

where the first and third terms in (3.4.32) sum to zero because of the periodicity boundary conditions, and the second and fourth terms are zero because $\delta\eta = 0$ on $y=0,L$. The first and fourth terms of (3.4.31) vanish upon integration by $x$ and another application of the boundary conditions for the perturbations. We are left with

$$-2\iint_\Omega(\delta\eta\delta h)_x\,dxdy=0. \tag{3.4.33}$$

This proves that $\delta^2\mathcal{H}(\eta_0,h_0)$ is invariant in time with respect to the linear stability equations.

If it can be shown that there exist criteria such that the second variation of the constrained hamiltonian is either positive or negative definite with respect

to all small perturbations, then it is possible to prove that the system is linearly stable in the sense of Liapunov when these criteria are met (Shepherd, 1990). We see immediately that, if $\gamma > 0$, we cannot guarantee the definiteness of $\delta^2\mathcal{H}(\eta_0, h_0)$ because both $\nabla\delta\eta \cdot \nabla\delta\eta$ and $(\delta h)^2$ in the integrand of (3.4.28) are always positive, but one is subtracted from the other. Therefore the steady state solution $(\eta_0, h_0) = (0, 1-\gamma y), \gamma > 0$, is not necessarily linearly stable in the sense of Liapunov with respect to the perturbation norm $||\delta\mathbf{q}|| = [\delta^2\mathcal{H}(\eta_0, h_0)]^{\frac{1}{2}}$ (the norm would be $||\delta\mathbf{q}|| = [-\delta^2\mathcal{H}(\eta_0, h_0)]^{\frac{1}{2}}$ if $\delta^2\mathcal{H}$ was negative definite - see Section 3.5 for a more detailed discussion of disturbance norms). This implies that there exists the possibility of linear instability in our model. In practice, such a result almost always means that instability is present, but there is no way to prove this fact.

If $\gamma < 0$, however, we see that the integrand of (3.4.28) is always positive definite, which means that for this case, the steady solution is linearly stable in the sense of Liapunov. This implies that if the gravity current depth *increases* in the positive $y$ direction, we have linear stability, but if it *decreases*, there exists the possibility of linear instability (note that the case $\gamma = 0$, which is not dealt with here or in the next section, is a special situation - see Chapter 6).

We now proceed to the nonlinear extension of this approach in order to develop convexity estimates for nonlinear stability. These estimates will be used to determine if there exists the possibility of nonlinear instability in our model.

### *3.5 Nonlinear Stability*

The definiteness of the second variation of the constrained hamiltonian for a system of partial differential equations does not ensure nonlinear stability as it would in a canonical finite dimensional case because the infinite dimensional phase

space is not compact, and as a result there are mathematical difficulties associated with convergence which do not otherwise arise (Ebin and Marsden, 1970). In order to derive criteria for nonlinear stability, we start by defining a new functional $\mathcal{L}$, equivalent to $\mathcal{H}(\mathbf{q}+\mathbf{q}_0)-\mathcal{H}(\mathbf{q}_0)$, so that

$$\mathcal{L}(\mathbf{q}) = H(\mathbf{q}+\mathbf{q}_0) - H(\mathbf{q}_0) + C(\mathbf{q}+\mathbf{q}_0) - C(\mathbf{q}_0), \tag{3.5.1}$$

where $H$ and $C$ are as defined in (3.2.8) and (3.3.12) respectively, $\Phi_1$ and $\Phi_2$ are defined by (3.4.16) and (3.4.17) respectively, $\mathbf{q}_0$ is the steady solution, and $\mathbf{q}$ represents a finite amplitude, time dependent adjustment to the steady state. It is important to note that $\mathcal{L}(\mathbf{q})$ is an invariant of the full nonlinear equations (3.2.1). We may rewrite (3.5.1) as

$$\begin{aligned}
\mathcal{L}(\mathbf{q}) = {} & \frac{1}{2}\int\!\!\int_\Omega \{\nabla(\eta+\eta_0)\cdot\nabla(\eta+\eta_0) + (h+h_0-y)^2 - y^2\}dxdy \\
& - \frac{1}{2}\int\!\!\int_\Omega \{\nabla\eta_0\cdot\nabla\eta_0 + (h_0-y)^2 - y^2\}dxdy \\
& + \int\!\!\int_\Omega \left(\int_{-y}^{q_1+q_{10}-y} F_1(\xi)d\xi\right)dxdy \\
& - \int\!\!\int_\Omega \left\{\left(\int_0^{q_2+q_{20}} F_2(\xi)d\xi\right) + \frac{1}{2}(q_2+q_{20})^2\right\}dxdy \\
& - \int\!\!\int_\Omega \left(\int_{-y}^{q_{10}-y} F_1(\xi)d\xi\right)dxdy + \int\!\!\int_\Omega \left\{\left(\int_0^{q_{20}} F_2(\xi)d\xi\right) + \frac{1}{2}q_{20}^2\right\}dxdy.
\end{aligned} \tag{3.5.2}$$

This may be rewritten as

$$\begin{aligned}
\mathcal{L}(\mathbf{q}) = {} & \frac{1}{2}\int\!\!\int_\Omega \{\nabla\eta\cdot\nabla\eta + 2\nabla\eta_0\cdot\nabla\eta + h^2 + 2hh_0 - 2hy\}dxdy \\
& + \int\!\!\int_\Omega \left(\int_{q_{10}-y}^{q_{10}+q_1-y} F_1(\xi)d\xi\right)dxdy \\
& - \int\!\!\int_\Omega \left\{\left(\int_{q_{20}}^{q_{20}+q_2} F_2(\xi)d\xi\right)dxdy + \frac{1}{2}q_2^2 + q_2q_{20}\right\}dxdy.
\end{aligned} \tag{3.5.3}$$

We now utilize (3.4.25) and the fact that $\eta_0 = 0$ and $q_2 = h$ to rewrite (3.5.3) as

$$\mathcal{L}(\mathbf{q}) = \frac{1}{2}\iint_\Omega \{\nabla\eta\cdot\nabla\eta + 2hF_2(h_0)\}dxdy + \iint_\Omega \left(\int_{q_{10}-y}^{q_{10}+q_1-y} F_1(\xi)d\xi\right)dxdy - \iint_\Omega \left(\int_{q_{20}}^{q_{20}+q_2} F_2(\xi)d\xi\right)dxdy, \tag{3.5.4}$$

which, upon rearranging, gives

$$\mathcal{L}(\mathbf{q}) = \frac{1}{2}\iint_\Omega \nabla\eta\cdot\nabla\eta\,dxdy + \iint_\Omega \left(\int_{q_{10}}^{q_{10}+q_1} F_1(\xi)d\xi\right)dxdy - \iint_\Omega \left[\left\{\int_{q_{20}}^{q_{20}+q_2} F_2(\xi)d\xi\right\} - F_2(h_0)h\right]dxdy. \tag{3.5.5}$$

Suppose that $F_1(\xi)$ and $F_2(\xi)$ satisfy the following inequalities

$$\alpha_1 < F_1'(\xi) < \beta_1, \tag{3.5.6}$$

$$\alpha_2 < F_2'(\xi) < \beta_2, \tag{3.5.7}$$

for all arguments $\xi$, where the primed superscript represents $d/d\xi$, and where $\alpha_1$, $\alpha_2$, $\beta_1$, and $\beta_2$ are real constants. Then, if these equations are integrated twice, we have criteria which may be used to develop bounds on the functional $\mathcal{L}(\mathbf{q})$. We integrate (3.5.6) as an example. The first integration gives

$$\int_{q_{10}-y}^{q_{10}+q_1-y} \alpha_1 d\xi < \int_{q_{10}-y}^{q_{10}+q_1-y} F_1'(\xi)d\xi < \int_{q_{10}-y}^{q_{10}+q_1-y} \beta_1 d\xi, \tag{3.5.8}$$

which gives

$$\alpha_1 q_1 < F_1(q_{10}+q_1-y) - F_1(q_{10}-y) < \beta_1 q_1. \tag{3.5.9}$$

We then integrate (3.5.9) with respect to $q_1$ as follows

$$\alpha_1 \int_0^{q_1} q_1^* dq_1^* < \int_0^{q_1} F_1(q_{10} + q_1^*) dq_1^* < \beta_1 \int_0^{q_1} q_1^* dq_1^*, \tag{3.5.10}$$

where we have used the fact that $F_1(q_{10} - y) = 0$, and where $q_1^*$ represents a dummy integration variable. Inequality (3.5.10) may be rewritten as

$$\frac{1}{2}\alpha_1 q_1^2 < \int_{q_{10}-y}^{q_1+q_{10}-y} F_1(\xi) d\xi < \frac{1}{2}\beta_1 q_1^2. \tag{3.5.11}$$

We may also integrate (3.5.7) in exactly the same way to obtain

$$\frac{1}{2}\alpha_2 h^2 < \int_{q_{20}}^{q_{20}+q_2} F_2(\xi) d\xi - F_2(h_0)h < \frac{1}{2}\beta_2 h^2. \tag{3.5.12}$$

By selecting the appropriate segments of the inequalities (3.5.11) and (3.5.12) and substituting these into (3.5.5), we may develop the following inequality for $\mathcal{L}(\mathbf{q})$. If we replace the second term in (3.5.5) with the term on the left hand side of the inequality (3.5.11), and the third term in (3.5.5) with the term on the right hand side of the inequality (3.5.12), then the result must be less than $\mathcal{L}(\mathbf{q})$. We may write

$$\mathcal{L}(\mathbf{q}) > \frac{1}{2} \iint_\Omega \{\nabla\eta \cdot \nabla\eta + \alpha_1(\Delta\eta + h)^2 - \beta_2 h^2\} \, dxdy. \tag{3.5.13}$$

Similarily, if we replace the second and third terms in (3.5.5) with the reverse of what was done to develop (3.5.13), we have constructed a term which must be greater than $\mathcal{L}(\mathbf{q})$, viz.

$$\frac{1}{2} \iint_\Omega \{\nabla\eta \cdot \nabla\eta + \beta_1(\Delta\eta + h)^2 - \alpha_2 h^2\} \, dxdy > \mathcal{L}(\mathbf{q}). \tag{3.5.14}$$

If we put (3.5.13) and (3.5.14) together, the result is the following estimate for $\mathcal{L}(\mathbf{q})$

$$\frac{1}{2}\iint_{\Omega}\{\nabla\eta\cdot\nabla\eta+\alpha_1(\Delta\eta+h)^2-\beta_2 h^2\}dxdy<\mathcal{L}(\mathbf{q})$$
$$<\frac{1}{2}\iint_{\Omega}\{\nabla\eta\cdot\nabla\eta+\beta_1(\Delta\eta+h)^2-\alpha_2 h^2\}dxdy. \tag{3.5.15}$$

Now it is possible to develop criteria so that $\mathcal{L}(\mathbf{q})$ is positive definite. Since $\nabla\eta\cdot\nabla\eta$ is always positive (unless there is no disturbance at all), if

$$0\le\alpha_1<F_1'(\xi)<\beta_1<\infty, \tag{3.5.16}$$

$$-\infty<\alpha_2<F_2'(\xi)<\beta_2\le 0, \tag{3.5.17}$$

then the left hand side of (3.5.15) must always be positive, which guarantees the positive definiteness of $\mathcal{L}$.

The next step in this process is to select a norm which will be the measure of the disturbance, and to find bounds for it such that we have criteria for stability in the sense of Liapunov.

We have already indicated that norms are not identical in infinite dimensional space, which means there exists the possibility that the system could be nonlinearly stable with respect to one norm, but not necessarily so with respect to another (Shepherd, 1990). This suggests that some thought should go into the selection of the disturbance norm.

First, there are some basic requirements which the norm must meet, which derive from abstract functional analysis. The norm must be a *metric* on the space in question, which means that a) it must be positive for any non-zero vector $\mathbf{q}$ in the function space, b) it must satisfy the triangle inequality, i.e., $||\mathbf{q}_1+\mathbf{q}_2||\le$

$||\mathbf{q}_1|| + ||\mathbf{q}_2||$, and c) it must behave in such a way that $||c\mathbf{q}|| = |c|\,||\mathbf{q}||$ for any constant $c$ (McIntyre and Shepherd, 1987).

Second, the norm should make some physical sense, i.e., it should represent quantities which have an impact on a growing perturbation. For example, it seems reasonable to assume that disturbance growth should be related to disturbance energy, which makes the latter a possible norm.

In our case, because in (3.5.16) and (3.5.17) $\alpha_1$ and $\beta_2$ are not bounded away from zero, it turns out that we will require *two* norms to find bounds on the disturbance (the reason for this will be discussed later). The norms we choose are

$$||\mathbf{q}||_I^2 = \frac{1}{2}\int\int_\Omega \nabla\eta\cdot\nabla\eta\,dxdy, \tag{3.5.18}$$

and

$$||\mathbf{q}||_{II}^2 = \frac{1}{2}\int\int_\Omega \{\nabla\eta\cdot\nabla\eta + (\Delta\eta)^2 + h^2\}\,dxdy, \tag{3.5.19}$$

where $||\mathbf{q}||_I$ is simply the disturbance kinetic energy, and $||\mathbf{q}||_{II}$ is $||\mathbf{q}||_I$ plus the disturbance enstrophy (the square of the relative vorticity in the upper layer) and the square of the disturbance potential energy as a result of deflections in the gravity current thickness.

We now redefine slightly the notion of nonlinear stability in the sense of Liapunov, which in general takes the same form as (3.4.18) with $\delta\mathbf{q}$ replaced by $\mathbf{q}$, to take into account the two norms (see, e.g., Benjamin, 1972). We say that the steady solution $(\eta_0, h_0)$ is nonlinearly stable in the sense of Liapunov if for every $\epsilon > 0$, there exists a $\delta > 0$, such that

$$||\mathbf{q}||_{II} < \delta \quad \text{at} \quad t = 0 \Longrightarrow ||\mathbf{q}||_I < \epsilon \quad \text{for all} \quad t \geq 0. \tag{3.5.20}$$

We now proceed to find bounds on the norms. We have

$$\begin{aligned} ||\mathbf{q}||_I^2 &= \frac{1}{2}\iint_\Omega \nabla\eta\cdot\nabla\eta\,dxdy \\ &\leq \frac{1}{2}\iint_\Omega \{\nabla\eta\cdot\nabla\eta+\alpha_1(\Delta\eta+h)^2-\beta_2 h^2\}\,dxdy \\ &< \mathcal{L}(\mathbf{q})=\mathcal{L}(\tilde{\mathbf{q}}), \end{aligned} \tag{3.5.21}$$

where $\tilde{\mathbf{q}}=\mathbf{q}_{t=0}$, and we are using the invariance of $\mathcal{L}(\mathbf{q})$. Notice that we could not have developed the inequality (3.5.21) if we had used the norm $||\mathbf{q}||_{II}$, because quantities proportional to $\alpha_1/\inf(\alpha_1)$ and $\beta_2/\max(\beta_2)$ would be needed. The problem here is that $\inf(\alpha_1)$ and $\max(\beta_2)$ (the infimum of $\alpha_1$ and maximum of $\beta_2$), are zero (from (3.5.16) and (3.5.17)), thus making quantities in which it is part of the divisor undefined.

Continuing, we have

$$\begin{aligned} \mathcal{L}(\tilde{\mathbf{q}}) &< \frac{1}{2}\{\nabla\tilde{\eta}\cdot\nabla\tilde{\eta}+\beta_1(\Delta\tilde{\eta}+\tilde{h})^2-\alpha_2\tilde{h}^2\}\,dxdy \\ &\leq \frac{1}{2}\iint_\Omega \{\nabla\tilde{\eta}\cdot\nabla\tilde{\eta}+2\beta_1[(\Delta\tilde{\eta})^2+\tilde{h}^2]-\alpha_2\tilde{h}^2\}\,dxdy \\ &= \frac{1}{2}\iint_\Omega \{\nabla\tilde{\eta}\cdot\nabla\tilde{\eta}+2\beta_1(\Delta\tilde{\eta})^2-(\alpha_2-2\beta_1)\tilde{h}^2\}\,dxdy \\ &\leq \frac{\Gamma}{2}\iint_\Omega \{\nabla\tilde{\eta}\cdot\nabla\tilde{\eta}+(\Delta\tilde{\eta})^2+\tilde{h}^2\}\,dxdy \\ &= \frac{\Gamma}{2}||\tilde{\mathbf{q}}||_{II}^2, \end{aligned} \tag{3.5.22}$$

where $\Gamma=\max(1,2\beta_1,2\beta_1-\alpha_2)>0$, and where $[\tilde{\eta},\tilde{h}]=[\eta,h]_{t=0}$. So we have

$$||\mathbf{q}||_I < \left(\frac{\Gamma}{2}\right)^{\frac{1}{2}}||\tilde{\mathbf{q}}||_{II}, \tag{3.5.23}$$

for all time (Swaters, 1993). We see that for every $\epsilon<0$, if $||\tilde{\mathbf{q}}||_{II}<\epsilon(\Gamma/2)^{-\frac{1}{2}}$, then $||\mathbf{q}||_I<\epsilon$, and so if $\mathcal{L}(\mathbf{q})$ is positive definite, we have bounds on the

disturbance norms $||\mathbf{q}||_I$ and $||\mathbf{q}||_{II}$ such that the system is stable in the sense of Liapunov.

To examine our model for nonlinear stability, we review the criteria (3.5.16) and (3.5.17). We see that, if $\gamma > 0$, $F_2'(\xi) = 1/\gamma > 0$ if $\xi = h_0 = 1 - \gamma y$ (see equation (3.4.26)), and thus criteria (3.5.17) cannot be met for all arguments $\xi$. Therefore $\mathcal{L}(\mathbf{q})$ is not positive definite, and so if we can show that it is also not negative definite for $\gamma > 0$, then there exists the possibility of nonlinear instability. It turns out that in this case, the procedure and the results are exactly as set out in Swaters (1993), and so only the convexity estimates derived there will be presented. They are

$$-\infty < \alpha_1 < F_1'(\xi) < \beta_1 < -\tilde{C} < 0, \tag{3.5.24}$$

$$\tilde{C}\phi < \alpha_2 < F_2'(\xi) < \beta_2 < \infty, \tag{3.5.25}$$

where $\phi = \beta_1/(\tilde{C} + \beta_1)$ and $\tilde{C} > 0$ is a constant, which is obtained by the introduction of a Poincare inequality in the analysis. Swaters went on to find bounds on a disturbance norm, but, for our purposes, it is sufficient to point out that $F_1'(\xi) = 0$ when $\xi = q_{10} - y$ (see equation (3.4.25). Therefore, the inequality (3.5.24) is not met, and we have shown that there exists the possibility of nonlinear instability if $\gamma > 0$.

If $\gamma < 0$, we have, from (3.4.25), that $F_1(q_{10} - y) = 0$, and substituting in the steady solution (3.4.24), that $F_1(1-(1+\gamma)y) = 0$. We see that *any* value of $\gamma$ or $y$ sets $F_1$ to zero, and so it is not unreasonable to conclude that $F_1(\xi) = 0$ for all arguments $\xi$. We may then state that $F_1'(\xi) = 0$, which means that inequality (3.5.16) is satisfied.

We now rewrite (3.4.26), replacing $h_0$ with the arbitrary argument $\xi$,

so that

$$F_2(\xi) = \frac{\xi - 1}{\gamma}. \tag{3.5.26}$$

This means that $F_2'(\xi) = 1/\gamma$, which is always negative for $\gamma < 0$, and so inequality (3.5.17) is satisfied. We may therefore state that if $\gamma < 0$, then $\mathcal{L}(\mathbf{q})$ is positive definite, and so the steady solution is nonlinearly stable in the sense of Liapunov.

In summary, we cannot show that $\mathcal{L}(\mathbf{q})$ is either positive or negative definite if $\gamma > 0$, and so there exists the possibility of nonlinear instability in the sense of Liapunov in this case, but if $\gamma < 0$, then we have nonlinear stability. We therefore now turn to methods which will allow us to derive evolution equations, for the possibly unstable case $\gamma > 0$, which model the amplitude of an initial perturbation on the steady solution as it evolves in time, so that we may see the actual form of the instability, if it exists.

# Chapter 4

## The Linear Stability Problem

### *4.1 The Linear Stability Equations*

The first step in the process of examining the weakly nonlinear stability characteristics of steady solutions in our model is to perform a linear stability analysis. We do this because there is certain information essential to the weakly nonlinear work which is generated from the linear analysis, namely the marginal stability curve, whose meaning will be discussed at length in a later section.

Linear stability analysis is a procedure in which a small perturbation is applied to a steady solution of the governing equations in order to see if such disturbances will grow with time, indicating instability, or remain constant, oscillate, or recede, indicating stability of the steady solution to such perturbations. From a physical context, we are really determining if the steady solution exists, because it will never be seen in nature (or even in a laboratory setting) if it is susceptible to small perturbations since it is not possible to completely eliminate imperfections which give rise to small deviations from the steady solution (Drazin and Reid, 1981).

The work is carried out by adding a small perturbation to the steady solution to be studied, and substituting this into the governing equations. The key assumption in this analysis is that the perturbations are small, which allows us to ignore terms which are quadratic in the perturbations (which essentially means dropping the nonlinear terms). The result of applying this procedure is the linear stability equations, the solution of which dictates the form of the disturbances and provides a dispersion relation between the phase speed of the wave disturbance and the wavenumbers of the modes.

It is important to point out that if there is instability in linear stability analysis, the growing disturbance will always reach a size where the linear stability equations are no longer valid, because at that point the small perturbation assumption is violated. One then needs to appeal to nonlinear theories in order to follow the evolution in time of the disturbance, because the nonlinear terms can no longer be ignored.

In Swaters (1991), a comprehensive linear stability analysis was performed for a coupled density front on a semi-infinite sloping continental shelf with only one boundary. In this chapter, we apply this work to our model and derive the marginal stability curve for the subsequent nonlinear analysis.

In order to derive the stability equations, we introduce

$$h = h_0(y) + h'(x, y, t), \tag{4.1.1a}$$

$$\eta = \eta_0(y) + \eta'(x, y, t), \tag{4.1.1b}$$

where $\eta_0(y)$ and $h_0(y)$ are the steady solutions, and $\eta'$ and $h'$ are the perturbation quantities. We then substitute (4.1.1) into (2.4.8) and (2.4.9) using (2.4.12) to get (after dropping the primes)

$$[\partial_t + \mu U_0(y)\partial_x]\Delta\eta - (1 + \mu U_{0_{yy}})\eta_x - h_x + \mu J(\eta, \Delta\eta) = 0, \tag{4.1.2}$$

$$[\partial_t + (\mu U_0(y) + 1)\partial_x]h + \mu h_{0_y}\eta_x + \mu J(\eta, h) = 0. \tag{4.1.3}$$

These are the *nonlinear* perturbation equations, and they will be used in the weakly nonlinear analyses presented in the next two chapters. For our purposes here, we drop the Jacobian terms, which are quadratic in the perturbations, to

arrive at the equations

$$[\partial_t + \mu U_0(y)\partial_x]\Delta\eta - (1 + \mu U_{0_{yy}})\eta_x - h_x = 0, \tag{4.1.4}$$

$$[\partial_t + (\mu U_0(y) + 1)\partial_x]h + \mu h_{0_y}\eta_x = 0. \tag{4.1.5}$$

In this chapter, we assume that the steady solution for the gravity current takes the form, as we did in Chapter 3, of a simple wedge described by

$$h_0(y) = 1 - \gamma y. \tag{4.1.6}$$

Here $\gamma$ is the cross-channel rate of change of the thickness of the gravity current relative to the sloping bottom. The dimensional rate of change is given by $\gamma^* = (h^*/L^*)\gamma$.

We also concentrate on the "pure" baroclinic problem by setting the mean flow $U_0 = 0$. This approximation filters out any possible *barotropic* instability in the upper layer (Swaters, 1991). Applying (4.1.6) and the baroclinic approximation to (4.1.4) and (4.1.5) leads to

$$\Delta\eta_t - \eta_x - h_x = 0, \tag{4.1.7}$$

$$h_t + h_x - \mu\gamma\eta_x = 0. \tag{4.1.8}$$

These equations are the linear stability equations for our model (note that if we let $\mu = 1$, these equations are identical in form to equations (3.4.30)).

*4.2 Energetics*

It is possible to derive necessary conditions for linear instability from an energy form of the perturbation equations. We multiply equation (4.1.7) by $\eta$,

equation (4.1.8) by $h$, and then add the result (after dividing (4.1.8) by $\mu\gamma$) to obtain (after simplifying)

$$\eta\Delta\eta_t - \frac{1}{2}(\eta^2)_x + \frac{1}{2}\frac{[(h^2)_x + (h^2)_t]}{\mu\gamma} - (\eta h)_x = 0. \tag{4.2.1}$$

We now average this equation over one along-channel wavelength by applying the operator

$$\langle * \rangle = \frac{1}{2\lambda}\int_{-\lambda}^{\lambda}(*)\,dx, \tag{4.2.2}$$

and we integrate over $0 \le y \le L$ to obtain

$$\frac{1}{2\lambda}\iint_{\Omega}\eta\Delta\eta_t\,dxdy + \frac{1}{2\lambda}\iint_{\Omega}\frac{(h^2)_t}{2\mu\gamma}\,dxdy = 0, \tag{4.2.3}$$

where we have utilized the domain $\Omega$ as defined in (3.2.2). The second, third, and fifth terms on the left hand side of (4.2.1) are zero after carrying out an $x-$integration and applying the periodicity boundary conditions.

We now apply Green's first identity to rewrite the first term in (4.2.3), which gives

$$\frac{1}{2\lambda}\left\{\oint_{\partial\Omega}\eta(\mathbf{n}\cdot\nabla\eta_t)\,dS - \iint_{\Omega}\nabla\eta\cdot\nabla\eta_t\,dxdy + \iint_{\Omega}\frac{(h^2)_t}{2\mu\gamma}\,dxdy\right\} = 0, \tag{4.2.4}$$

which leaves after applying the averaging operator notation (4.2.2) and rearranging

$$\frac{\partial}{\partial t}\int_0^L\left\{\langle\nabla\eta\cdot\nabla\eta\rangle - \frac{\langle h^2\rangle}{2\mu\gamma}\right\}dy = 0. \tag{4.2.5}$$

The boundary integral in (4.2.4) contributes nothing because

$$\begin{aligned}\oint_{\partial\Omega} \eta(\mathbf{n}\cdot\nabla\eta_t)\,dS &= -\int_0^L [\eta\eta_{tx}]_{x=-\lambda}\,dy + \int_{-\lambda}^{\lambda} [\eta\eta_{ty}]_{y=L}\,dx \\ &\quad + \int_0^L [\eta\eta_{tx}]_{x=\lambda}\,dy - \int_{-\lambda}^{\lambda} [\eta\eta_{ty}]_{y=0}\,dx \\ &= 0, \end{aligned} \tag{4.2.6}$$

where the first and third integrals sum to zero by the periodicity boundary conditions on $\eta$ and its derivatives, and the second and fourth integrals are zero because $\eta = 0$ on $y = 0, L$.

If we integrate (4.2.5) with respect to time, we find that

$$\int_0^L \left\{ \langle \nabla\eta\cdot\nabla\eta\rangle - \frac{\langle h^2\rangle}{2\mu\gamma} \right\} dy = \text{constant}. \tag{4.2.7}$$

From (4.2.7), we see that if $\gamma > 0$ (note that $\mu > 0$ - see Chapter 2), then it is possible that the perturbation kinetic energy could grow large and the equality still be maintained, because the second term on the left hand side is negative. However, if $\gamma < 0$, then (4.2.7) is positive definite for all perturbation quantities $\eta$ and $h$, which implies stability. Therefore, from (4.2.7) we see that a necessary condition for instability is $\gamma > 0$, and $\gamma < 0$ is sufficient for stability. In physical terms, this means that if the rate of change of thickness of the gravity current is negative (i.e., the gravity current becomes thinner in the positive $y-$direction), then we have met a necessary (but not sufficient) condition for instability (note that these results agree with what was found in Section 3.4).

*4.3 Normal Mode Analysis*

In order for a system to be considered stable to small disturbances, it must be stable to all possible arbitrary perturbations (Chandrasekhar, 1961). To see

why this is so, suppose a system is stable when perturbed by all, except one, arbitrary disturbances. Then it is likely that at some time, as a result of natural imperfections in the system, that this perturbation will be realized, and instability is the inevitable result (Drazin and Reid, 1981).

From the discussion above, it is obvious that care must be taken to make sure that a method is used in the linear stability analysis which allows for the testing of all possible disturbances. The most widely applied procedure which meets this requirement is the method of *normal modes*. The basic idea behind this approach is to recognize that it is possible to represent arbitrary functions with Fourier series and transforms in space, and Laplace transforms in time (Drazin and Reid, 1981). If we can find a complete set of basis functions for solutions to the linear stability equations, then if the system is stable to each individual mode represented in the basis functions, it is stable to all arbitrary perturbations because each disturbance is nothing more than a particular superposition of these modes (Chandrasekhar, 1961).

It was mentioned in Chapter 3 that stability in the sense of Liapunov hinged on whether a disturbance grows in time to a finite size, or remains bounded by the size of the initial perturbation. In the normal mode analysis, the time component will be represented by the basis function of the complex Laplace transform, i.e., $\exp(-ikct)$ , where $c = c_R + ic_I$ is a complex phase speed with $c_R$ and $c_I$ representing the real and imaginary parts, respectively. We see that if $c_I > 0$, then the mode will grow exponentially in time until it is a finite size, and therefore may be termed unstable.

With the above discussion in mind, we now introduce along-front normal

mode instabilities of the form

$$[\eta, h] = [\tilde{\eta}(y), \tilde{h}(y)]\exp[ik(x - ct)] + \text{c.c}, \tag{4.3.1}$$

where c.c means the complex conjugate, $k$ is the real-valued along-channel wavenumber, and $c$ is the along-channel complex wave speed. Substituting (4.3.1) into (4.1.7) and (4.1.8) gives (after dropping the tildes)

$$c(\eta_{yy} - k^2\eta) + [1 - \mu\gamma(c-1)^{-1}]\eta = 0, \tag{4.3.2}$$

$$h = -\mu\gamma(c-1)^{-1}\eta, \tag{4.3.3}$$

where we take $\gamma > 0$ here, and from now on. We may rewrite these equations as

$$\eta_{yy} - \left\{k^2 - \frac{1}{c} + \frac{\mu\gamma}{c(c-1)}\right\}\eta = 0, \tag{4.3.4}$$

$$h = -\frac{\mu\gamma}{c-1}\eta. \tag{4.3.5}$$

The boundary conditions on the channel walls (2.4.11) become

$$\left.\begin{matrix}\eta = 0 \\ h = 0\end{matrix}\right\} \quad \text{on} \quad y = 0, L. \tag{4.3.6}$$

The solution to (4.3.4), subject to (4.3.6), is

$$\eta(y) = a_1 \sin\left(\frac{n\pi y}{L}\right) \qquad \text{for} \quad n = 1, 2, 3, \ldots, \tag{4.3.7}$$

where $a_1$ is a free constant.

We have found, therefore, the general form of the normal mode solutions to the perturbation equations, which are

$$\eta(x,y,t) = a_1 \sin(ly)\exp[ik(x-ct)] + \text{c.c.},$$
$$h(x,y,t) = -a_1 \frac{\mu\gamma}{c-1}\sin(ly)\exp[ik(x-ct)] + \text{c.c.}, \qquad (4.3.8)$$

where $l = n\pi/L$.

We note, however, that the equations (4.3.8) are not solutions for arbitrary $k, l,$ and $c,$ rather they will be so only for $c$ as a specific function of $k$ and $l$. To determine what this function is, we simply substitute (4.3.8) into the perturbation equation (4.1.7) (since (4.1.8), after substitution, gives nothing but a simple identity). We have

$$\left\{(-k^2-l^2)(-ikc) - ik + \frac{\mu\gamma ik}{c-1}\right\} a_1 \sin(ly)\exp[ik(x-ct)] + \text{c.c.} = 0. \qquad (4.3.9)$$

Dividing (4.3.9) through by $ik\eta(x,y,t)$ and rearranging leaves

$$(k^2+l^2)c^2 - (k^2+l^2+1)c + (1+\mu\gamma) = 0. \qquad (4.3.10)$$

Application of the quadratic formula to (4.3.10) provides the solution for $c,$ which is

$$c = \frac{k^2+l^2+1 \pm [(k^2+l^2+1)^2 - 4(k^2+l^2)(1+\mu\gamma)]^{\frac{1}{2}}}{2(k^2+l^2)}. \qquad (4.3.11)$$

The equation (4.3.11) is known as the "dispersion relation" for the perturbation wave solution. In wave theory, it is said that if $c$ is not a constant function of $k^2+l^2,$ then the waves are *dispersive*, which means that waves of different wavelengths have different phase speeds (Kundu, 1990). We see from (4.3.11) that

waves will be dispersive for all but certain special cases, one of which we will discuss below.

For instability to occur, $c$ must have a complex component. The boundary between instability and stability will be given, therefore, by setting the quantity in equation (4.3.11) under the square root sign to zero. This gives us the marginal stability curve, whose equation can be written in the form

$$\gamma_c = \frac{1}{\mu}\left[\frac{(K^2-1)^2}{4K^2}\right], \tag{4.3.12}$$

where $\gamma_c$ is the critical value of $\gamma$ above which the $K^2 \equiv k^2 + l^2$ mode goes unstable.

The marginal stability curve, as mentioned above, represents the boundary between stable modes and unstable modes for a particular $\gamma_c$. The technical definition for marginal stability is that a point on the curve must be neutrally stable (i.e., $c_I = 0$), but there must be at least one neighboring point to it which is unstable (i.e., $c_I > 0$) for a particular value of $\gamma_c$ (Drazin and Reid, 1981).

Figure 2 shows the marginal stability curve, plotted on the program *Mathematica*, where the interaction parameter has been set to $\mu = 2$ (the reason for this is given below equation (2.2.24)). The minimum of the marginal stability curve is located at $K = 1$ and $\gamma_c = 0$. Thus for every $\gamma_c > 0$, there exists wavenumbers which are unstable (independently of $\mu$; see (4.3.12)).

It can easily be deduced that, since $l = n\pi/L$, as $n$ increases a larger range of values for the along-channel wavenumber $k$ give stable $K$ modes for a given $\gamma$. For example, suppose $K = K_0 > 1$ and $n = 1$ for a particular $\gamma_c$. Then if $n$ is set to, say, $n = 2$, $K$ must increase beyond $K_0$, and $\gamma_c$

will be larger for this $K$. This implies that the $n = 1$ mode for a particular $K$ is the *first* mode to go unstable for a particular value of $\gamma_c$. With this in mind, for the remainder of this thesis we set $l = \pi/L$, the first across-channel harmonic, because this is the first cross-channel mode to go unstable. We also see from the dispersion relation (4.3.11) that if $K = 1$ and $\gamma_c = 0$ then $c = 1$, which means that this horizontal mode is nondispersive. This has important ramifications for the nonlinear theory developed for this mode in Chapter 6. Furthermore, we see that $\pi/L < 1$ for the $K = 1$ mode to exist, and that if $L$ is in fact very large then we have a useful model for continental shelf dynamics because the offshore boundary will be effectively unbounded.

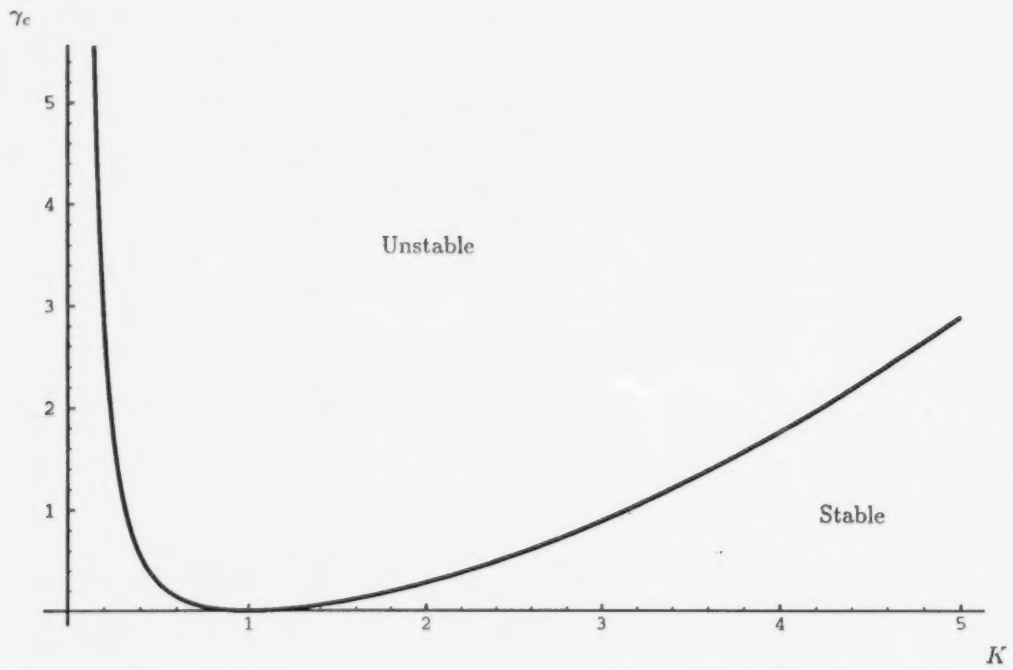


Figure 2. Marginal stability curve as determined from equation (4.3.12) using $\mu = 2.0$.

## Chapter 5

## Weakly Nonlinear Analysis for Unstable Modes other than K=1

In order to see how the unstable modes as determined by linear theory actually evolve in time and space we must allow the nonlinear interactions to be included in the description of the physical process. That is, we must develop a finite amplitude theory which follows the evolution of the wave when it has reached amplitudes for which the linear theory is no longer valid. This occurs when the amplitude has grown to the point where the assumption that the terms quadratic in the perturbations (i.e., the nonlinear terms) are small compared to the linear terms is no longer applicable. Up to this time, the amplitude has grown essentially at the linear rate, which is purely exponential, but after this time, we expect the nonlinear terms to modify this growth in a meaningful way.

However, the fully nonlinear set of governing equations (2.4.8) and (2.4.9) are intractible analytically as they stand. In order to get around this problem, we employ a method called *weakly nonlinear analysis*, which essentially allows us to utilize the fully nonlinear equations as long as the mode being studied is only *weakly* unstable. This allows the use of asymptotic methods to derive amplitude equations which follow the evolution of the disturbance associated with a slightly supercritical mode.

The reason for doing this analysis is twofold. First, it is essential to show that the disturbances saturate (do not show unbounded growth) with the inclusion of nonlinear effects, or the physicality of the model itself is thrown into question. Second, it is of interest to determine the form that the finite amplitude solutions take; for example, they may be oscilliatory, or the amplitude may stabilize at some new level after a period of time.

*5.1 Derivation of the Amplitude Equation*

In this section, we derive a temporal amplitude evolution equation for a weakly unstable mode which has a wavenumber modulus *different* than $K = 1$. In this situation, there will always be other modes with different wavenumbers which are unstable at smaller values of $\gamma$. For this reason, in this section we do not utilize a slow space variable which would follow the evolution of a wavepacket centred on the mode in question. This problem will be examined in the next section, where the amplitude equation is derived for the $K = 1$ mode.

To determine the proper scaling for the slow time variable, we look at the dispersion relation (4.3.11). From this it can be seen that if $\gamma_c$ is increased to $\gamma_c + \Delta$, where $\Delta$ is a small number, we have

$$c = \frac{K^2 + 1 \pm \{(K^2+1)^2 - 4K^2[1 + \mu(\gamma_c + \Delta)]\}^{\frac{1}{2}}}{2K^2}. \tag{5.1.1}$$

Substituting for $\gamma_c$ from the marginal stability curve (4.3.12) gives

$$c = \frac{K^2 + 1 \pm \{(K^2+1)^2 - 4K^2[1 + (K^2-1)^2/4K^2 + \mu\Delta]\}^{\frac{1}{2}}}{2K^2}$$

$$= \frac{K^2 + 1 \pm \{-4K^2\mu\Delta\}^{\frac{1}{2}}}{2K^2} = \frac{K^2 + 1 \pm i\{4K^2\mu\Delta\}^{\frac{1}{2}}}{2K^2}, \tag{5.1.2}$$

so that the growth rate $\sigma = kc_I$ is

$$\sigma = \frac{k(\mu\Delta)^{\frac{1}{2}}}{K} = \left(\frac{k^2\mu\Delta}{k^2 + l^2}\right)^{\frac{1}{2}} \propto \Delta^{\frac{1}{2}}. \tag{5.1.3}$$

Thus the corresponding increase in the growth rate will be proportional to $\Delta^{\frac{1}{2}}$. This means that if we let $\epsilon^2 = \Delta$ (for convenience), then we write the following

to represent a small supercriticality in $\gamma$

$$\gamma = \gamma_c + \epsilon^2, \tag{5.1.4}$$

which, according to the above discussion, leads us to introduce a slow timescale with the following scaling

$$T = \epsilon t, \tag{5.1.5}$$

where $T$ will be the timescale over which the nonlinear interactions make an O(1) contribution to the dynamics. The method used here is known as *multiple scales*, and it is based on the premise that the dynamics evolve (in this case) over two distinct time scales, where the "fast" scale is the advective time scale for the plane waves themselves, and the "slow" scale dictates the evolution of the *form* of these waves over time. In other words, the slow scale is the time scale over which the envelope bounding the amplitude of the fast moving plane waves evolves.

We take equations (4.1.2) and (4.1.3), which are the nonlinear perturbation equations, and substitute in (5.1.4) and (5.1.5), set $U_0 = 0$ in order to concentrate on baroclinic instability, and notice that the time derivative mapping as a result of (5.1.5) is $\partial_t \longmapsto \partial_t + \epsilon\partial_T$. This yields

$$\Delta\eta_t - \eta_x - h_x = -\epsilon\Delta\eta_T - \mu J(\eta, \Delta\eta), \tag{5.1.6a}$$

$$h_t + h_x - \mu\gamma_c\eta_x = -\epsilon h_T + \epsilon^2\mu\eta_x - \mu J(\eta, h). \tag{5.1.6b}$$

We now apply a straightforward asymptotic expansion to these equations

(in order to exploit the small parameter $\epsilon$)

$$\eta(x,y,t,T) = \epsilon\eta_0(x,y,t,T) + \epsilon^2\eta_1(x,y,t,T) + \dots , \tag{5.1.7a}$$

$$h(x,y,t,T) = \epsilon h_0(x,y,t,T) + \epsilon^2 h_1(x,y,t,T) + \dots . \tag{5.1.7b}$$

We remind the reader that henceforth throughout this paper the "0" subscript on the perturbation thickness $h(x,y,t)$ and the upper layer perturbation geostrophic pressure $\eta(x,y,t)$ will denote the respective leading order term in the asymptotic expansion utilized in the finite amplitude instability theory.

The O(1) problem associated with substituting (5.1.7) into (5.1.6), is given by

$$\Delta\eta_{0_t} - \eta_{0_x} - h_{0_x} = 0, \tag{5.1.8a}$$

$$h_{0_t} + h_{0_x} - \mu\gamma_c\eta_{0_x} = 0. \tag{5.1.8b}$$

The solution for the equations (5.1.8) will be in the form

$$\eta_0 = A(T)\sin(ly)\exp(ik\theta) + \text{c.c}, \tag{5.1.9a}$$

$$h_0 = B(T)\sin(ly)\exp(ik\theta) + \text{c.c}, \tag{5.1.9b}$$

where $\theta = x - ct$, $c$ is a *real* phase speed, $l = \pi/L$, c.c is complex conjugate, and $A, B$ are the amplitude coefficients.

After substitution of (5.1.9) into (5.1.8), we obtain

$$c = \frac{k^2 + l^2 + 1}{2(k^2 + l^2)}, \tag{5.1.10}$$

which is the dispersion relation found in Chapter 4 using linear theory after uti-

lizing (4.3.12), and

$$B = \frac{\mu\gamma_c A}{1-c} = \frac{(k^2+l^2-1)A}{2}, \tag{5.1.11}$$

which is the equation relating the amplitude of $h$ to that of $\eta$. Notice that if $k^2 + l^2 = K^2 = 1$, then $B \equiv 0$ to leading order. This has important ramifications for the scaling of the gravity current equations in the $K = 1$ mode analysis, as will be seen in Chapter 6.

The $O(\epsilon)$ problem is given by

$$\Delta\eta_{1_t} - \eta_{1_x} - h_{1_x} = -\Delta\eta_{0_T} - \mu J(\eta_0, \Delta\eta_0), \tag{5.1.12a}$$

$$h_{1_t} + h_{1_x} - \mu\gamma_c\eta_{1_x} = -h_{0_T} - \mu J(\eta_0, h_0). \tag{5.1.12b}$$

Substituting in the solutions from the $O(1)$ problem, we find

$$\Delta\eta_{1_t} - \eta_{1_x} - h_{1_x} = A_T(k^2+l^2)\sin(ly)\exp(ik\theta) + \text{c.c}, \tag{5.1.13}$$

$$h_{1_t} + h_{1_x} - \gamma_c\mu\eta_{1_x} = -B_T\sin(ly)\exp(ik\theta) + \text{c.c}. \tag{5.1.14}$$

The solution to (5.1.13) and (5.1.14) may be written in the general form

$$\eta_1 = E(T)\sin(ly)\exp(ik\theta) + \text{c.c}, \tag{5.1.15a}$$

$$h_1 = \phi(y,T) + F(T)\sin(ly)\exp(ik\theta) + \text{c.c}, \tag{5.1.15b}$$

where $\phi(y,T)$ is a homogeneous solution which will be required to balance adjustments to the mean flow resulting from nonlinear interactions in the $O(\epsilon^2)$

problem. Now substitute (5.1.15) into (5.1.13) and (5.1.14) to obtain

$$ikE[c(k^2+l^2)-1]-ikF = A_T(k^2+l^2), \tag{5.1.16a}$$

$$ikF(1-c)-ik\mu\gamma_c E = -\frac{\mu\gamma_c A_T}{1-c}. \tag{5.1.16b}$$

Thus, from (5.1.16b) we find an expression for $F$, which is

$$F = \frac{\mu\gamma_c E}{1-c} + i\frac{\mu\gamma_c A_T}{k(1-c)^2}. \tag{5.1.17}$$

Now we use (5.1.17) in (5.1.16a) to obtain, after making use of the dispersion relation (5.1.10) and the expression for the marginal stability curve (4.3.12)

$$ikE\left(\frac{k^2+l^2-1}{2}\right) - ikE\left(\frac{k^2+l^2-1}{2}\right) + A_T(k^2+l^2) = A_T(k^2+l^2). \tag{5.1.18}$$

We see that (5.1.18) is an identity, which implies that the "E" mode is simply proportional to the O(1) solution. We may thus absorb this contribution directly into the O(1) solution (Newell, 1985; Pedlosky, 1970). We therefore set $E \equiv 0$, which produces $O(\epsilon)$ solutions in the form

$$\eta_1 = 0, \tag{5.1.19a}$$

$$h_1 = \phi(y,T) + i\frac{\mu\gamma_c A_T}{k(1-c)^2}\sin(ly)\exp(ik\theta) + \text{c.c.} \tag{5.1.19b}$$

The required evolution equation for $A(T)$ is determined by examining the $O(\epsilon^2)$ problem given by

$$\Delta\eta_{2_t} - \eta_{2_x} - h_{2_x} = -\Delta\eta_{1_T} - \mu J(\eta_1, \Delta\eta_0) - \mu J(\eta_0, \Delta\eta_1), \tag{5.1.20a}$$

$$h_{2_t} + h_{2_x} - \gamma_c\mu\eta_{2_x} = -h_{1_T} + \mu\eta_{0_x} - \mu J(\eta_1, h_0) - \mu J(\eta_0, h_1). \tag{5.1.20b}$$

Using (5.1.19) and (5.1.9) in (5.1.20) we find

$$\Delta\eta_{2_t} - \eta_{2_x} - h_{2_x} = 0, \tag{5.1.21a}$$

$$h_{2_t} + h_{2_x} - \gamma_c\mu\eta_{2_x} = \left[-\frac{i}{k}\left(\frac{\gamma_c\mu A_{TT}}{(1-c)^2}\right) + ik\mu A - ik\mu A\phi_y\right]\sin(ly)\exp(ik\theta) + \text{c.c.}$$
$$-\phi_T - \mu[2ikl(AD_T{}^* - A^*D_T)\sin(ly)\cos(ly)], \tag{5.1.21b}$$

where

$$D_T = i\frac{\gamma_c\mu A_T}{k(1-c)^2}. \tag{5.1.22}$$

Now we apply solvability conditions to (5.1.21b) in order to determine the amplitude equation. Since all the terms in the left hand side operator of this equation contain derivatives in either $x$ or $t$, the coefficient of the inhomogeneities on the right hand side which are independent of $x$ and $t$ must be set to zero. This is done because if it is not, the particular solution to the homogeneous equation involving these terms will grow linearly in time (i.e., it will be a term or terms multiplied by $t$). This means that eventually the solution will grow to the point where it violates the basic requirements of the asymptotic expansion, namely that the terms in the series will remain O(1) quantities multiplied by the various orders of $\epsilon$.

From a physical standpoint, solutions which grow linearly in time imply that there exists the possibility of an infinite amount of energy associated with the perturbations. This is an unacceptable, unphysical result, which makes it necessary to set these so-called *secular* terms to zero and avoid these consequences.

Setting the secular terms to zero in (5.1.21b) leads to

$$\phi_T = -2\mu ikl(AD_T^* - A^* D_T)\sin(ly)\cos(ly). \tag{5.1.23}$$

Using the expression for $D_T$ and the trigonometric identity $\sin(2x) = 2\sin(x)\cos(x)$, this may be written as

$$\phi_T = -\frac{\gamma_c \mu^2 l}{(1-c)^2}(|A|^2)_T \sin(2ly). \tag{5.1.24}$$

Now integrating with respect to $T$, we find, after applying (4.3.12) and the dispersion relation (5.1.10)

$$\phi = -\mu l K^2(|A|^2 - |A_0|^2)\sin(2ly), \tag{5.1.25}$$

where $A_0 = A(T=0)$. It is important to note that $\phi$, the adjustment to the mean flow, is always strictly real.

Another point to appreciate is that the differential equation for $\phi(y,T)$ given by (5.1.24) does not contain any derivatives with respect to the cross-channel coordinate $y$. Thus, it is not possible to impose additional auxilliary boundary conditions at $y = 0, L$ on $\phi$ as one needs to do in quasigeostrophic theory (Pedlosky (1970)). The reason why there are no $y$-derivatives in (5.1.24) arises from the fact that the convective time derivatives in the momentum equations for the gravity current have been completely filtered out in the derivation of the governing equations (2.4.8) and (2.4.9). The additional auxilliary boundary conditions for the $x$-independent mean flow required in finite amplitude quasigeostrophic baroclinic instability are derived from the local time rate of change of momentum terms which are retained in quasigeostrophic theory. Since these terms are not retained here in any form it is inappropriate to expect that $\phi$ should satisfy

conditions which are derived from them. We note, however, that the $\sin(2ly)$ dependence in the solution for $\phi$ will imply that there is no net along-channel mass flux associated with the mean flow, i.e., generated by the self-interaction of the perturbation wave field to this order. This means that

$$\int_0^L \phi_y dy = 0. \tag{5.1.26}$$

To derive the required evolution equation for $A(T)$ it is convenient to first eliminate $h_2$ between (5.1.21a) and (5.1.21b) to yield

$$(\partial_t + \partial_x)(\Delta\partial_t - \partial_x)\eta_2 - \gamma_c\mu\eta_{2xx} = \left[\frac{\gamma_c\mu A_{TT}}{(1-c)^2} - k^2\mu A - \frac{2\gamma_c\mu^3k^2l^2A}{(1-c)^2}(|A|^2 - |A_0|^2)\cos(2ly)\right]\exp(ik\theta)\sin(ly) + \text{c.c.} \tag{5.1.27}$$

where we have substituted the $y-$derivative of (5.1.25) for $\phi_y$ in (5.1.21b).

Using another trigonometric identity we may re-write $\cos(2ly)\sin(ly)$ as $[\sin(3ly) - \sin(ly)]/2$. The only terms which produce secular growth are those terms on the right hand side of (5.1.27) which are proportional to $\sin(ly)\exp(ik\theta)$ and its complex conjugate. Setting the coefficient of these terms to zero gives

$$(k^2+l^2)A_{TT} - k^2\mu A + \mu^2k^2l^2(k^2+l^2)A(|A|^2 - |A_0|^2) = 0, \tag{5.1.28}$$

where we have used (4.3.12) and (5.1.10) to replace $\gamma_c/(1-c)^2$ with $(k^2 + l^2)/\mu$.

Equation (5.1.28) may be simplified by dividing through by $(k^2+l^2)$ and rearranging, so that the evolution equation for the perturbation amplitude $A$ is

$$A_{TT} = \sigma^2 A - k^2 N A(|A|^2 - |A_0|^2), \tag{5.1.29}$$

where $\sigma \equiv \left(\frac{\mu k^2}{k^2+l^2}\right)^{\frac{1}{2}}$ and $N \equiv \mu^2 l^2$. Note that $\sigma$ represents the growth rate for the unstable mode as would be determined from linear theory (see (5.1.3)). Pedlosky (1970) derived a similar evolution equation from a two-layer, rigid-lid model of quasigeostrophic baroclinic instability on a $\beta$-plane.

*5.2 Solution to the Evolution Equation*

The method of solution for (5.1.29) follows Pedlosky (1987, Ch.7) exactly, and so we merely provide an outline. Assuming a solution to (5.1.29) of the form

$$A(T) = R(T)\exp[i\theta(T)], \tag{5.2.1}$$

leads to, after separating the real and imaginary parts,

$$\theta_T = \frac{M}{R^2}, \tag{5.2.2a}$$

$$R_{TT} - \frac{M^2}{R^3} = \sigma^2 R - k^2 N R(R^2 - {R_0}^2), \tag{5.2.2b}$$

where $M$ is a constant. If we assume that the phase is constant in time, then $M = 0$ and (5.2.2b) becomes

$$R_{TT} = \sigma^2 R - k^2 N R(R^2 - {R_0}^2). \tag{5.2.3}$$

The constant phase for $A$ means that at the $T = 0$, $dA/dT = \sigma A$, that is, the amplitude increases initially according to the growth rate specified by linear theory.

If (5.2.3) is multiplied by $R_T$ and integrated, we obtain

$$\frac{1}{2}(R_T)^2 + V(R) = E, \tag{5.2.4}$$

where $V(R) = -\frac{R^2}{2}[\sigma^2 + k^2 N {R_0}^2] + \frac{kNR^4}{4}$ and $E$ is a constant. Since (5.2.4) implies that the amplitude behaves like a harmonic oscillator, we may utilize the "potential" function $V(R)$ to determine maximum and minimum amplitudes for the oscillating system. We do this by setting $V(R) = E$ (Pedlosky (1987)), where we take $E$ to be the energy evaluated at $T = 0$ (i.e. $E = [\frac{1}{2}R_T^2 + V(R)]_{T=0}$). We obtain

$$-\frac{R^2(\sigma^2 + k^2 N R_0^2)}{2} + \frac{k^2 N R^4}{4} = \frac{Q_0^2}{2} - \frac{R_0^2(\sigma^2 + k^2 N R_0^2)}{2} + \frac{k^2 N R_0^4}{4}, \qquad (5.2.5)$$

where $Q_0^2 = R_T^2|_{T=0}$. We may rewrite this as

$$R^4 - \frac{2R^2}{k^2 N}(\sigma^2 + k^2 N R_0^2) = \frac{2Q_0^2}{k^2 N} - \frac{2R_0^2}{k^2 N}(\sigma^2 + k^2 N R_0^2) + R_0^4. \qquad (5.2.6)$$

We use the quadratic formula to solve for $R^2$, which is, after some simplification

$$R^2_{\text{max,min}} = \frac{\sigma^2 + k^2 N R_0^2}{k^2 N} \pm \frac{\sigma^2}{k^2 N}\sqrt{1 + \frac{2Q_0^2 k^2 N}{\sigma^4}}, \qquad (5.2.7)$$

or

$$R^2{}_{\text{max,min}} = {R_0}^2 + \frac{\sigma^2}{k^2 N}\left[1 \pm \left(1 + \frac{2k^2 N {R_0}^2}{\sigma^2}\right)^{\frac{1}{2}}\right], \qquad (5.2.8)$$

where we have let $Q_0^2 = R_T^2|_{T=0} = \sigma^2 R_0^2$, for reasons indicated earlier (see description after equation (5.2.3)), and where the maximum and minimum are associated with the plus and minus signs, respectively.

From the derivation of $R_{\text{max,min}}$, we see that we are able to rewrite (5.2.4) as

$$\frac{1}{2}(R_T)^2 = -\left(\frac{k^2 N}{4}\right)(R^2 - R^2_{\text{max}})(R^2 - R^2_{\text{min}}), \qquad (5.2.9)$$

because $R_{max}$ and $R_{min}$ are the roots of the expression $V(R) - E = 0$ in terms of $R^2$ (the $k^2N/4$ factor was divided out in the derivation, so it must be multiplied back in as a coefficient).

Now apply the change of variables (Pedlosky (1987))

$$\xi = \frac{R}{R_{max}}, \tag{5.2.10}$$

which allows us to rewrite (5.2.9) as

$$(\xi_T)^2 = \left(\frac{k^2 N R_{max}^2}{2}\right)(1-\xi^2)\left(\xi^2 - \frac{R_{min}^2}{R_{max}^2}\right). \tag{5.2.11}$$

Now let

$$\alpha = \frac{R_{min}^2}{R_{max}^2}; \quad \tau = \left(\frac{k^2 N R_{max}^2}{2}\right)^{\frac{1}{2}} T, \tag{5.2.12}$$

and we may rewrite (5.2.11) as

$$d\tau = \frac{d\xi}{[(1-\xi^2)(\xi^2-\alpha^2)]^{\frac{1}{2}}}. \tag{5.2.13}$$

Integrating (5.2.13) leads to

$$\xi = \mathrm{dn}(\tau - \tau_0 | m), \tag{5.2.14}$$

where

$$\tau_0 = \mathrm{dn}^{-1}\left(\frac{R_0}{R_{max}} \mid m\right). \tag{5.2.15}$$

Here dn is the Jacobi elliptic dnoidal function (following the notation of Milne-Thomson, 1950), $m = (1-\alpha^2)$, and $\tau_0$ is chosen in such a way as to ensure

that $R = R_0$ at $\tau = 0$. The period of the disturbance is given by

$$\tau_p = 2E(m), \tag{5.2.16}$$

where $E(m)$ is the complete Jacobi elliptic integral of the first kind, given by (Abramowitz and Stegun, 1964)

$$E(m) = \int_0^1 \frac{dt}{[(1-t^2)(1-mt^2)]^{\frac{1}{2}}}. \tag{5.2.17}$$

The evolution of $A$ follows the form of a dnoidal wave, and therefore is periodic in time. This means that after the initial exponential increase of the unstable mode the effect of the nonlinearities in the equations for $A$ is to slow and eventually reverse the growth of the disturbance. The amplitude falls until it reaches a point where the linear growth rate becomes dominant again, and the cycle begins anew.

*5.3 Description of the Solutions for the Dnoidal Wave Equation*

In this subsection, we examine the amplitude function derived in the previous subsection, redimensionalize it, and see what it means for the physical problem that was enunciated at the outset.

The scalings presented in Chapter 2, as mentioned before, suggest horizontal lengthscales of order 15 km, advective timescales of order 7 days, and a scale height for the gravity current of about 40m. Let us consider a channel width $L = \pi$ in non-dimensional units, so that we set the cross-channel wavenumber, $l = \pi/L$, equal to 1 (this corresponds to a dimensional channel width of about 47 km).

As an example, if we set $k = 1$, then the solution (5.2.14) corresponds to the horizontal mode $K = \sqrt{2}$. We also let $\mu = 2$, $\epsilon = 0.1$, and the

initial nondimensional perturbation pressure amplitude $A_0 = 0.1$. With these parameters, the amplitude function $A(T)$ is found to vary with slow time as depicted in Figure 3 (see Program 1 in the Appendix for the *Mathematica* program used to plot this figure). From this plot, it can be seen that the oscillations at this wavenumber are such that $R$ grows to about 7 times its initial amplitude before saturating. The period is about 10 slow time units. The ultra-long period is indicative of nothing more than the fact that the supercriticality is very small (i.e. $O(\epsilon^2)$). This produces a small growth rate which eventually is balanced by a similarly scaled nonlinearity. This is certainly a weakness in the model, but our main purpose has been to show that the nonlinearities will slow and reverse the linear growth rate of the disturbance. Since this is the situation, we expect that in the full nonlinear case, where the supercriticality could be much larger than $\gamma_c + \epsilon^2$, there exists the possibility that the wave will be large enough to break up the gravity current into coherent travelling eddies or, equally likely, accelerate the instability further.

Analyses similar to what is presented above may be done for each along-channel wavenumber. To see how the key parameters change as $k$ changes, we present the following plots. Figure 4, plotted on *Mathematica* from equation (5.2.8), shows how the maximum amplitude, $R_{\max}$, varies with wavenumber. It can be seen that as the wavelength becomes shorter, the maximum amplitude decreases, becoming more or less constant with about an 80% reduction from small $k$ at the high wavenumber limit. Figure 5, plotted on *Mathematica* from equation (5.2.16), is a plot of the period of the disturbance as it varies with $k$. From this figure, we see that the period falls off as the along-channel wavenumber increases, very much like the period of the fast along-channel oscillations would be expected to change. So from the above discussion it can be concluded that as the

wavenumber increases, the maximum amplitude of the disturbance falls off and the period becomes shorter, which suggests that the low wavenumber disturbances should dominate if instability is present.

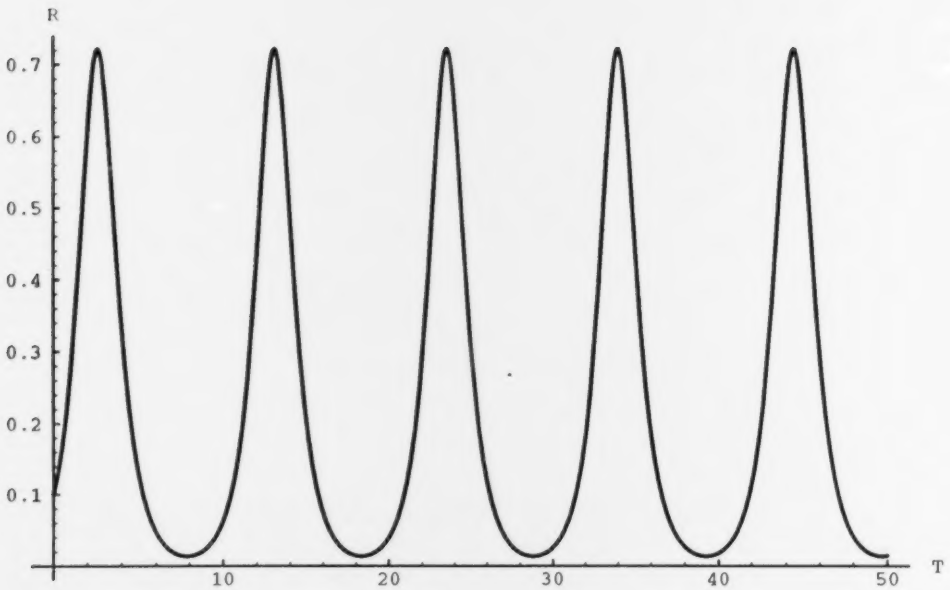


Figure 3. Plot of nondimensional perturbation pressure amplitude $R(T)$ versus time $T$, where $k = l = 1.0$, $N = 4.0$, $\epsilon = 0.1$ and where $\eta = \epsilon\eta_0 + \mathrm{O}(\epsilon^2)$.

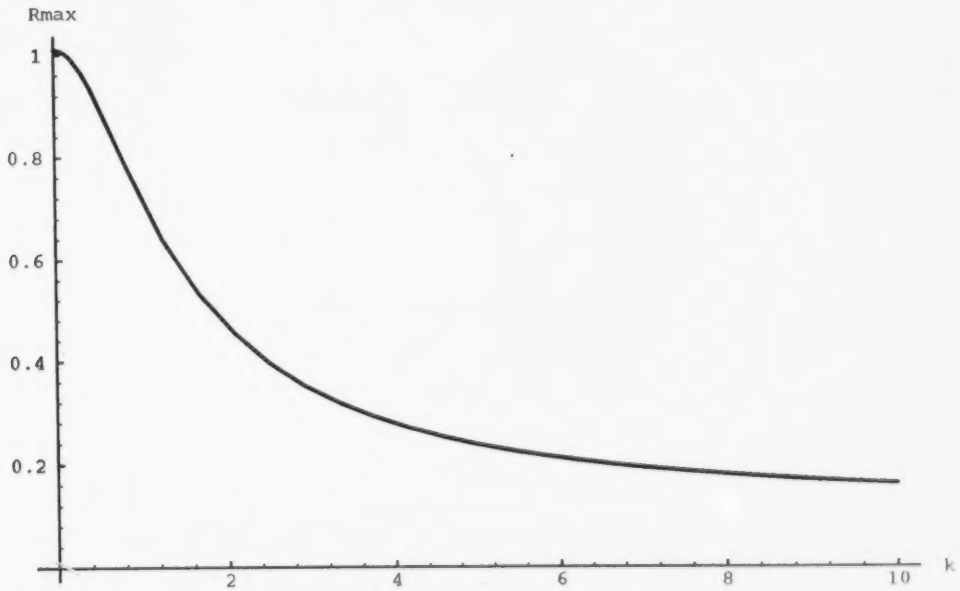


Figure 4. Plot of $R_{\max}$ versus $k$ for $l = 1.0$, $\mu = 2.0$ (from equation (5.2.8)).

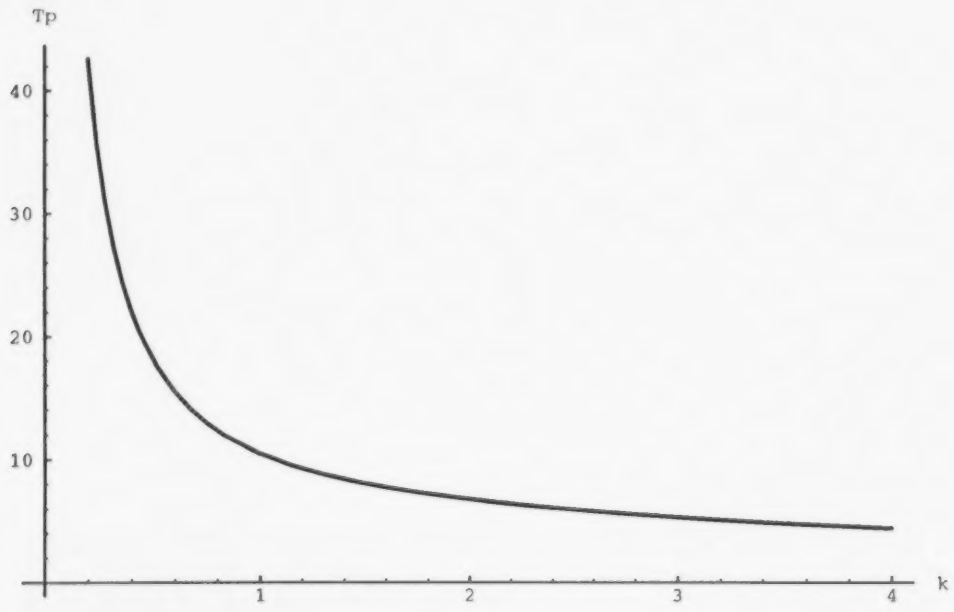


Figure 5. Plot of period versus $k$ for $l = 1.0$, $\mu = 2.0$ (from equation (5.2.16)).

## Chapter 6

## Amplitude Equations for the K=1 Mode

### *6.1 Derivation of the Equations*

In this section, we examine a supercriticality which is centred on the $K = 1$ mode, which is the wavenumber modulus found at the bottom of the marginal stability curve (see Figure 2). Under these conditions, a finite but small increase in $\gamma$ over $\gamma_c$ will excite initially a small, finite band of unstable modes. We wish to follow the evolution of the resulting "baroclinic wave packet," and so a slow space scale is introduced along with the slow time scale adopted in the last section. The scalings will now be

$$\begin{aligned} \gamma &= \epsilon^2, \\ T &= \epsilon t, \\ X &= \epsilon x. \end{aligned} \tag{6.1.1}$$

Note that $\gamma_c = 0$ at $K = 1$, which changes the scaling for $\gamma$ to (6.1.1) from what was used in (5.1.4). Since the rate of change of channel thickness is extremely small in this scenario, it can easily be shown by the use of an asymptotic analysis that the gravity current perturbation height is not an O(1) quantity as it was in Chapter 5. This can be seen by inserting $K = 1$ into (5.1.11), which yields $h = 0$ to leading order. This implies that we should introduce

$$h = \epsilon \tilde{h}, \tag{6.1.2}$$

as the scaling for $h$.

As in the previous section, we now take the nonlinear perturbation equations (4.1.2) and (4.1.3) with $U_0 \equiv 0$ and substitute the scalings (6.1.1) and (6.1.2), drop the "0" subscript and use the mappings $\partial_t \longmapsto \partial_t + \epsilon\partial_T$ and $\partial_x \longmapsto \partial_x + \epsilon\partial_X$ . The scaled equations are (after dropping the tildes)

$$\nabla^2\eta_t - \eta_x + \mu J(\eta, \Delta\eta) = \epsilon[h_x - \Delta\eta_T - 2\eta_{Xxt} + \eta_X] + \mathrm{O}(\epsilon^2), \quad (6.1.3a)$$

$$h_t + h_x + \mu J(\eta, h) = \epsilon[\mu\eta_x - h_T - h_X] + \mathrm{O}(\epsilon^2). \quad (6.1.3b)$$

Now we exploit the small parameter $\epsilon$ by introducing a standard asymptotic expansion for $\eta$ and $h$ in the form

$$\eta(x, y, t, X, T) = \epsilon\eta_0(x, y, t, X, T) + \epsilon^2\eta_1(x, y, t, X, T) + \ldots, \quad (6.1.4a)$$

$$h(x, y, t, X, T) = \epsilon h_0(x, y, t, X, T) + \epsilon^2 h_1(x, y, t, X, T) + \ldots. \quad (6.1.4b)$$

The $\mathrm{O}(1)$ problem is given by

$$\Delta\eta_{0_t} - \eta_{0_x} = 0, \quad (6.1.5a)$$

$$h_{0_t} + h_{0_x} = 0. \quad (6.1.5b)$$

Note that to leading order the thickness and pressure perturbations are uncoupled. The solution to (6.1.5) may be written in the form

$$\eta_0 = A(X, T)\sin(ly)\exp(ik\theta) + \text{c.c}, \quad (6.1.6a)$$

$$h_0 = f(\theta, y, X, T), \quad (6.1.6b)$$

where $\theta = x - ct$ and the form of $h$ is left unspecified at this point because

it cannot be determined from (6.1.5). The phase speed satisfies, of course,

$$c = \frac{1}{k^2 + l^2} = 1, \tag{6.1.7}$$

since $k^2 + l^2 = 1$ at $\gamma_c = 0$.

The $O(\epsilon)$ problem is

$$\Delta\eta_{1_t} - \eta_{1_x} = h_{0_x} - \mu J(\eta_0, \Delta\eta_0) - \Delta\eta_{0_T} - 2\eta_{0_{XXt}} + \eta_{0_X}, \tag{6.1.8a}$$

$$h_{1_t} + h_{1_x} = \mu\eta_{0_x} - \mu J(\eta_0, h_0) - h_{0_T} - h_{0_X}. \tag{6.1.8b}$$

The simple hyperbolic nature of the left hand side operator in (6.1.8b) implies that *any* dependence on the variable $\theta$ in the right hand side of (6.1.8b) produces secular growth. This means that the solvability condition for (6.1.8b) is

$$\mu\eta_{0_x} - \mu J(\eta_0, h_0) - h_{0_T} - h_{0_X} = 0. \tag{6.1.9}$$

The structure of the solution for $\eta_0$ as given by (6.1.6a) implies that $h_0$ takes the form

$$h_0 = \phi(y, X, T) + \left\{ \sum_{m=1}^{\infty} \sum_{n=1}^{\infty} B_{m,n}(X, T) \sin(nly) \exp(mik\theta) + \text{c.c} \right\}, \tag{6.1.10}$$

where $\phi(y, X, T)$ is a mean flow adjustment term whose form is determined as a result of the balance between the growth of the disturbance and the extraction of potential energy from the ambient flow. It can be seen that the form for the solution for $h_0$ is such that all possible along and cross-channel modes are represented. This is because nonlinear interactions (through the Jacobian term in (6.1.8b)) will generate higher modes from lower modes, which will result in secular growth if they too are not included in the solution for $h_0$.

The phase velocities calculated from (6.1.5a) and (6.1.5b) for the upper and lower layers, respectively, are equivalent (see (6.1.7)), but the group velocities will be different, viz

$$c_{g_1} = \frac{d}{dk}\left[\frac{k}{k^2+l^2}\right] = 1 - 2k^2, \tag{6.1.11}$$

(since $k^2 + l^2 = 1$) and from (6.1.5b), we have

$$c_{g_2} = 1, \tag{6.1.12}$$

where the subscripts 1 and 2 denote the upper and lower layer, respectively. The phase velocities "coalesce" at the $K = 1$ mode, but the group velocities remain distinct. This is exactly the same observation made by Pedlosky (1972) for the Phillips model.

Substituting (6.1.6a) and (6.1.10) into the right side of (6.1.8a) leads to

$$\begin{aligned}\nabla^2\eta_{1_t} - \eta_{1_x} = ik \sum_{m=1}^{\infty}\sum_{n=1}^{\infty} mB_{m,n}\sin(nly)\exp(mik\theta) \\ +[A_T + (1-2k^2)A_X]\sin(ly)\exp(ik\theta) + \text{c.c.}\end{aligned} \tag{6.1.13}$$

The only terms which cause resonant behavior for the left hand side of (6.1.13) are those which are proportional to $\sin(ly)\exp(ik\theta)$, which means the solvability condition for this equation may be written in the form

$$ikB_{1,1} + A_T + (1-2k^2)A_X = 0. \tag{6.1.14}$$

This equation determines $B_{1,1}$ as a function of $A(X,T)$.

Substituting (6.1.6a) and (6.1.10) into (6.1.9) yields

$$\mu ikA(1-\phi_y)\sin(ly)\exp(ik\theta)$$

$$-\frac{\mu i k l A}{2}\sum_{m=1}^{\infty}\sum_{n=1}^{\infty}\Big\{nB_{m,n}\sin[(n+1)ly]-(n+1)B_{m,n+1}\sin(nly)$$
$$-mB_{m,n}\sin[(n+1)ly]-mB_{m,n+1}\sin(nly)\Big\}\exp[(m+1)ik\theta]$$

$$+\frac{\mu i k l A^{*}}{2}\sum_{m=1}^{\infty}\sum_{n=1}^{\infty}\Big\{nB_{m,n}\sin[(n+1)ly]-(n+1)B_{m,n+1}\sin(nly)$$
$$+mB_{m,n}\sin[(n+1)ly]+mB_{m,n+1}\sin(nly)\Big\}\exp[(m-1)ik\theta]$$

$$-\sum_{m=1}^{\infty}\sum_{n=1}^{\infty}(B_{m,n_X}+B_{m,n_T})\sin(nly)\exp(mik\theta)+\text{c.c.}-\phi_X-\phi_T=0. \tag{6.1.15}$$

This expression is a double Fourier series in the basis functions $\{\sin(nly)\}_{n=1}^{\infty}$ and $\{\exp(mik\theta)\}_{m=0}^{\infty}$. The evolution equations are obtained by demanding that each individual Fourier coefficient be identically zero.

The terms which are independent of the fast phase $\theta$ are given by

$$\phi_X+\phi_T=\frac{\mu i k l A^{*}}{2}\sum_{n=1}^{\infty}\Big\{nB_{1,n}\sin[(n+1)ly]-(n+1)B_{1,n+1}\sin(nly)$$
$$+B_{1,n}\sin[(n+1)ly]+B_{1,n+1}\sin(nly)\Big\}+\text{c.c.} \tag{6.1.16}$$

Simplifying and including the complex conjugate explicitly, we find that

$$\phi_X+\phi_T=\frac{\mu i k l}{2}\sum_{n=1}^{\infty}\Big\{n(AB_{1,n+1}^{*}-A^{*}B_{1,n+1})$$
$$-n(AB_{1,n-1}^{*}-A^{*}B_{1,n-1})\Big\}\sin(nly). \tag{6.1.17}$$

The solution to (6.1.17) may be written in the form

$$\phi=\frac{\mu l}{2}\sum_{n=1}^{\infty}\alpha_n(X,T)n\sin(nly). \tag{6.1.18}$$

Substituting (6.1.18) into (6.1.17) leads to the following set of equations for $\alpha_n$

$$\alpha_{n_X} + \alpha_{n_T} = ik[(AB^*_{1,n+1} - A^*B_{1,n+1}) - (AB^*_{1,n-1} - A^*B_{1,n-1})]. \qquad (6.1.19)$$

We shall now examine the $\exp(ik\theta)$ terms. Extracting from (6.1.15) all terms of this form yields

$$\begin{aligned}\mu ikA(1-\phi_y)\sin(ly) + \frac{\mu iklA^*}{2}\sum_{n=1}^{\infty}\Big\{ & nB_{2,n}\sin[(n+1)ly] \\ & - (n+1)B_{2,n+1}\sin(nly) + 2B_{2,n}\sin[(n+1)ly] + 2B_{2,n+1}\sin(nly)\Big\} \\ & - \sum_{n=1}^{\infty}(B_{1,n_X} + B_{1,n_T})\sin(nly) = 0. \qquad (6.1.20)\end{aligned}$$

If (6.1.18) is substituted into (6.1.20), we find, after some manipulation

$$\mu ikA + \mu^2 l^2 ikA\alpha_2 - B_{1,1_X} - B_{1,1_T} = 0, \qquad (6.1.21)$$

from the $\sin(ly)$ terms, and from the $\sin(nly)$ terms $(n > 1)$

$$\begin{aligned}-\frac{\mu^2 l^2 ikA}{4}[(n-1)^2\alpha_{n-1} - (n+1)^2\alpha_{n+1}] & \\ + \frac{\mu iklA^*}{2}[(n+1)B_{2,n-1} - (n-1)B_{2,n+1}] & \\ - (B_{1,n_X} + B_{1,n_T}) = 0 \qquad (n = 2,3,\ldots). & \qquad (6.1.22)\end{aligned}$$

Finally, the equations associated with the modes where $m > 1$ are found in exactly an analogous way, and are given by

$$\begin{aligned}B_{m,n_T} + B_{m,n_X} = & \frac{\mu iklA^*}{2}[(n+m)B_{m+1,n-1} - (n-m)B_{m+1,n+1}] \\ & - \frac{\mu iklA}{2}[(n-m)B_{m-1,n-1} - (n+m)B_{m-1,n+1}] \\ & (m = 2,3,\ldots, \quad n = 1,2,\ldots). \qquad (6.1.23)\end{aligned}$$

Equation (6.1.23) can be consolidated with (6.1.22) to yield equations for all $B_{m,n}$ and if (6.1.14) is substituted into (6.1.19) and (6.1.21) to generate equations for $A$ and $\alpha_2$, then a complete, closed, infinite set of nonlinear partial differential equations is the result. To simplify these resulting equations, we introduce the transformations

$$\alpha_n = -\tilde{\alpha}_n,$$
$$B_{m,n} = -i\tilde{B}_{m,n}, \qquad \text{(except for } B_{1,1}\text{)}, \tag{6.1.24}$$

which yields the coupled system (after dropping the tildes)

$$(\partial_T + \partial_X)(\partial_T + (1-2k^2)\partial_X)A = \mu k^2 A - \mu^2 l^2 k^2 A\alpha_2, \tag{6.1.25}$$

$$(\partial_T + \partial_X)\alpha_2 = (\partial_T + (1-2k^2)\partial_X)|A|^2 + k(AB^*_{1,3} + A^*B_{1,3}), \tag{6.1.26}$$

$$(\partial_T + \partial_X)\alpha_n = k[(AB^*_{1,n+1} + A^*B_{1,n+1}) - (AB^*_{1,n-1} + A^*B_{1,n-1})] \tag{6.1.27}$$
$$(n = 1,3,4,\dots),$$

$$\begin{aligned}(\partial_T + \partial_X)B_{m,n} = &-\frac{\mu^2 l^2 kA}{4}[(n-1)^2\alpha_{n-1} - (n+1)^2\alpha_{n+1}]\delta_{1,m} \\ &+ \frac{\mu ikl A^*}{2}[(n+m)B_{m+1,n-1} - (n-m)B_{m+1,n+1}] \\ &- \frac{\mu ikl A}{2}[(n-m)B_{m-1,n-1} - (n+m)B_{m-1,n+1}]\end{aligned} \tag{6.1.28}$$
$$(m = 1,2,\dots, n = 1,2,3,\dots \quad \text{(except} \quad m = n = 1)).$$

Equations (6.1.25) - (6.1.28) define the evolution in slow time and space of the perturbation pressure amplitude $A(X,T)$, all the modes of the gravity

current height $B_{m,n}(X,T)$, and all the mean flow modes $\alpha_n(X,T)$. It is important to note that each mode does not interact directly with all the others; a mode interacts only with a small band of its nearest "neighbours". This makes the system more tractible numerically, especially if $\partial_X$ or $\partial_T$ is set to zero. The major problem here is the determination of an appropriate point to truncate the system so as to work with a closed, finite set of equations, but at the same time retain as much of the physics that the infinite system represents as possible.

There is an interesting point to notice about the equations (6.1.25) - (6.1.28) before any analysis is done. It can immediately be seen that the "ladder" of excited modes is initiated by the presence of the $B_{1,3}$ amplitude coefficient in (6.1.26). This "odd" mode excites only "even" mean flow modes (i.e. $\alpha_{2n}$s) and only "even-even" or "odd-odd" pairs of height perturbation modes (i.e. $B_{2,3}$, $B_{2,5}$ etc. $= 0$). So although the excluded coefficients are represented in the equations, they are not forced by the perturbation pressure.

*6.2 Solitary Wave Solution*

It is possible to derive a steadily-travelling solution to a truncated set of the equations (6.1.25) - (6.1.28). If we retain only (6.1.25) and (6.1.26) and neglect $B_{1,3}$ and higher order terms, we are left with the coupled set of equations

$$(\partial_T + \partial_X)(\partial_T + (1-2k^2)\partial_X)A = \mu k^2 A - \mu^2 k^2 l^2 A\alpha_2, \tag{6.2.1}$$

$$(\partial_T + \partial_X)\alpha_2 = (\partial_T + (1-2k^2)\partial_X)|A|^2. \tag{6.2.2}$$

These equations correspond to retaining only the fundamental harmonic and its accompanying mean flow, and are identical in form to those derived by Pedlosky (1972) in a marginally unstable wave packet analysis of the Phillips model of

baroclinic instability. It should be noted here that Pedlosky revised his 1972 work in two papers published in 1982 (Pedlosky (1982a,b)), which are further discussed in Section 6.4. For our purposes here, however, the truncation at the primary modes is still interesting, and useful to analyze and compare to solutions which *do* include higher harmonics.

It is straightforward to verify that there exists a steadily-travelling solution to these truncated equations of the form (Pedlosky, 1972)

$$\begin{aligned} A(X,T) &= A(\xi), \\ \alpha_2(X,T) &= \alpha_2(\xi), \end{aligned} \tag{6.2.3}$$

where $\xi = X - VT$. Substituting (6.2.3) into (6.2.1) and (6.2.2) leads to the solution

$$A(\xi) = A_0 \mathrm{sech}(\kappa\xi), \tag{6.2.4}$$

$$\alpha_2(\xi) = \left(\frac{1-2k^2-V}{1-V}\right) {A_0}^2 \mathrm{sech}^2(\kappa\xi), \tag{6.2.5}$$

where $A_0$ is the maximum envelope amplitude, and where

$$V = \frac{2\mu k^2 - {A_0}^2 \mu^2 l^2 k^2 (1-2k^2)}{2\mu k^2 - {A_0}^2 \mu^2 l^2 k^2}, \tag{6.2.6}$$

$$\kappa = \left(\frac{{A_0}^2 \mu^2 l^2 k^2}{2}\right)^{\frac{1}{2}} \frac{2\mu k^2 - {A_0}^2 \mu^2 l^2 k^2}{2{A_0}^2 \mu^2 l^2 k^4}. \tag{6.2.7}$$

We may determine the perturbation thickness amplitude from (6.1.14) which yields

$$B_{1,1}(\xi) = i\left[\frac{A_0 \kappa (V - 1 + 2k^2)}{k}\right] \mathrm{sech}(\kappa\xi)\tanh(\kappa\xi). \tag{6.2.8}$$

We now follow a similar procedure to that employed in Section 5.2 and analyze this solution in the context of a channel. A plot of the envelope phase speed $V$ versus the along-channel wavenumber $k$ is found in the upper panel of Figure 6. We see that $V$ is greater than both group speeds if $k$ is between 0 and 1. This effect was explained by Pedlosky (1972), who suggested it essentially is a result of a combination of the linear instability and nonlinear stability of the ambient fluid in which the wavepacket is propagating. Behind the packet, the ambient fluid is returning energy to the mean flow at a faster and faster rate as the amplitude falls off, which gives the packet an extra "push" to speeds beyond the group speeds. The same effect in reverse is provided by the fluid in front of the packet, with the same result.

The bottom panel of Figure 6 is a plot of $\kappa$ versus $k$, and we see that as $k$ tends to 0 or 1, $\kappa$ becomes infinite. This simply means that the envelope becomes extremely small in the along-channel direction for these values of $k$, vanishing at the endpoints.

Figures 7a, b, and c are contour plots for the upper layer perturbation pressure

$$\eta_0(x, y, 0, X, 0) = 2A_0 \mathrm{sech}(\kappa X)\cos(kx)\sin(ly), \tag{6.2.9}$$

assuming an initial nondimensional amplitude of $A_0 = 0.5$, assuming time is fixed (i.e. a "snapshot" in time), with $\epsilon = 0.1$, and where $k = 0.2$, $0.5$, and $0.8$, respectively. The plot was produced by the program *Spyglass* from data generated by a Fortran program using (6.2.9) - see Program 2 in the Appendix for an example. The figures show that as $k$ increases, the solitary wave envelope broadens and so includes more fast plane-wave oscillations. Since $V$, the speed of the solitary wave, is larger than the phase speed $c$ the fast oscillations will

appear in front of the wave, reach their apex at the maximum amplitude of the solitary wave, and then disappear again behind the moving wavepacket.

Plots of the gravity current thickness perturbation

$$h_0(x,y,0,X,0) = -\mu l\frac{(1-2k^2-V)}{(1-V)}A_0^2\mathrm{sech}^2(\kappa X)\sin(2ly)+ \\ 2A_0\kappa\frac{(V-1+2k^2)}{k}\mathrm{sech}(\kappa X)\tanh(\kappa X)\cos(kx+\pi/2)\sin(ly), \tag{6.2.10}$$

using the same data as above is shown in Figure 8a, b, and c. These contour plots were produced in exactly the same manner as those for Figure 7a, b, and c, using Program 2 in the Appendix to generate the data. We see that the mean flow adjustment dominates and that the plane wave component simply distorts these cross-channel high and low thickness cells. Figure 9a, b, and c are plots, done the same way as Figures 7 and 8, of the $O(\epsilon^2)$ contribution to the *total* current height, i.e., the leading order nonconstant part of the total current height given by $[(4.1.6)+\epsilon^2(6.2.10)-1]/\epsilon^2$ (i.e., $-y+h_0$) where it is understood that $\gamma=\epsilon^2$.

We note however that there is some question regarding the stability of this solitary wave solution over time. Gibbon *et al.* (1979) examined Pedlosky's equations in detail, and from them derived a sine-Gordon equation (see Chapter 7). They concluded from this derivation that if the linear growth rate is positive, then the disturbance is itself unstable to small perturbations on the "tail" of the wave because there is a source of available potential energy there. We have not been able to determine the role of the higher harmonics in the evolution of this solution, or whether similar solutions exist for higher order truncations.

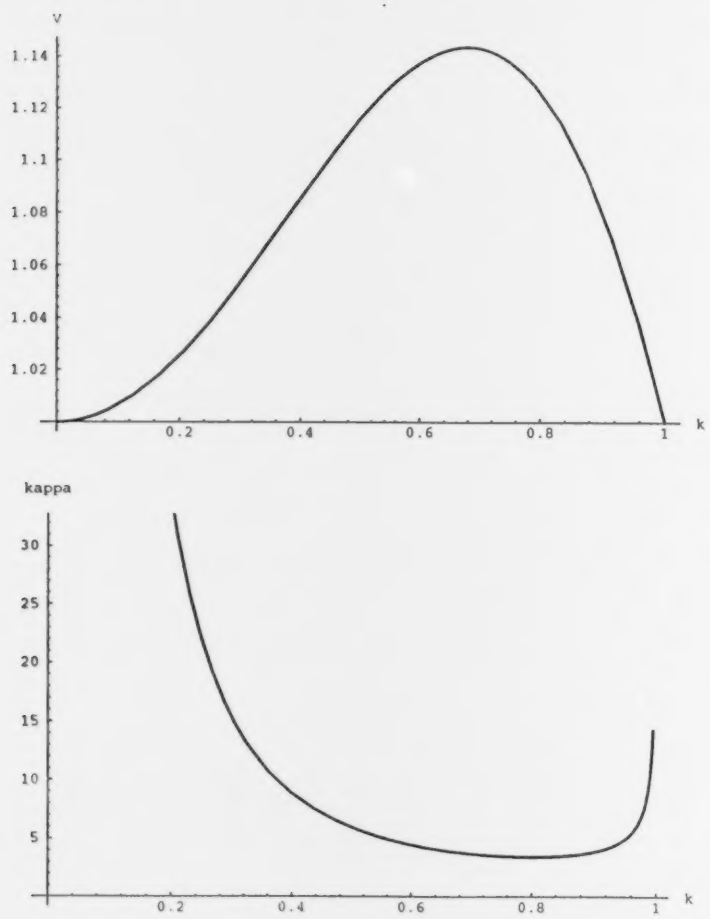


Figure 6. Upper panel - Envelope speed $V$ versus $k$ (from equation (6.2.6)) for the soliton solution. Lower panel - $\kappa$ versus $k$ (from equation (6.2.7)) for the soliton solution.

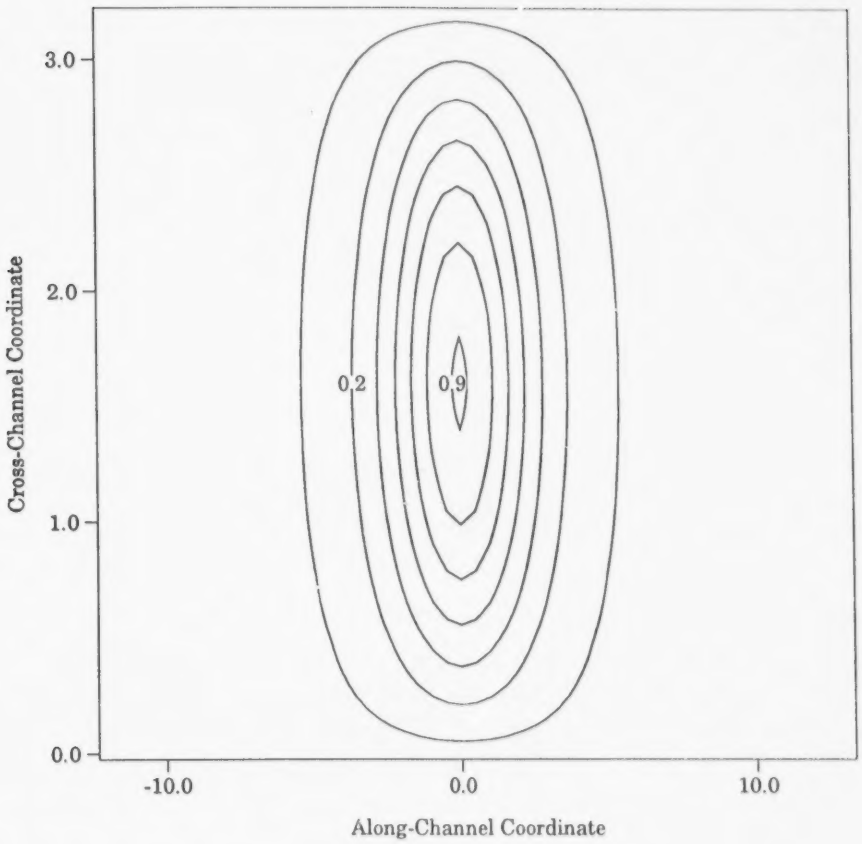


Figure 7a. Contour plot of the leading order nondimensional perturbation pressure (from equation (6.2.9)) where $k = 0.2$, $l = 0.978$, $\mu = 2.0$ and $A_0 = 0.5$. Contour intervals $\pm 0.15$.

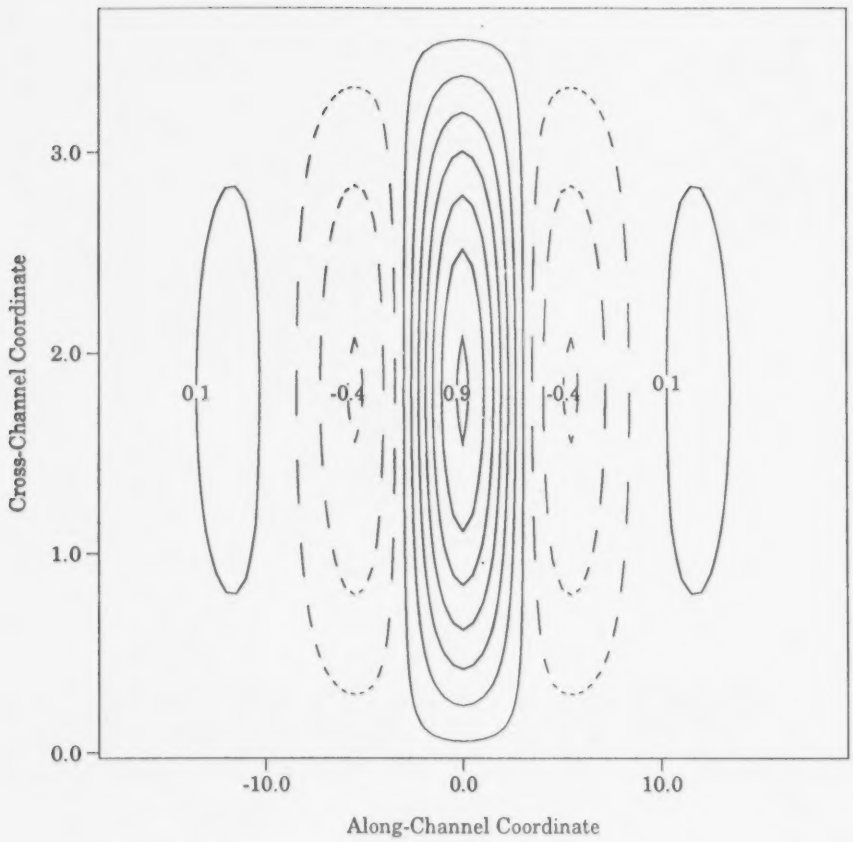


Figure 7b. Contour plot of the leading order nondimensional perturbation pressure (from equation (6.2.9)) where $k = 0.5$, $l = 0.866$, $\mu = 2.0$ and $A_0 = 0.5$. Contour intervals $\pm 0.15$.

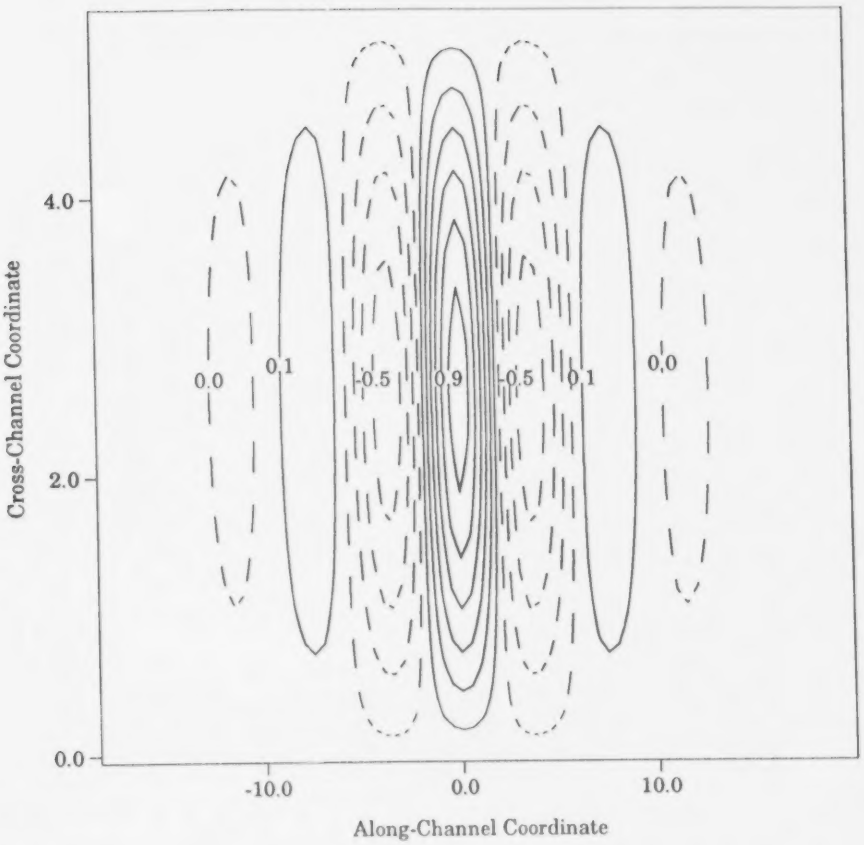


Figure 7c. Contour plot of the leading order nondimensional perturbation pressure (from equation (6.2.9)) where $k = 0.8$, $l = 0.600$, $\mu = 2.0$ and $A_0 = 0.5$. Contour intervals $\pm 0.15$.

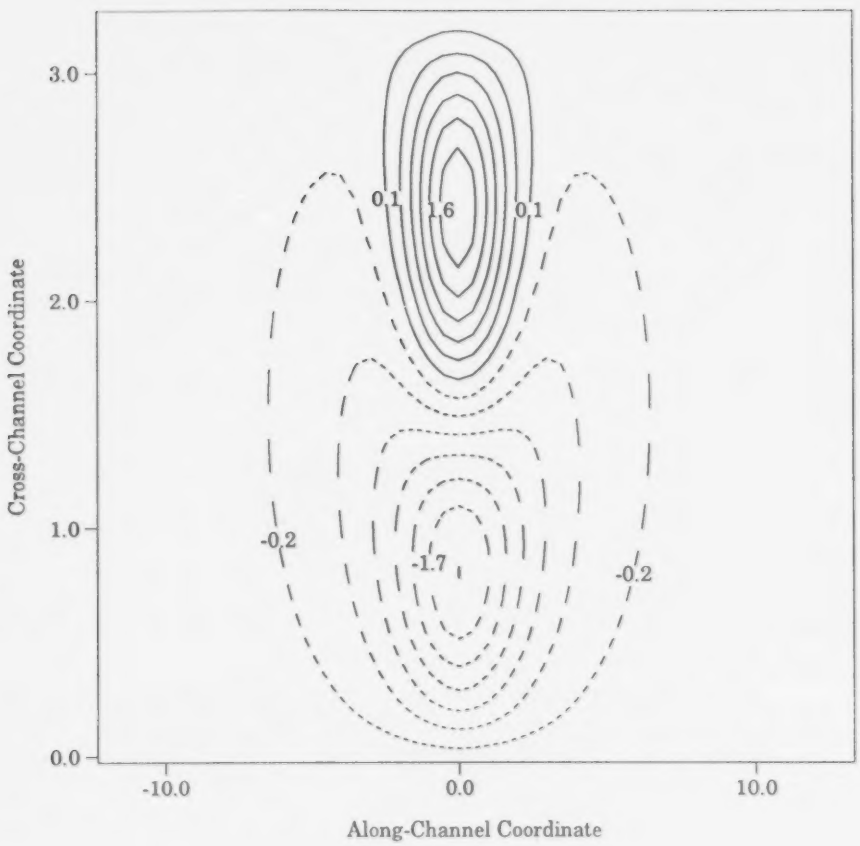


Figure 8a. Contour plot of the leading order nondimensional gravity current perturbation thickness (from equation (6.2.10)) where $k = 0.2$, $l = 0.978$, $\mu = 2.0$ and $A_0 = 0.5$. Contour intervals $\pm 0.03$.

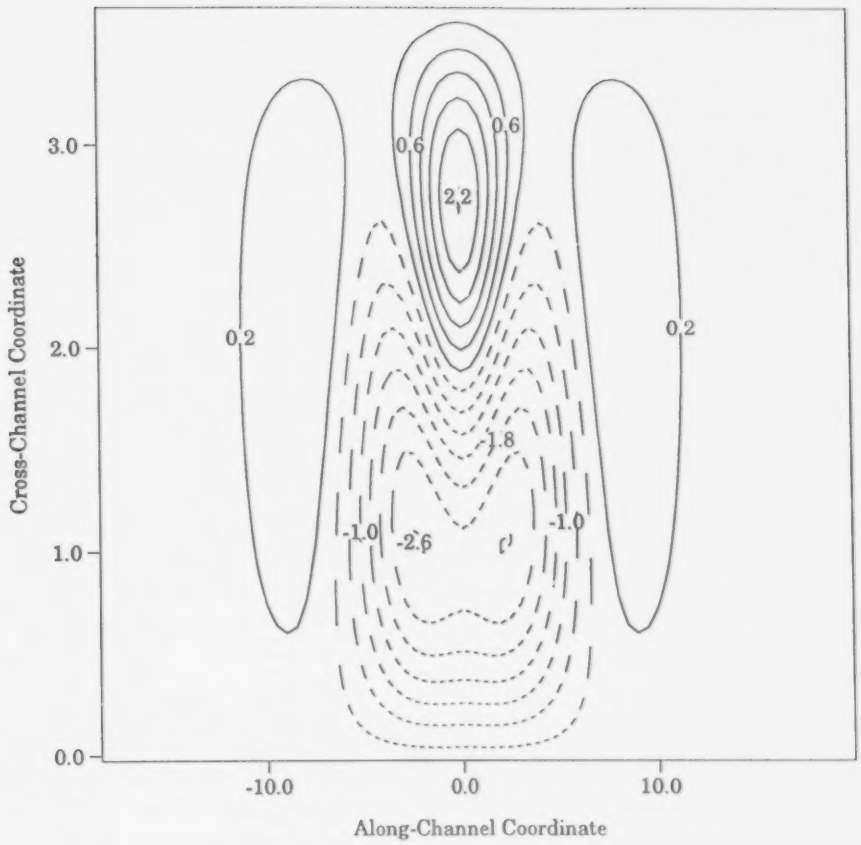


Figure 8b. Contour plot of the leading order nondimensional gravity current perturbation thickness (from equation (6.2.10)) where $k = 0.5$, $l = 0.866$, $\mu = 2.0$ and $A_0 = 0.5$. Contour intervals $\pm 0.04$.

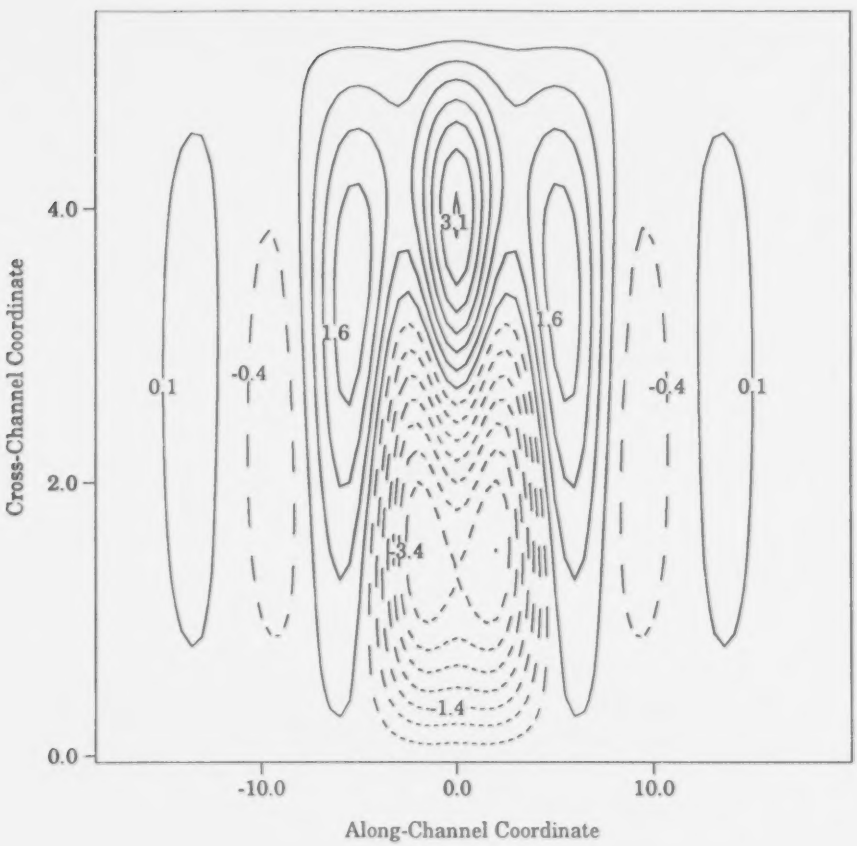


Figure 8c. Contour plot of the leading order nondimensional gravity current perturbation thickness (from equation (6.2.10)) where $k = 0.8$, $l = 0.600$, $\mu = 2.0$ and $A_0 = 0.5$. Contour intervals $\pm 0.05$.

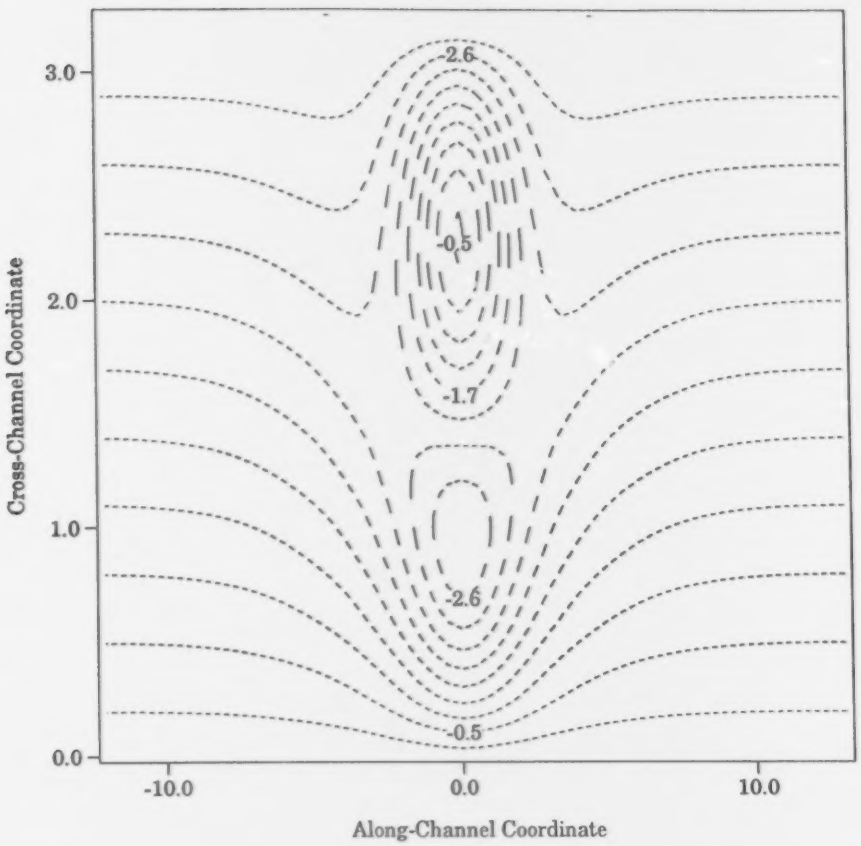


Figure 9a. Contour plot of the leading order nondimensional variable part of the total current height scaled by $\epsilon^{-2}$ where $k = 0.2$, $l = 0.978$, $\mu = 2.0$ and $A_0 = 0.5$. Contour intervals $\pm 0.03$.

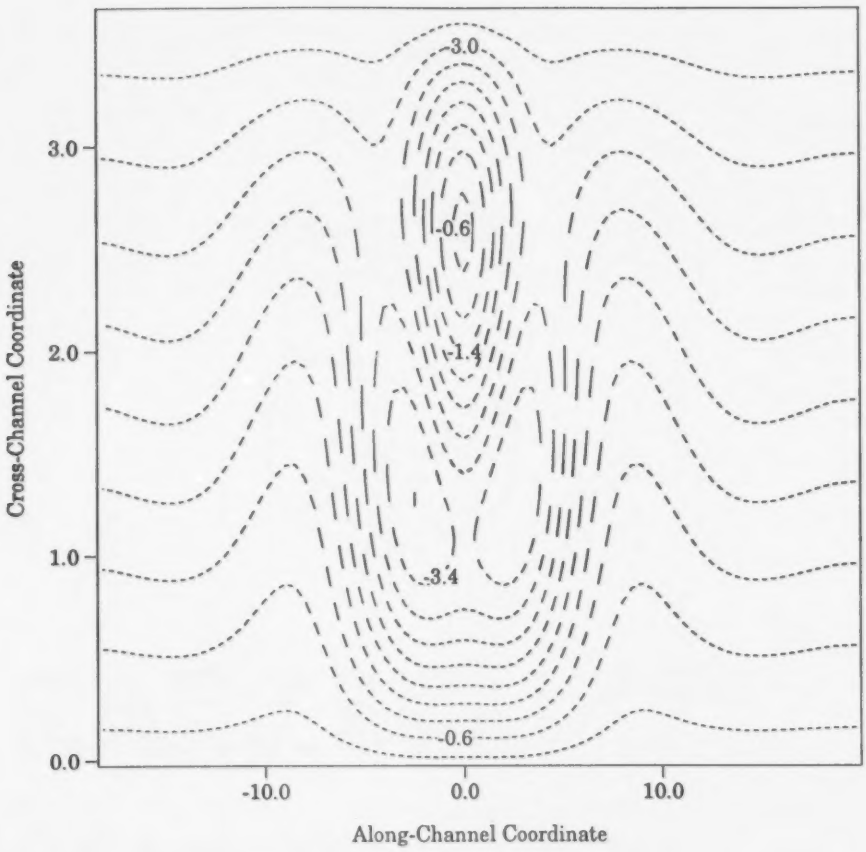


Figure 9b. Contour plot of the leading order nondimensional variable part of the total current height scaled by $\epsilon^{-2}$ where $k = 0.5$, $l = 0.866$, $\mu = 2.0$ and $A_0 = 0.5$. Contour intervals $\pm 0.04$.

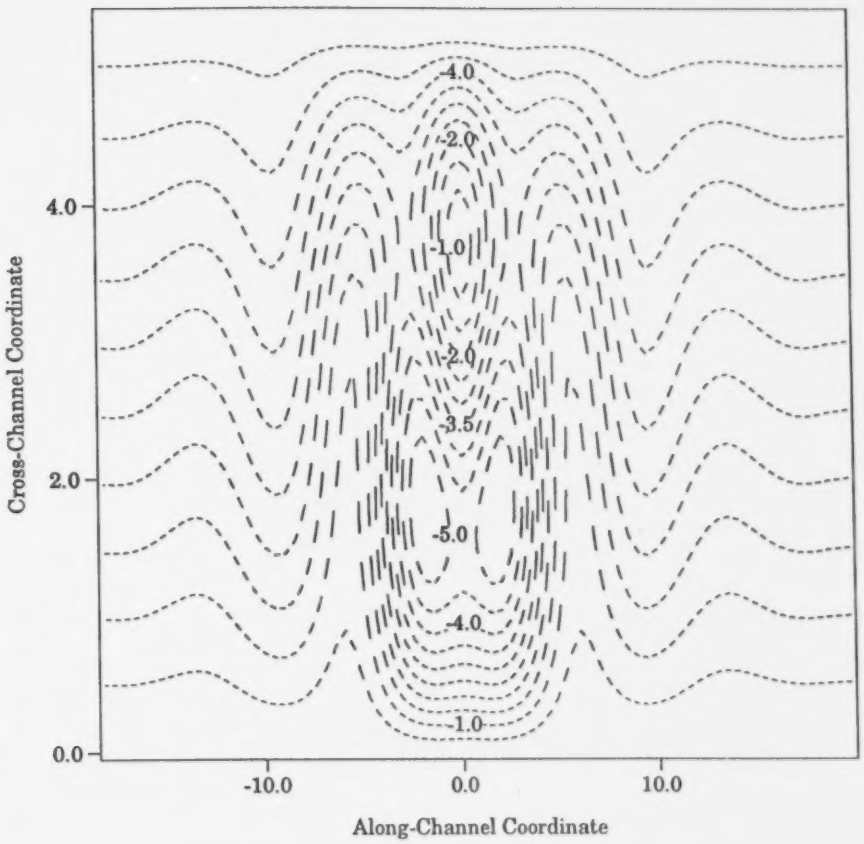


Figure 9c. Contour plot of the leading order nondimensional variable part of the total current height scaled by $\epsilon^{-2}$ where $k = 0.8$, $l = 0.600$, $\mu = 2.0$ and $A_0 = 0.5$. Contour intervals $\pm 0.05$.

*6.3 Multiple Equation Representation*

All of the remaining spectral analysis will be done by setting $\partial_X = 0$ in the system (6.1.25) - (6.1.28). We do this because the partial differential equations in their present form are intractable analytically, and are very difficult to resolve numerically, so we content ourselves with examining the time evolution of the various modes as described by the resulting set of ordinary differential equations. With this assumption made, some points of interest should be noted here. First, if $B_{1,3}$ is set to zero in (6.1.26) and the equation is then integrated with respect to the slow time $T$, we find that

$$\alpha_2(T) = |A(T)|^2 + |A(0)|^2. \tag{6.3.1}$$

If this equation is substituted into (6.1.25), we find that the result is equivalent to (5.1.29) if we apply it to the most unstable mode (i.e set $k^2 + l^2 = 1$ in that equation). Another interesting aspect here is that if we *sum* all equations represented by (6.1.27) and add them to (6.1.26), we find the following

$$\sum_{n=1}^{\infty} \frac{d\alpha_{2n}}{dT} = \frac{d|A|^2}{dT}, \tag{6.3.2}$$

which leads immediately to

$$\sum_{n=1}^{\infty} \alpha_{2n} = |A|^2 + |A_0|^2. \tag{6.3.3}$$

Equation (6.3.3) implies that, if all the excited modes are represented, that the sum of *all* the mean flow adjustment amplitudes at any time $T$ is equal to the modulus squared of the free surface perturbation amplitude to within a constant. This suggests strongly that, if the assumption is made that $A$ is bounded, the

mean flow modes fall off in importance as the "ladder" is climbed (but there is no proof for this because we cannot claim that $\alpha_{n+2} < \alpha_n$ for all $n$).

We now examine in more detail the system of equations (6.1.25) - (6.1.28). Three different truncation points are applied, and standard Runge-Kutta methods are used to integrate the resulting set of equations numerically. We first derive a simple system of four equations, where two mean flow modes are included as follows

$$\frac{d^2A}{dT^2} = \mu k^2 A - \mu^2 l^2 k^2 A \alpha_2,$$

$$\frac{d\alpha_2}{dT} = \frac{d|A|^2}{dT} + k(AB^*_{1,3} + A^* B_{1,3}),$$

$$\frac{dB_{1,3}}{dT} = -\frac{\mu^2 l^2 k A}{4}(4\alpha_2 - 16\alpha_4),$$

$$\frac{d\alpha_4}{dT} = -k(AB^*_{1,3} + A^* B_{1,3}). \tag{6.3.4}$$

In order to simplify the system (6.3.4), we assume that all variables have constant phases, which allows us to use the linear theory growth rate as an initial condition (as mentioned in Section 5.1) on the perturbation pressure amplitude. We use the same parameter settings as in the previous subsection, except here we set the nondimensional initial amplitude $A_0 = 0.01$. A fourth-order Runge-Kutta scheme for solving systems of ODEs numerically was then applied (see Program 3 in the Appendix), and the results for the perturbation pressure amplitude are plotted in Figure 10a. The nondimensional perturbation pressure amplitude reaches about 130 times the initial perturbation amplitude before non-

linear effects finally halt the growth. The timescale of the disturbance is again very long, similar to what was found in Chapter 5, and it is again due to the very small supercriticality applied to the gravity current thickness.

In Figure 10b, we plot, using an eighth-order Runge-Kutta scheme (see Program 4 in the Appendix for an example - note that the fourth-order and eighth-order Runge-Kutta methods produce results with essentially the same level of accuracy, because the solutions in this section are well-behaved), the results from performing exactly the same procedure for a system of 12 equations, which essentially amounts to adding one more mean flow mode $(\alpha_6)$ and including perturbation thickness modes up to $B_{2,4}$ and $B_{3,5}$ .to make a complete set (to work with real valued functions only, we set $\tilde{B}_{2m,2n} = -i\hat{B}_{2m,2n}$). The figure shows a very similar result, where the pressure amplitude again grows to approximately 130 times the initial amplitude before nonlinearities stop and reverse the growth. It is interesting to note that the amplitude oscillates as before, but several more cycles are required to form a period than in the 4 equation system.

Another set of equations was developed by truncating after the mean flow mode $\alpha_{10}$ and after the even thickness mode $B_{10,10}$ and the odd thickness mode $B_{9,9}$. The perturbation pressure amplitude is plotted in Figure 11a, again using an eighth-order Runge-Kutta scheme (see Program 4 in the Appendix - all of Figures 11 and 12 were calculated using this program), and we see that the amplitude is now constricted somewhat, with a secondary longwave periodicity also appearing. From this evidence it may be suggested that this amplitude, if enough equations were integrated, may stabilize at some new finite level and remain there for all time.

Figures 11b and 11c show the corresponding primary perturbation thickness mode $-iB_{1,1}$ and primary mean flow mode $\alpha_2$. Figure 11d is a plot of the

mode $B_{8,6}$, which shows that this higher mode has a much smaller maximum and minimum amplitude than do the primary modes (about 20 times smaller), lending credence to the suggestion made previously that the higher modes will tend to fall off in significance.

Figures 12a and 12b are plots of $A(T)$ for the 56 equation set where $k = 0.2$ and $k = 0.8$, respectively. It is easy to see from these plots that as the along-channel wavenumber increases, the frequency of the oscillation also increases (see Figure 11a as well for the $k = 0.5$ plot).

Other truncations were applied and it was found, in general, that if the cutoff was applied too soon after (but not directly after) a mean flow mode, then exponentially growing solutions resulted for $A(T)$. In particular, if $B_{1,3}$ is included but not the second mean flow mode $\alpha_4$, then exponentially growing solutions are obtained. If the truncation was applied directly after a mean flow mode, then the equation set yielded bounded oscillating solutions, where the cycles forming a period became more complex with each increase in size of the set. This would seem to indicate that the mean flow modes have a stabilizing influence on the solutions, possibly by acting to restrict the potential energy available to the higher modes. We were unable to rigorously establish whether or not increasing the number of modes always leads to an increase in the number of cycles needed to form a period, although the numerical evidence seems to indicate this.

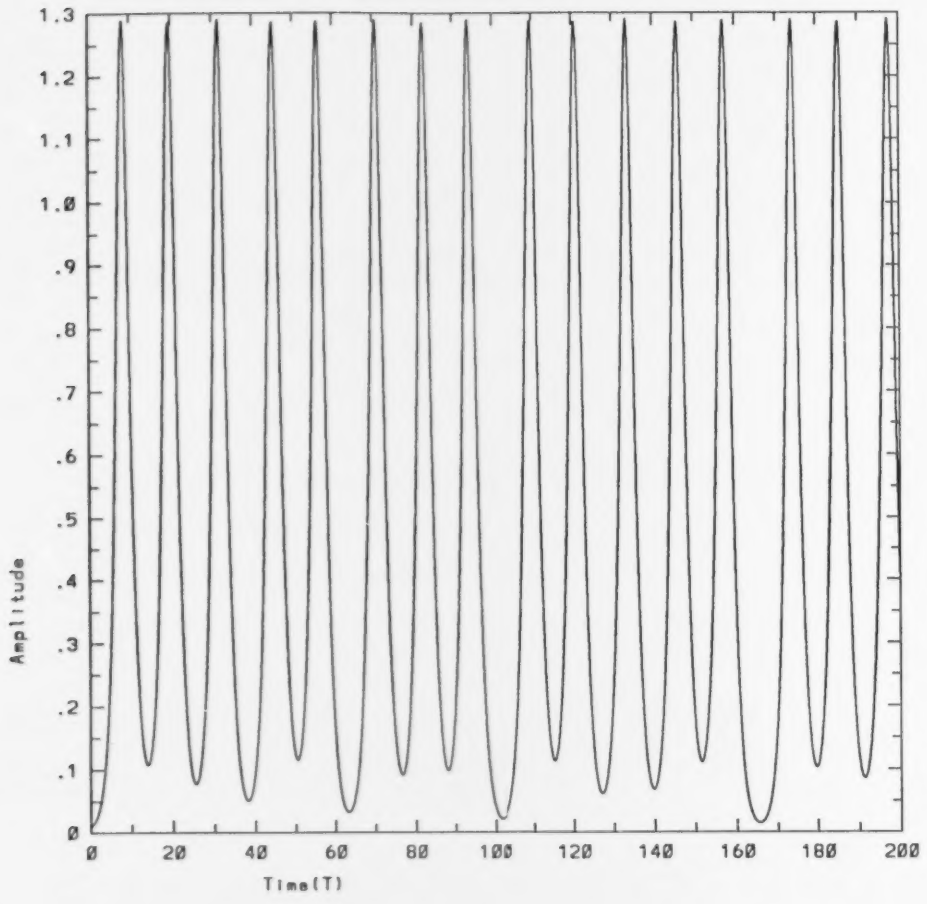


Figure 10a. Plot of temporal solution for $A(T)$ for the 4 equation set (from equations (6.3.4)) where $k = 0.5$, $l = 0.866$, $\mu = 2.0$ and $A_0 = 0.01$.

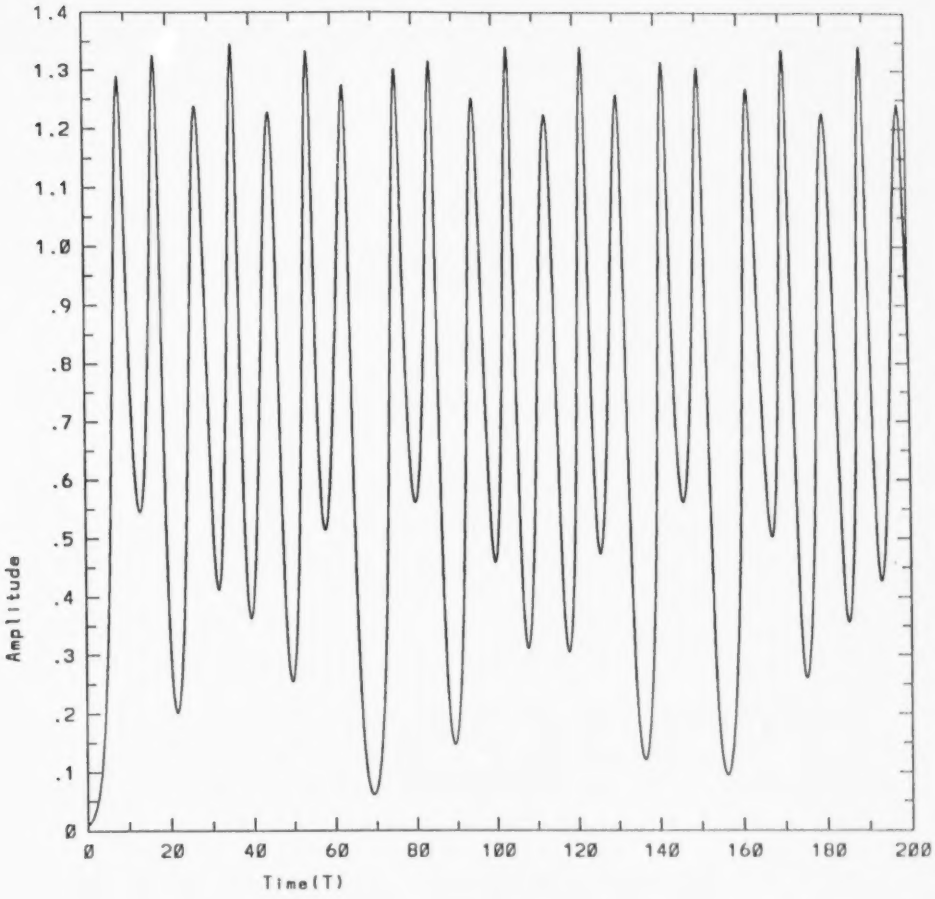


Figure 10b. Plot of temporal solution for $A(T)$ for the 12 equation set where $k = 0.5$, $l = 0.866$, $\mu = 2.0$ and $A_0 = 0.01$.

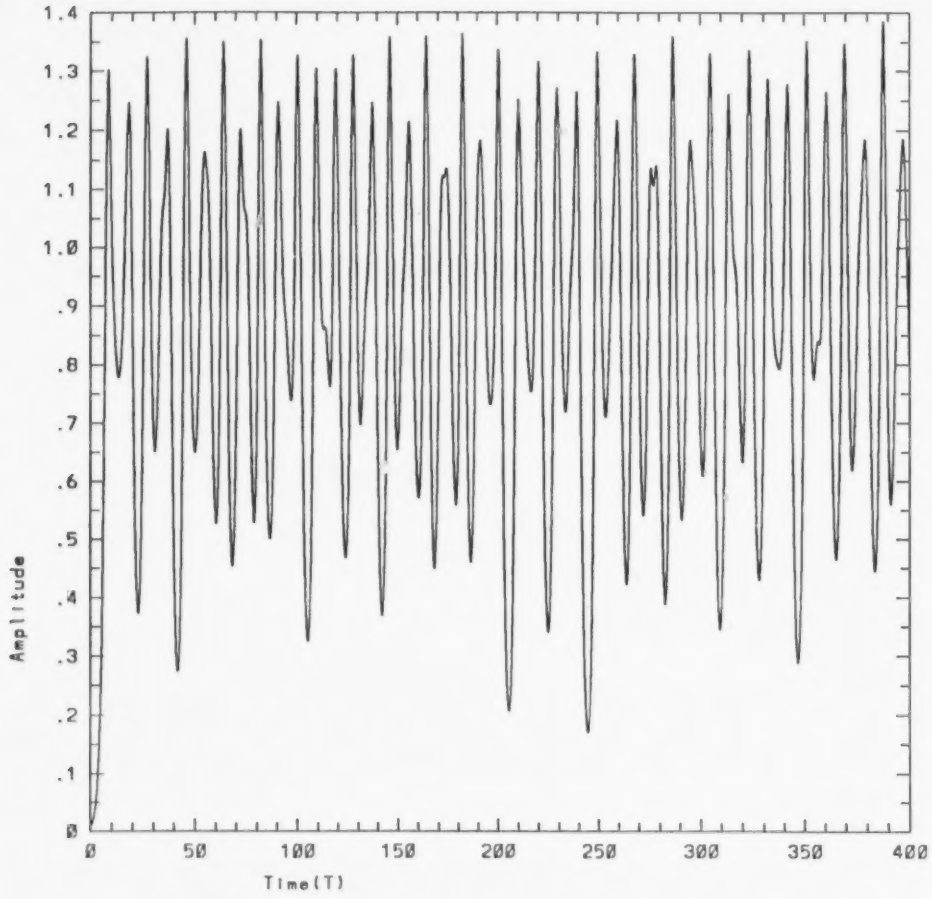


Figure 11a. Plot of temporal solution for $A(T)$ for the 56 equation set where $k = 0.5$, $l = 0.866$, $\mu = 2.0$ and $A_0 = 0.01$.

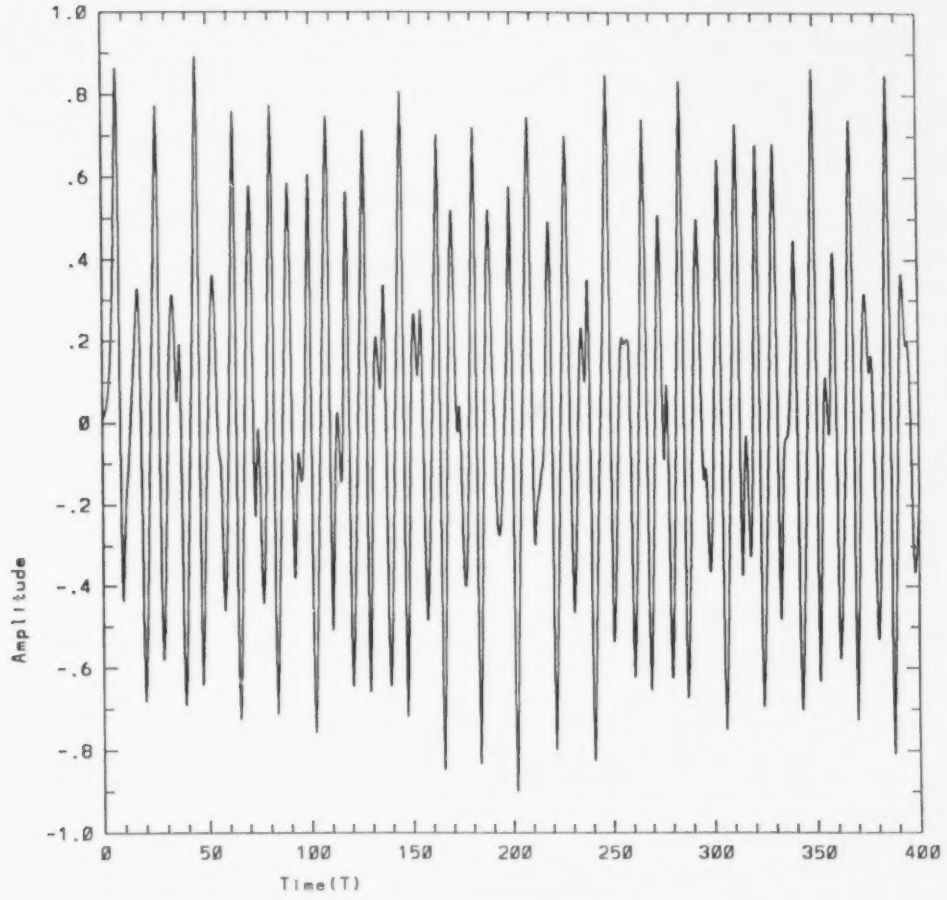


Figure 11b. Plot of temporal solution for $-iB_{1,1}$ for the 56 equation set where $k = 0.5$, $l = 0.866$, $\mu = 2.0$ and $A_0 = 0.01$.

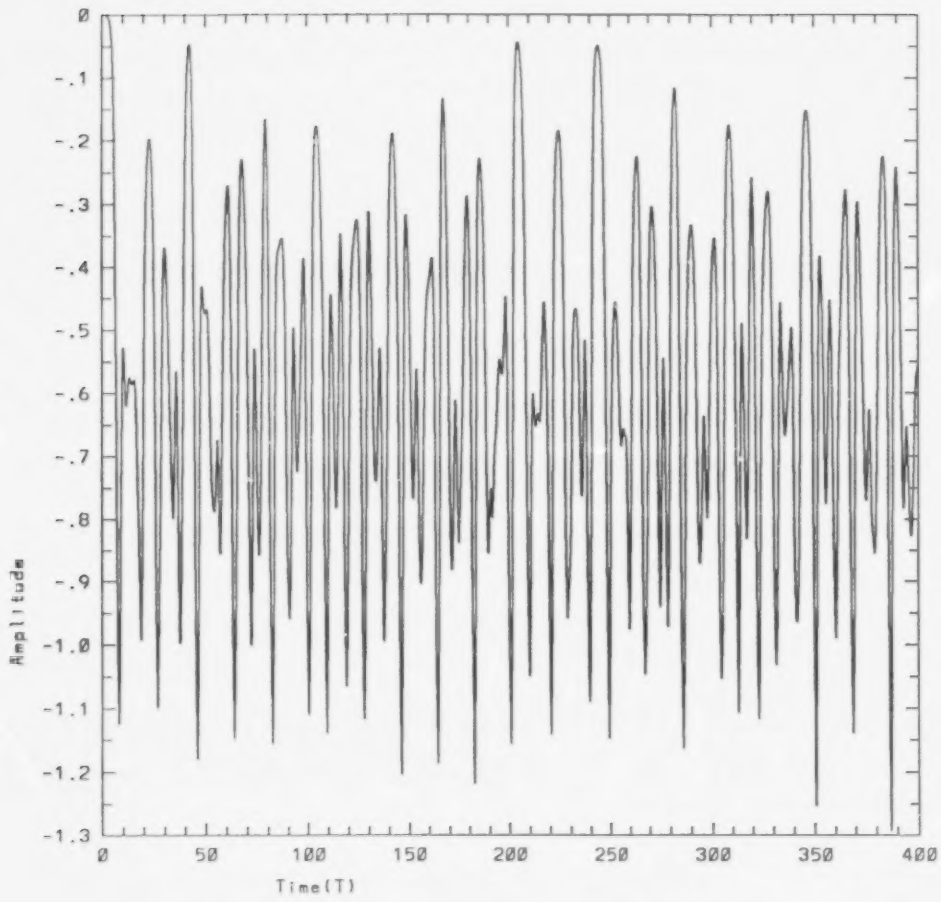


Figure 11c. Plot of temporal solution for $\alpha_2$ for the 56 equation set where $k = 0.5$, $l = 0.866$, $\mu = 2.0$ and $A_0 = 0.01$.

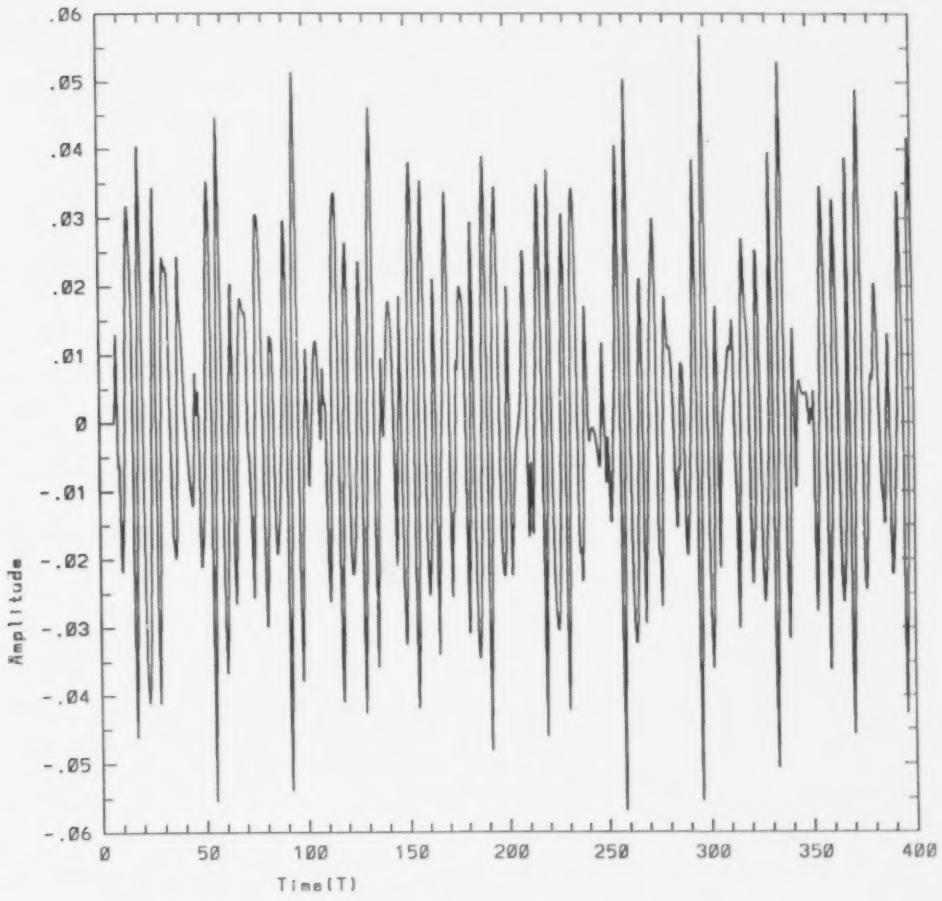


Figure 11d. Plot of temporal solution for $B_{s,6}$ for the 56 equation set where $k = 0.5$, $l = 0.866$, $\mu = 2.0$ and $A_0 = 0.01$.

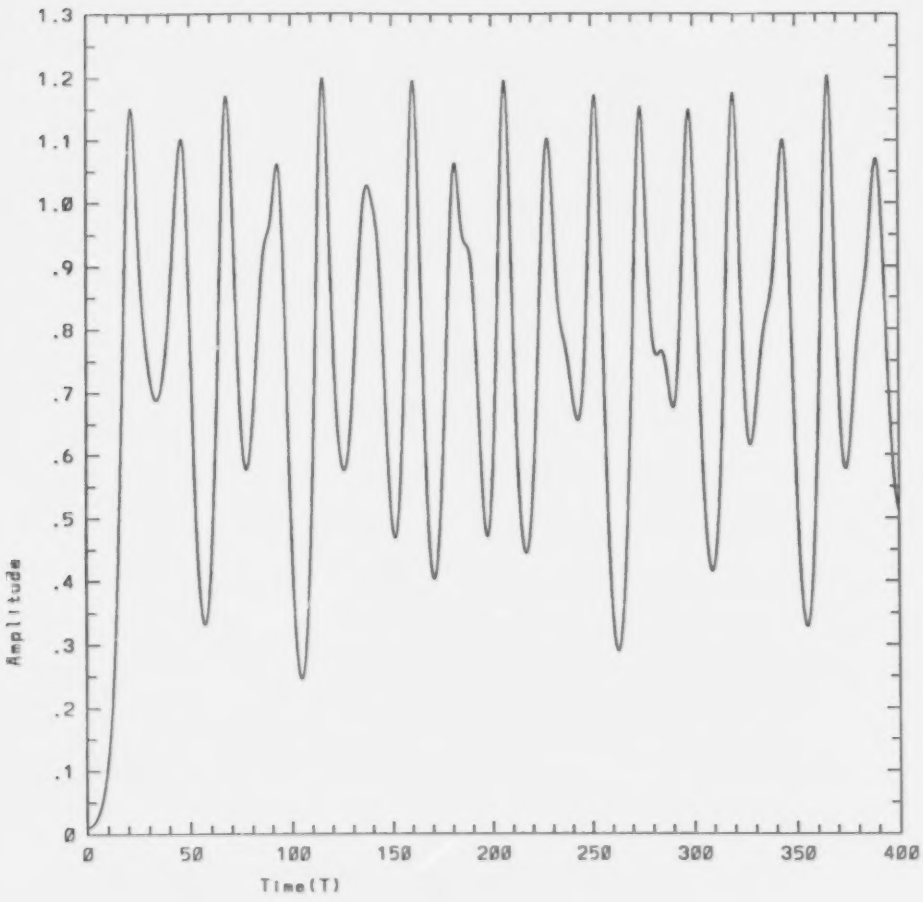


Figure 12a. Plot of temporal solution for $A(T)$ for the 56 equation set where $k = 0.2$, $l = 0.978$, $\mu = 2.0$ and $A_0 = 0.01$.

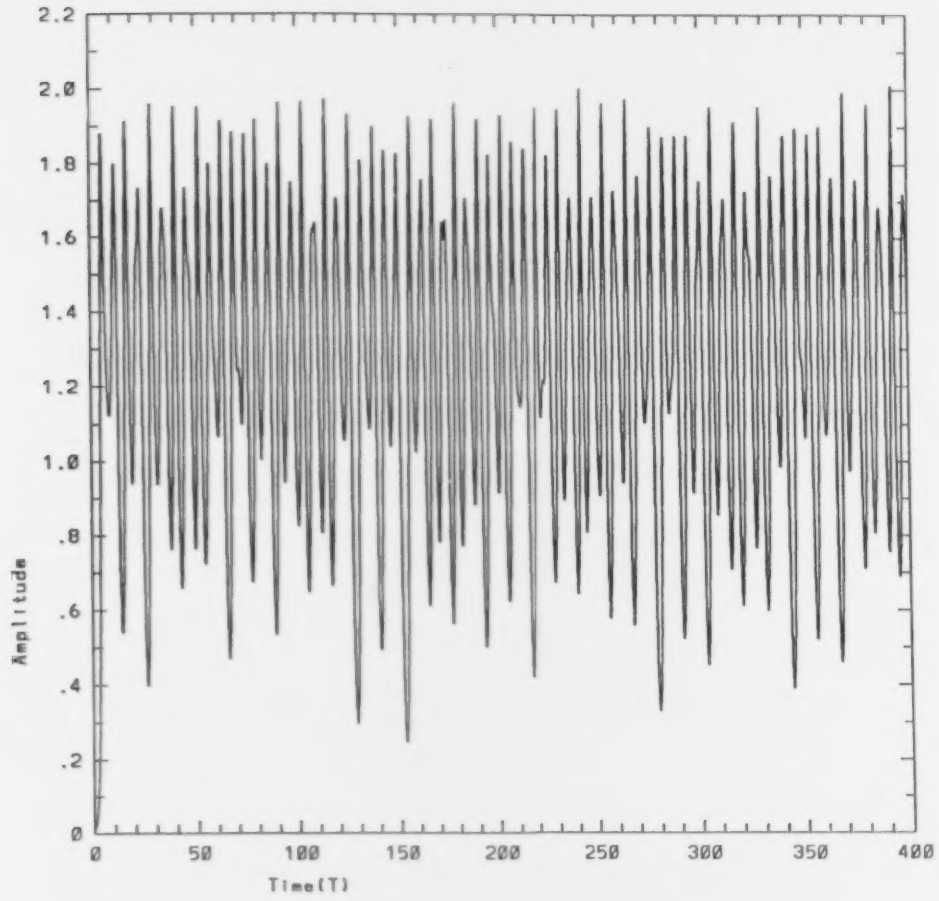


Figure 12b. Plot of temporal solution for $A(T)$ for the 56 equation set where $k = 0.8$, $l = 0.600$, $\mu = 2.0$ and $A_0 = 0.01$.

*6.4 A Solution to the Complete Multiple Equation Set*

As has been alluded to previously, Pedlosky (1982a,b) revised his 1972 calculations for the mode at the bottom of the marginal stability curve which he had derived from the Phillips model. In the new work, he found an infinite system of coupled nonlinear partial differential equations which have substantially the same form as those presented in (6.1.25) - (6.1.28). This revision was motivated by some numerical results presented by Boville (1981), which showed that there were important differences between these and Pedlosky's analytical results for this mode, which manifested themselves in the form of higher harmonics not seen in Pedlosky's 1972 analysis. As an explanation for the existence of these higher modes, Pedlosky (1982a) points out that the potential vorticity gradient disappears in one of the layers, as well as the Doppler-shifted frequency of the wave. This generates a singularity in the linearized equations, and so the whole layer is a critical layer for this wavenumber. This then implies (Warn and Gauthier, 1989) that since the mean advection of potential vorticity is no longer important, the initial form of the perturbation will dominate the dynamics, and higher harmonics will be generated rather quickly.

For example, in our model, the leading order potential vorticity in the lower layer, from equation (2.3.35), is $1/h_0$, and so the gradient in the across-channel direction is

$$\mathrm{PV}_y = -\frac{h_{0y}}{h_0^2}. \tag{6.4.1}$$

But $h_0 = 1 - \gamma y$, so $h_{0y} = -\gamma = 0$ for the critical mode, and so the basic state potential vorticity gradient vanishes. Also, equation (4.3.4), which is the linearized normal mode equation, shows that if $c = 1$, which is the phase speed

for the lower (and upper) layer when $\gamma_c = 0$, then there exists a singularity in the equation. This implies the existence of a critical layer there. These similarities between Pedlosky's model and our model explain why the analysis results in similar wavepacket equations for the minimum critical thickness.

Warn and Gauthier (1989) found an analytical solution to Pedlosky's infinite set of equations (Pedlosky (1982b)) by changing the focus of the analysis from a spectral approach, which we have already outlined in this chapter, to an attempt to find a solution to the solvability conditions directly by casting them in the form of an initial value problem. We now will outline this solution as it relates to our model.

We first write down the solvability conditions. From equation (6.1.9), we have

$$\mu\eta_{0x} - \mu J(\eta_0, h_0) - h_{0T} - h_{0X} = 0, \tag{6.4.2}$$

for the gravity current equation, and for the upper layer, we note that the right hand side of equation (6.1.13) indicates a condition of the form

$$\langle [(A_T + (1-2k^2)A_X)\Phi + h_{0x}]\Phi^* \rangle = 0, \tag{6.4.3}$$

where $\Phi = \sin(ly)\exp(ik\theta)$ and

$$\langle (*) \rangle = \frac{1}{2\lambda}\int_{-\lambda}^{\lambda}\int_0^L (*)\,dxdy = \frac{1}{2\lambda}\int\int_{\Omega}(*)\,dxdy, \tag{6.4.4}$$

is the area average over the domain. This is simply the statement that, since the left hand side operator is dispersive, only terms multiplied by $\Phi$ will give rise to secular growth. This is essentially an application of the Fredholm Alternative Theorem (Boyce and DiPrima, 1986).

Now let us work with the purely temporal problem in the slow variables (i.e., set $\partial_X = 0$). Then (6.4.3) may be rewritten as

$$A_T\langle\Phi\Phi^*\rangle = -\langle h_{0x}\Phi^*\rangle, \tag{6.4.5}$$

or

$$A_T = -\frac{\langle h_{0x}\Phi^*\rangle}{\langle\Phi\Phi^*\rangle} = \Gamma\langle h_{0x}\Phi^*\rangle, \tag{6.4.6}$$

where $\Gamma = -1/\langle\Phi\Phi^*\rangle$.

Now insert the solution for $\eta_0$ (i.e. (6.1.6a)) into (6.4.2), to get

$$\mu A\Phi_x - \mu J(A\Phi, h_0) - h_{0T} + \text{c.c.} = 0. \tag{6.4.7}$$

We may let $A$ be real without loss of generality; in fact, if $A$ is real initially, then it remains so for all time (Warn and Gauthier, 1989). We may prove this statement in the following way. First, (6.4.6) is differentiated with respect to $T$ to obtain

$$A_{TT} = \Gamma\langle h_{0xT}\Phi^*\rangle. \tag{6.4.8}$$

Also, we rewrite (6.4.7) as, after differentiation with respect to $x$

$$\begin{aligned} h_{0Tx} &= -\mu J(A\Phi + A^*\Phi^*, h_0 - y)_x \\ &= -\mu A J(\Phi, h_0 - y)_x - \mu A^* J(\Phi^*, h_0 - y)_x. \end{aligned} \tag{6.4.9}$$

Inserting (6.4.9) into (6.4.8) leaves

$$A_{TT} = -\mu\Gamma A\langle J(\Phi, h_0 - y)_x\Phi^*\rangle - \mu\Gamma A^*\langle J(\Phi^*, h_0 - y)_x\Phi^*\rangle. \tag{6.4.10}$$

We look at each of the terms on the right hand side of (6.4.10) separately. The first term becomes

$$\begin{aligned}-\mu\Gamma A\langle J(\Phi,h_0-y)_x\Phi^*\rangle &= -\mu\Gamma A\langle J(\Phi,h_0-y)\Phi^*_x\rangle\\ &= -ik\mu\Gamma A\langle J(\Phi,h_0-y)\Phi^*\rangle\\ &= -ik\mu\Gamma A\langle \Phi_x\Phi^*(h_0-y)_y-\Phi_y\Phi^*(h_0-y)_x\rangle,\end{aligned} \tag{6.4.11}$$

where in the first line of (6.4.11), we have integrated by parts with respect to $x$ and used the periodic boundary conditions on $\Phi$ and $h_0$. The quantity $\Phi_y\Phi^* = l\cos(ly)\sin(ly)$ is independent of $x$, and so the second term on the right hand side of (6.4.11) is zero after an $x-$integration and application of the periodicity boundary conditions on $h_0$. The first term may be rewritten as

$$\begin{aligned}-ik\mu\Gamma A\langle \Phi_x\Phi^*(h_0-y)_y\rangle &= k^2\mu\Gamma A\langle \Phi^*\Phi(h_0-y)_y\rangle\\ &= k^2\mu\Gamma A\langle |\Phi|^2(h_0-y)_y\rangle.\end{aligned} \tag{6.4.12}$$

The second term on the right hand side of (6.4.10) becomes

$$\begin{aligned}-\mu\Gamma A^*\langle J(\Phi^*,h_0-y)_x\Phi^*\rangle &= -\mu\Gamma A^*\langle J(\Phi^*,h_0-y)\Phi^*_x\rangle\\ &= -ik\mu\Gamma A^*\langle J(\Phi^*,h_0-y)\Phi^*\rangle\\ &= -\frac{ik\mu\Gamma A^*}{2}\langle J(\Phi^{*2},h_0-y)\rangle\\ &= \frac{ik\mu\Gamma A^*}{4\lambda}\iint_\Omega \nabla\cdot[\Phi^{*2}\hat{e}_3\times\nabla(h_0-y)]\,dxdy\\ &= \frac{ik\mu\Gamma A^*}{4\lambda}\oint_{\partial\Omega}\Phi^{*2}[\mathbf{n}\cdot\hat{e}_3\times\nabla(h_0-y)]\,dS\end{aligned}$$

$$
\begin{aligned}
=&\frac{ik\mu\Gamma A^*}{4\lambda}\Big\{-\int_0^L[-\Phi^{*2}(h_0-y)_y]_{x=-\lambda}\,dy+\int_{-\lambda}^{\lambda}[\Phi^{*2}(h_0-y)_x]_{y=L}\,dx\\
&+\int_0^L[-\Phi^{*2}(h_0-y)_y]_{x=\lambda}\,dy-\int_{-\lambda}^{\lambda}[\Phi^{*2}(h_0-y)_x]_{y=0}\,dx\Big\}\\
=&0,
\end{aligned}
\tag{6.4.13}
$$

where the first and third terms in the last two lines of (6.4.13) sum to zero by the periodicity boundary condition, and the second and fourth terms are zero because $h_{0x}=0 \quad \text{on} \quad y=0,L.$

We may therefore rewrite (6.4.10) as

$$
A_{TT}=k^2\mu\Gamma A\langle|\Phi|^2(h_0-y)_y\rangle. \tag{6.4.14}
$$

It is clear from (6.4.14) that if $A$ is real at $t=0,$ then it is real for all time $t,$ which proves the assertion.

With this in mind, we may rewrite (6.4.7) as

$$
h_{0T}+2\mu AJ(\Phi,h_0-y)=0. \tag{6.4.15}
$$

We also rescale the independent variables, to simplify the subsequent calculations

$$
\tau=klT; \quad \mathcal{X}=kx; \quad \mathcal{Y}=ly-\pi/2, \tag{6.4.16}
$$

so that (6.4.15) becomes

$$
h_{0\tau}+2\mu AJ(\Phi,h_0-(\mathcal{Y}+\pi/2)/l)=0, \tag{6.4.17}
$$

where $J(A,B)=A_{\mathcal{X}}B_{\mathcal{Y}}-A_{\mathcal{Y}}B_{\mathcal{X}},$ and we revise (6.4.6) to

$$
A_\tau=\Gamma_1\langle h_{0\mathcal{X}}\Phi^*\rangle, \tag{6.4.18}
$$

where $\Gamma_1 = -1/(l\langle\Phi\Phi^*\rangle)$.

We now define a new variable $\nu$

$$\nu = 2\mu \int_0^\tau A(\tau')d\tau', \tag{6.4.19}$$

which allows (6.4.17) to be written in the simpler form

$$h_{0_\nu} + J(\Phi, h_0 - (\mathcal{Y} + \pi/2)/l) = 0. \tag{6.4.20}$$

Finally, if we let $h_0 - (\mathcal{Y} + \pi/2)/l = g$, we may write

$$g_\nu + J(\Phi, g) = 0. \tag{6.4.21}$$

Now we derive an equation for $A(\tau)$. If (6.4.21) is multiplied by $\mathcal{Y}$ and then the area average is taken, the following expression is obtained after transforming the independent variable $\nu$ back to $\tau$ using (6.4.19).

$$\langle \mathcal{Y} g\rangle_\tau + 2\mu A\langle \mathcal{Y} J(\Phi, g)\rangle = 0, \tag{6.4.22}$$

where the area average is now taken to be over the $(\mathcal{X}, \mathcal{Y})$ coordinates. If we

rewrite the Jacobian using (3.2.24) and rearrange, we find

$$\begin{aligned}
\langle \mathcal{Y} g\rangle_\tau =& 2\mu A\langle \mathcal{Y}\nabla\cdot(\Phi\hat{e}_3\times\nabla g)\rangle \\
=& 2\mu A\langle \nabla\cdot(\mathcal{Y}\Phi\hat{e}_3\times\nabla g)\rangle - \langle \Phi(\hat{e}_3\times\nabla g)\cdot\nabla\mathcal{Y}\rangle \\
=& 2\mu A\oint_{\partial\Omega}\mathcal{Y}\Phi\mathbf{n}\cdot(\hat{e}_3\times\nabla g)\,dS \\
& - 2\mu A\langle \Phi\nabla\cdot(\mathcal{Y}\hat{e}_3\times\nabla g)+\Phi\mathcal{Y}\nabla\cdot(\hat{e}_3\times\nabla g)\rangle \\
=& 0 - 2\mu A\langle \Phi\nabla\cdot\mathcal{Y}(-g_{\mathcal{Y}},g_{\mathcal{X}})\rangle \\
=& -2\mu A\langle \Phi(-\mathcal{Y}g_{\mathcal{Y}\mathcal{X}}+g_{\mathcal{X}}+\mathcal{Y}g_{\mathcal{X}\mathcal{Y}})\rangle \\
=& -2\mu A\langle \Phi g_{\mathcal{X}}\rangle,
\end{aligned} \tag{6.4.23}$$

where the vector identity (3.2.49) has been used twice, and (3.2.52) has been applied. The boundary integral is zero because

$$\begin{aligned}
&\oint_{\partial\Omega}\mathcal{Y}\Phi\mathbf{n}\cdot(\hat{e}_3\times\nabla g)\,dS = \\
&\quad -\int_{\frac{\pi}{2}/l}^{(L+\frac{\pi}{2})/l}[\mathcal{Y}\Phi(-g_{\mathcal{Y}})]_{\mathcal{X}=-\lambda/k}\,d\mathcal{Y}+\int_{-\lambda/k}^{\lambda/k}[\mathcal{Y}\Phi(g_{\mathcal{X}})]_{\mathcal{Y}=(L+\pi/2)/l}\,d\mathcal{X} \\
&\quad +\int_{\frac{\pi}{2}/l}^{(L+\frac{\pi}{2})/l}[\mathcal{Y}\Phi(-g_{\mathcal{Y}})]_{\mathcal{X}=\lambda/k}\,d\mathcal{Y}-\int_{-\lambda/k}^{\lambda/k}[\mathcal{Y}\Phi(g_{\mathcal{X}})]_{\mathcal{Y}=(\pi/2)/l}\,d\mathcal{X} \\
&\quad = 0,
\end{aligned} \tag{6.4.24}$$

where the first and third terms of (6.4.24) sum to zero because of the periodicity boundary conditions, and the second and fourth terms are zero because $\Phi = 0$ on $\mathcal{Y} = [(0, L) + \pi/2]/l$.

If equation (6.4.23) is inserted in (6.4.18), and noting that $h_{0\mathcal{X}} = g_{\mathcal{X}}$ and that $\Phi$ is real, we get

$$AA_\tau = -\frac{\Gamma_1}{2\mu}\langle \mathcal{Y} g\rangle_\tau, \tag{6.4.25}$$

or

$$(A^2)_\tau = -\frac{\Gamma_1}{\mu}\langle \mathcal{Y} g\rangle_\tau. \tag{6.4.26}$$

Integrating with respect to $\tau$ gives, after using (6.4.19) and taking $A(\tau = 0) = 0$

$$\left(\frac{d\nu}{d\tau}\right)^2 = -4\mu\Gamma_1\langle \mathcal{Y} g\rangle|_0^\tau. \tag{6.4.27}$$

If we now define a "potential" (Warn and Gauthier, 1989) such that

$$V(\nu) = 4\mu\Gamma_1\langle \mathcal{Y} g\rangle|_0^\nu, \tag{6.4.28}$$

where $g = g(\nu)$ now, we may write

$$\left(\frac{d\nu}{d\tau}\right)^2 + V(\nu) = 0. \tag{6.4.29}$$

Now Warn and Gauthier introduce a transformation of the spatial variables to

$$\alpha = \alpha(\mathcal{X}, \mathcal{Y}); \quad m = m(\mathcal{X}, \mathcal{Y}), \tag{6.4.30}$$

such that

$$\frac{\partial \mathcal{X}}{\partial \alpha} = -\frac{\partial \Phi}{\partial \mathcal{Y}}; \quad \frac{\partial \mathcal{Y}}{\partial \alpha} = \frac{\partial \Phi}{\partial \mathcal{X}}. \tag{6.4.31}$$

It can be shown easily that the result of the conditions set out in (6.4.31) is that $\Phi$ is independent of $\alpha$; i.e. $\Phi = \Phi(m)$. Now since $\Phi = \cos(kx)\sin(ly) =$

$\cos\mathcal{X}\cos\mathcal{Y}$, we have

$$\begin{aligned}\frac{\partial\mathcal{Y}}{\partial\alpha} = \frac{\partial\Phi}{\partial\mathcal{X}} &= -\sin\mathcal{X}\cos\mathcal{Y} \\ &= -\frac{m^{\frac{1}{2}}\sin\mathcal{X}\cos\mathcal{Y}}{(1-\cos^2\mathcal{X}\cos^2\mathcal{Y})^{\frac{1}{2}}} \\ &= -m^{\frac{1}{2}}(1-m^{-1}\sin^2\mathcal{Y})^{\frac{1}{2}}, \qquad (6.4.32)\end{aligned}$$

where we have let $m = 1-\Phi^2$. Now it is possible to rewrite (6.4.32) in the form

$$\int \frac{d\mathcal{Y}}{(1-m^{-1}\sin^2\mathcal{Y})^{\frac{1}{2}}} = -m^{\frac{1}{2}}\alpha, \qquad (6.4.33)$$

which may be put in the form of elliptic functions, so that

$$\begin{aligned}\sin\mathcal{Y} &= \mathrm{sn}(-m^{\frac{1}{2}}\alpha|1/m) \\ &= -\mathrm{sn}(m^{\frac{1}{2}}\alpha|1/m) \\ &= -m^{\frac{1}{2}}\mathrm{sn}(\alpha|m), \qquad (6.4.34)\end{aligned}$$

where identity (16.11.2) for Jacobi elliptic functions listed in Abramowitz and Stegun (1964) has been used along with the fact that $\mathrm{sn}(-x|m) = -\mathrm{sn}(x|m)$.

The $\mathcal{X}$ coordinate gives a very similar integral

$$\frac{\partial\mathcal{X}}{\partial\alpha} = m^{\frac{1}{2}}(1-m^{-1}\sin^2\mathcal{X})^{\frac{1}{2}}, \qquad (6.4.35)$$

so that

$$\sin\mathcal{X} = m^{\frac{1}{2}}\mathrm{sn}(\alpha|m), \qquad (6.4.36)$$

but Warn and Gauthier shift this solution over by a quarter period, so that

$$\begin{aligned} \mathrm{sn}(\alpha + K|m) &= \mathrm{cd}(\alpha|m) \\ &= \frac{\mathrm{cn}(\alpha|m)}{\mathrm{dn}(\alpha|m)}, \end{aligned} \tag{6.4.37}$$

where $K$ represents a quarter period of the sn function (Dixon, 1894). We may then rewrite (6.4.36) as

$$\sin \mathcal{X} = m^{\frac{1}{2}} \frac{\mathrm{cn}(\alpha|m)}{\mathrm{dn}(\alpha|m)}. \tag{6.4.38}$$

We now substitute these transformations into equation (6.4.21) to get

$$\begin{aligned} g_\nu &= -J(\Phi, g) \\ &= -\Phi_{\mathcal{X}} g_{\mathcal{Y}} + \Phi_{\mathcal{Y}} g_{\mathcal{X}} \\ &= -\mathcal{Y}_\alpha g_{\mathcal{Y}} - \mathcal{X}_\alpha g_{\mathcal{X}}. \end{aligned} \tag{6.4.39}$$

But the right hand side of (6.4.39) is just $-g_\alpha$. So we may write

$$\frac{\partial g}{\partial \nu} + \frac{\partial g}{\partial \alpha} = 0. \tag{6.4.40}$$

The solution to this equation is given by

$$g = \tilde{g}(\alpha - \nu, m), \tag{6.4.41}$$

where $\tilde{g}$ is the initial $g$ in $(\alpha, m)$ coordinates. This implies that

$$\tilde{g} = \tilde{h}_0[\mathcal{X}(\alpha, m), \mathcal{Y}(\alpha, m)] - (\tilde{\mathcal{Y}}(\alpha, m) + \pi/2)/l. \tag{6.4.42}$$

Now define

$$\begin{aligned}\sin \mathcal{Y}' &= -m^{\frac{1}{2}} \mathrm{sn}(\alpha - \nu|m) \\ \sin \mathcal{X}' &= m^{\frac{1}{2}} \frac{\mathrm{cn}(\alpha - \nu|m)}{\mathrm{dn}(\alpha - \nu|m)},\end{aligned} \tag{6.4.43}$$

where $(\mathcal{X}', \mathcal{Y}')$ represents the initial position of a particle now at $(\mathcal{X}, \mathcal{Y})$, then the solution may be written as

$$\begin{aligned} g(\mathcal{X}, \mathcal{Y}, \nu) &= \tilde{h}_0(\mathcal{X}', \mathcal{Y}') - \mathcal{Y}' \qquad |\mathcal{X}| < \pi/2 \\ &= \tilde{h}_0(\pi - \mathcal{X}', \mathcal{Y}') - \mathcal{Y}' \qquad |\pi - \mathcal{X}| < \pi/2. \end{aligned} \tag{6.4.44}$$

Using the addition theorem (16.17.1) for elliptic functions (Abramowitz and Stegun, 1964), we may write

$$\begin{aligned} \sin \mathcal{Y}' &= -m^{\frac{1}{2}} \mathrm{sn}(\alpha - \nu|m) \\ &= -m^{\frac{1}{2}} \frac{\mathrm{sn}(\alpha|m)\mathrm{cn}(\nu|m)\mathrm{dn}(\nu|m) - \mathrm{sn}(\nu|m)\mathrm{cn}(\alpha|m)\mathrm{dn}(\alpha|m)}{1 - m\,\mathrm{sn}^2(\alpha|m)\mathrm{sn}^2(\nu|m)}. \end{aligned} \tag{6.4.45}$$

It is possible to eliminate the dependence on $\alpha$ in the above expressions by utilizing (6.4.34) and (6.4.38). After the use of the identity $\mathrm{cn}^2(x|m) = 1 - \mathrm{sn}^2(x|m)$, we finally obtain

$$\sin \mathcal{Y}' = \frac{\sin \mathcal{Y}\mathrm{cn}(\nu|m)\mathrm{dn}(\nu|m) + \mathrm{sn}(\nu|m)\cos^2 \mathcal{Y} \sin \mathcal{X}}{1 - \sin^2 \mathcal{Y}\mathrm{sn}^2(\nu|m)}. \tag{6.4.46}$$

Similarily, we find

$$\sin \mathcal{X}' = \frac{2\mathrm{cn}(\nu|m)\mathrm{dn}(\nu|m)\sin \mathcal{Y} + \mathrm{sn}(\nu|m)\sin \mathcal{X}\cos 2\mathcal{Y}}{2\mathrm{dn}(\nu|m)\cos \mathcal{Y} - \mathrm{sn}(\nu|m)\mathrm{cn}(\nu|m)\sin \mathcal{X}\sin 2\mathcal{Y}}. \tag{6.4.47}$$

It is now possible to write an expression for $V(\nu)$ as

$$V(\nu) = 4\mu\Gamma_1 \left[ \langle \mathcal{Y} \check{g}(\mathcal{X}', \mathcal{Y}') \rangle + \langle \mathcal{Y} \check{g}(\mathcal{X}, \mathcal{Y}) \rangle \right] . \tag{6.4.48}$$

where the first term on the right hand side is actually the thickness at the current position (see equation (6.4.44)) multiplied into $\mathcal{Y}$ and area averaged. The second term is the area average of $\mathcal{Y}$ multiplied into the initial form of $g$ evaluated at the *current* coordinates.

It turns out that calculating $\nu(\tau)$ is quite difficult, since $V(\nu)$ must be determined at all $(\mathcal{X}, \mathcal{Y})$ in the domain for each value of $\nu$, utilizing (6.4.48), with area integrals carried out over the arcsins of the transformation functions (6.4.46) and (6.4.47). Then this result must be included in the differential equation (6.4.29), and again integrated numerically. In fact, Warn and Gauthier (1989) present two calculations of $V(\nu)$ in their work, but they do not attempt the calculation of $\nu(\tau)$ from equation (6.4.29) at all.

So although an analytical solution has been derived for the complete infinite set of equations (6.1.25) - (6.1.28), its utility is limited by the difficulty in actually calculating the solution numerically. In fact, integrating many equations in the spectral approach is much easier, and the physics is much clearer. The role of the higher harmonics and the mean flow distortion are explicit in the spectral approach, whereas these effects are hidden in the analytical solution presented here.

# Chapter 7

## The Sine-Gordon Equation

It was shown in the previous chapter that there exists a solitary wave solution to the truncated set of equations (6.2.1) - (6.2.2). A solitary wave is a disturbance which retains its form as it propagates for all time, and is a result of a balance between dispersive and amplitude steepening effects in a nonlinear system. The existence of such solutions for this set of equations suggests that there may be other forms of these waves, or perhaps even more than one such disturbance may co-exist at the same time in the same domain. These multiple solitary waves are known as *solitons*, and have been much studied in the last two decades. The most interesting property of solitons is that they retain their form after interactions, or collisions, with one another (except possibly for a phase change), and so, in a sense, behave like particles (Lamb, 1980). The purpose of this chapter is to derive an equation from the truncated set, called the sine-Gordon equation, whose solutions include solitons as well as other permanent wave disturbances.

A method for solving certain nonlinear partial differential equations such as the sine-Gordon equation, called the "inverse scattering transform," or IST, was developed in the early 1970's by Ablowitz and coworkers (Ablowitz and Segur, 1981) as an extension to similar methods which generated soliton solutions to the nonlinear Korteweg-deVries (KdV) equation. It proves the existence of multiple soliton solutions for the sine-Gordon equation, which implies that if it is possible to derive this equation from our truncated set, then we must allow for the existence of such solutions to our problem.

The IST as applied to the sine-Gordon equation is beyond the scope of

this thesis, so our approach here will be to examine some well-known solutions to this equation which were developed long before the advent of IST, and apply them to our problem. We still are able to show, however, that there exists the equivalent of solitary wave solutions to our sine-Gordon equation, including a 2-soliton disturbance (it will be seen later that a differentiation is required to obtain the classic "hump" form of the soliton).

*7.1 Derivation of the Sine-Gordon Equation*

We derive the sine-Gordon equation from the set (6.2.1) - (6.2.2), rewritten with minor changes as

$$(\partial_T + c_1\partial_X)(\partial_T + c_2\partial_X)A = \sigma^2 A - NA\alpha_2, \tag{7.1.1}$$

$$(\partial_T + c_2\partial_X)\alpha_2 = (\partial_T + c_1\partial_X)|A|^2, \tag{7.1.2}$$

where $c_1 = 1 - 2k^2$, $c_2 = 1$, $\sigma^2 = \mu k^2$, and $N = \mu^2 k^2 l^2$ and where $A \to 0$ as $|X| \to \infty$. The derivation which follows is based on that given by Gibbon, James and Moroz (1979) (or GJM), with certain of the steps expanded for clarity.

First the following substitution may be made

$$S = 1 - N\alpha_2/\sigma^2; \qquad R = \sqrt{2}A. \tag{7.1.3}$$

If (7.1.3) is inserted into (7.1.1) and (7.1.2), we obtain

$$(\partial_T + c_1\partial_X)(\partial_T + c_2\partial_X)(R/\sqrt{2}) = (\sigma^2/\sqrt{2})R - (N/\sqrt{2})(\sigma^2(-S+1)/N)R, \tag{7.1.4}$$

$$(\partial_T + c_2\partial_X)(\sigma^2(-S+1)/N) = (1/2)(\partial_T + c_1\partial_X)|R|^2. \tag{7.1.5}$$

The dependent variables are then transformed as follows

$$\xi = \frac{-N^{\frac{1}{2}}(X - c_1 T)}{c_1 - c_2}; \qquad \tau = \frac{\sigma^2 (X - c_2 T)}{N^{\frac{1}{2}}(c_1 - c_2)}. \tag{7.1.6}$$

Utilizing the chain rule, (7.1.6) applied to (7.1.4) gives

$$\begin{aligned}
&\left( \frac{N^{\frac{1}{2}} c_1}{c_1 - c_2} \partial_\xi - \frac{\sigma^2 c_2}{N^{\frac{1}{2}}(c_1 - c_2)} \partial_\tau - \frac{c_1 N^{\frac{1}{2}}}{c_1 - c_2} \partial_\xi + \frac{\sigma^2 c_1}{N^{\frac{1}{2}}(c_1 - c_2)} \partial_\tau \right) \times \\
&\left( \frac{N^{\frac{1}{2}} c_1}{c_1 - c_2} \partial_\xi - \frac{\sigma^2 c_2}{N^{\frac{1}{2}}(c_1 - c_2)} \partial_\tau - \frac{c_2 N^{\frac{1}{2}}}{c_1 - c_2} \partial_\xi + \frac{\sigma^2 c_2}{N^{\frac{1}{2}}(c_1 - c_2)} \partial_\tau \right) R \\
&= \sigma^2 R - (\sigma^2(-S+1)R).
\end{aligned} \tag{7.1.7}$$

This simplifies to

$$\left( \frac{\sigma^2}{N^{\frac{1}{2}}} \partial_\tau \right) \cdot \left( N^{\frac{1}{2}} \partial_\xi \right) R = \sigma^2 R - [\sigma^2(-S+1)R], \tag{7.1.8}$$

which becomes

$$R_{\xi\tau} = RS. \tag{7.1.9}$$

From equation (7.1.5) we get

$$\begin{aligned}
&\left( \frac{N^{\frac{1}{2}} c_1}{c_1 - c_2} \partial_\xi - \frac{\sigma^2 c_2}{N^{\frac{1}{2}}(c_1 - c_2)} \partial_\tau - \frac{c_2 N^{\frac{1}{2}}}{c_1 - c_2} \partial_\xi + \frac{\sigma^2 c_2}{N^{\frac{1}{2}}(c_1 - c_2)} \partial_\tau \right) \left( \frac{\sigma^2(-S+1)}{N} \right) \\
&= \frac{1}{2} \left( \frac{N^{\frac{1}{2}} c_1}{c_1 - c_2} \partial_\xi - \frac{\sigma^2 c_2}{N^{\frac{1}{2}}(c_1 - c_2)} \partial_\tau - \frac{c_1 N^{\frac{1}{2}}}{c_1 - c_2} \partial_\xi - \frac{\sigma^2 c_1}{N^{\frac{1}{2}}(c_1 - c_2)} \partial_\tau \right) |R|^2.
\end{aligned} \tag{7.1.10}$$

This simplifies to

$$N^{\frac{1}{2}} \partial_\xi \left( \frac{\sigma^2(-S+1)}{N} \right) = \frac{\sigma^2}{2N^{\frac{1}{2}}} (|R|^2)_\tau, \tag{7.1.11}$$

which becomes

$$S_\xi = -\frac{1}{2}(|R|^2)_\tau. \tag{7.1.12}$$

The boundary conditions becomes

$$R \to 0 \quad \text{as} \quad |\xi| \to \infty \quad (\text{or as} \quad |\tau| \to \infty). \tag{7.1.13}$$

GJM were able to derive a conservation law from these equations by first rewriting (7.1.12) as

$$S_\xi = -\frac{1}{2}[RR^*_\tau + R^* R_\tau]. \tag{7.1.14}$$

Then multiplying both sides of (7.1.14) by $S$ and rearranging gives

$$(S^2)_\xi = -[RSR^*_\tau + R^* S R_\tau]. \tag{7.1.15}$$

But $S$ is real (because $\alpha_2$ is real). Therefore substitute for $RS$ and $R^*S$ from (7.1.9) to obtain

$$(S^2)_\xi = -[R_{\xi\tau}R^*_\tau + R^*_{\xi\tau}R_\tau] = (|R|^2_\tau)_\xi. \tag{7.1.16}$$

Integration with respect to $\xi$ of (7.1.16) leads to

$$S^2 = -|R_\tau|^2 + C. \tag{7.1.17}$$

By a simple scaling, we may set $C = 1$ which means that

$$S^2 + |R_\tau|^2 = 1. \tag{7.1.18}$$

Therefore, if $R \to 0$ as $|\xi| \to \infty$, we must have

$$S \to \pm 1 \quad \text{as} \quad |\xi| \to \infty. \tag{7.1.19}$$

To finish the derivation, we assume that $R$ is *real* and then make the following substitutions

$$R = \phi_\xi; \qquad S = \cos\phi. \tag{7.1.20}$$

The sine-Gordon equation may be derived from either (7.1.9) and (7.1.12). Using (7.1.12) we have

$$-\phi_\xi \sin\phi = -\frac{1}{2}(\phi_\xi)_\tau^2 = -\phi_\xi \phi_{\xi\tau}, \tag{7.1.21}$$

or

$$\phi_{\xi\tau} = \sin\phi. \tag{7.1.22}$$

This is the sine-Gordon equation. GJM point out that (7.1.9) and (7.1.12) cannot be simplified further if $R$ is complex, but that such a system is still solvable by using the IST.

*7.2 Cnoidal Wave Solutions to the Sine-Gordon Equation*

We start the analysis of the sine-Gordon equation by looking for permanent wave solutions in the form

$$\phi(\xi, \tau) = \phi(\xi - c\tau) = \phi(\Gamma), \tag{7.2.1}$$

where $\Gamma = \xi - c\tau$ and $c$ is a constant (see Drazin, (1983), or Drazin and Johnson, (1989), for more details). In this way, we hope to find any solitary *or* periodic wave solutions which exist.

We start by inserting (7.2.1) into (7.1.22). This gives

$$-c\phi'' = \sin\phi, \tag{7.2.2}$$

where the prime indicates differentiation with respect to the variable $\Gamma$. We then multiply both sides by $\phi'$ and rearrange to obtain

$$(c/2)[(\phi')^2]' = (\cos\phi)'. \tag{7.2.3}$$

Integrating once and taking the square root of both sides leaves, again after rearranging

$$\frac{d\phi}{\pm\sqrt{\frac{2}{c}\cos\phi + K_1}} = d\Gamma, \tag{7.2.4}$$

where $K_1$ is a constant of integration. Now we rewrite the integrand on the left hand side of (7.2.4) by using the trigonometric identity $\cos\theta = 1 - 2\sin^2(\frac{1}{2}\theta)$, and obtain

$$\frac{d\phi}{\pm\sqrt{K_2 - \frac{4}{c}\sin^2(\frac{1}{2}\phi)}} = d\Gamma, \tag{7.2.5}$$

where $K_2$ is a constant. The next step is to let $\gamma = \frac{1}{2}\phi$ and then integrate both sides of (7.2.5) to arrive at

$$\Gamma - \Gamma_0 = 2\int_0^{\gamma} \frac{d\theta}{\pm\sqrt{K_2 - \frac{4}{c}\sin^2\theta}}$$

$$= \frac{2}{\sqrt{K_2}}\int_0^{\gamma} \frac{d\theta}{\pm\sqrt{1 - m\sin^2\theta}}, \tag{7.2.6}$$

where $m = 4/cK_2$, $\theta$ is a dummy variable of integration, and $\Gamma_0$ is the initial value for $\Gamma$.

The integral on the right hand side of equation (7.2.6) is an elliptic integral, and so, *if* $0 \leq m \leq 1$, we may make use of the Jacobi elliptic functions to represent the solution. We choose the "cn" function (the "sn" function would do just as well), and write the solution in the form (we have chosen the positive sign)

$$\mathrm{cn}\left[\frac{\sqrt{K_2}}{2}(\Gamma - \Gamma_0)|m\right] = \cos\gamma = \cos(\frac{1}{2}\phi), \tag{7.2.7}$$

so that

$$\phi(\xi,\tau) = 2\cos^{-1}\left\{\mathrm{cn}\left[\frac{\sqrt{K_2}}{2}(\Gamma - \Gamma_0)|m\right]\right\}. \tag{7.2.8}$$

This is the cnoidal wave solution for the sine-Gordon equation.

We may find the amplitude function by making use of (7.1.20) and (7.1.3) to find

$$\phi_\xi = R = \sqrt{2}A = -\frac{2}{\sqrt{1-\mathrm{cn}^2[\omega|m]}}(-\mathrm{sn}[\omega|m]\,\mathrm{dn}[\omega|m])(\sqrt{K_2}/2), \tag{7.2.9}$$

where we have let $\omega = (\sqrt{K_2}/2)(\Gamma - \Gamma_0)$. But we may use the identity $\mathrm{cn}^2 x + \mathrm{sn}^2 x = 1$ to simplify (7.2.9), which becomes

$$\begin{aligned} A &= \sqrt{\frac{K_2}{2}}\,\mathrm{dn}[\omega|m] \\ &= \sqrt{\frac{K_2}{2}}\,\mathrm{dn}\left[\frac{\sqrt{K_2}}{2}(\Gamma - \Gamma_0)|m\right]. \end{aligned} \tag{7.2.10}$$

Thus we have obtained dnoidal wave solutions analogous to equation (5.2.14), derived in Chapter 5 for the modes not at the bottom of the marginal stability curve.

*7.3 Single Soliton Solution to the Sine-Gordon Equation*

There are several approaches which have been developed over the years to

solve the sine-Gordon equation. For example, it has been known for a long time that various forms of arctan functions are solutions to this equation, and they generally represent solitary waves.

We may see why this is the case by simply setting $K_2 = 0$ in equation (7.2.5), and require that $c < 0$. Letting $c = -\tilde{c}$, this equation becomes, choosing the positive form of the integrand (this derivation is based on Drazin (1983))

$$d\Gamma = \frac{d\phi}{\frac{2}{\sqrt{\tilde{c}}}\sin(\frac{1}{2}\phi)}. \tag{7.3.1}$$

Integrating both sides of this equation gives

$$\Gamma - \Gamma_0 = \sqrt{\tilde{c}}\ln|\csc\gamma - \cot\gamma|, \tag{7.3.2}$$

where we have again let $\gamma = \frac{1}{2}\phi$. Exponentiating and rearranging leads to

$$\frac{1-\cos\gamma}{\sin\gamma} = \exp\left[\frac{1}{\sqrt{\tilde{c}}}(\Gamma - \Gamma_0)\right]. \tag{7.3.3}$$

We use the trigonometric identities $\sin 2x = 2\sin x\cos x$ and $2\sin^2 x = 1 - \cos 2x$ to rewrite the left hand side of (7.3.3) so that we obtain

$$\tan(\frac{1}{2}\gamma) = \tan(\frac{1}{4}\phi) = \exp\left[\frac{1}{\sqrt{\tilde{c}}}(\Gamma - \Gamma_0)\right]. \tag{7.3.4}$$

Finally, we may write

$$\phi(\Gamma) = 4\tan^{-1}\left\{\exp\left[\frac{1}{\sqrt{\tilde{c}}}(\Gamma - \Gamma_0)\right]\right\}. \tag{7.3.5}$$

Rewriting in terms of $(\xi, \tau)$ coordinates, we find that

$$\phi(\xi,\tau) = 4\tan^{-1}\left\{\exp[a\xi + \tau/a + \nu]\right\}, \tag{7.3.6}$$

where we have let $\nu = \exp\left(-\frac{\Gamma_0}{\sqrt{\tilde{c}}}\right)$, and $a = \sqrt{\tilde{c}}/\tilde{c}$. This constant is determined by the initial form of the solution $\phi(\xi(T=0), \tau(T=0))$, and plays the role of a phase factor only.

To proceed, we take the derivative of (7.3.6) with respect to $\xi$ to obtain (letting $\theta = a\xi + \tau/a$)

$$\phi_\xi = R = \frac{4a\exp(\theta)}{1+\exp(2\theta)} = \frac{4a}{\exp(-\theta)+\exp(\theta)} = 2a\mathrm{sech}(\theta). \tag{7.3.7}$$

GJM show that the transformation

$$\begin{aligned}
&\theta_i = \kappa_i(X - v_i T),\\
&v_i = c_1 + (c_1 - c_2)[N a_i^2 \sigma^{-2} - 1]^{-1},\\
&\kappa_i = (\sigma^2 - a_i^2 N)[a_i N^{\frac{1}{2}}(c_1 - c_2)]^{-1} \qquad i = 1, 2, \ldots, n,
\end{aligned} \tag{7.3.8}$$

converts (7.3.7) into

$$R = 2a_1\mathrm{sech}[\kappa_1(X - v_1 T)], \tag{7.3.9}$$

where in this case, of course, $i = 1$ only. Using the fact that $R = \sqrt{2}A$, we see that if we set $\sqrt{2}\,a = A_0$ and $a_1 = a$, then (7.3.9) is precisely the solitary wave solution presented in Chapter 6 as equation (6.2.4).

*7.4 A 2-Soliton Solution*

More solutions to (7.1.22) may be found by making a transformation of the independent variables, which is motivated by the form of the solution found in

Section 7.3, given by (see Lamb, 1980)

$$p = b\xi + \tau/b,$$
$$q = b\xi - \tau/b, \tag{7.4.1}$$

where we take $b$ to be a constant, so that the sine-Gordon equation becomes

$$\phi_{pp} - \phi_{qq} = \sin\phi. \tag{7.4.2}$$

We look for solutions of the form (this derivation is based on Lamb, 1980)

$$\phi(p,q) = 4\tan^{-1}\left[\frac{u(p)}{v(q)}\right]. \tag{7.4.3}$$

Taking the required derivatives gives

$$\phi_{pp} = \frac{4u''v(u^2+v^2) - (2uu')(4u'v)}{(u^2+v^2)^2},$$
$$\phi_{qq} = -\frac{4v''u(u^2+v^2) - (2vv')(4v'u)}{(u^2+v^2)^2}, \tag{7.4.4}$$

where the prime denotes differentiation with respect to $p$ when it is a superscript for $u$, and $q$ when it is a superscript for $v$. We also have (see Shen (1993))

$$\begin{aligned}\sin[4\tan^{-1}(u/v)] &= \sin 4\theta \\ &= 4\sin\theta\cos\theta(\cos^2\theta - \sin^2\theta) \\ &= \frac{4\tan\theta(1-\tan^2\theta)}{(1+\tan^2\theta)^2} \\ &= \frac{4uv(v^2-u^2)}{(u^2+v^2)^2},\end{aligned} \tag{7.4.5}$$

where we have let $\theta = \tan^{-1}(u/v)$.

Substituting (7.4.4) and (7.4.5) into (7.4.2) gives

$$4u''v(u^2+v^2) - 8(u')^2uv + 4v''u(u^2+v^2) - 8(v')^2uv = 4uv(v^2-u^2), \quad (7.4.6)$$

which may be simplified to

$$(u''v + v''u)(u^2+v^2) - 2uv[(u')^2 + (v')^2] - uv(v^2-u^2) = 0, \quad (7.4.7)$$

or

$$\left(\frac{u''}{u} + \frac{v''}{v}\right)(u^2+v^2) - 2(u')^2 - 2(v')^2 - v^2 + u^2 = 0. \quad (7.4.8)$$

We take the derivative of (7.4.8) with respect to $p$ to get

$$2uu'\left(\frac{u''}{u} + \frac{v''}{v}\right) + (u^2+v^2)\left(\frac{u''}{u}\right)' - 4u''u' + 2uu' = 0. \quad (7.4.9)$$

The derivative of (7.4.8) with respect to $q$ is

$$2vv'\left(\frac{u''}{u} + \frac{v''}{v}\right) + (u^2+v^2)\left(\frac{v''}{v}\right)' - 4v''v' - 2vv' = 0. \quad (7.4.10)$$

The next step is to divide equation (7.4.9) by $uu'(u^2+v^2)$ and equation (7.4.10) by $vv'(u^2+v^2)$ and add the results together to obtain, after some rearranging

$$\frac{2\left(\frac{u''}{u} + \frac{v''}{v}\right) - 4\frac{u''}{u} + 2}{u^2+v^2} + \frac{1}{uu'}\left(\frac{u''}{u}\right)' + \frac{2\left(\frac{u''}{u} + \frac{v''}{v}\right) - 4\frac{v''}{v} - 2}{u^2+v^2} + \frac{1}{vv'}\left(\frac{v''}{v}\right)' = 0, \quad (7.4.11)$$

which becomes after simplifying

$$\frac{1}{uu'}\left(\frac{u''}{u}\right)' + \frac{1}{vv'}\left(\frac{v''}{v}\right)' = 0, \quad (7.4.12)$$

or

$$\frac{1}{uu'}\left(\frac{u''}{u}\right)' = -\frac{1}{vv'}\left(\frac{v''}{v}\right)' = -4k^2, \tag{7.4.13}$$

where $k$ is a constant, because $u$ is a function of $p$ only, and $v$ is a function of $q$ only. The form of the constant is chosen for simplicity, as we shall see later. Now let us integrate the left hand side of (7.4.13). We first rearrange the equation to get

$$\left(\frac{u''}{u}\right)' = -4k^2uu' = -2k^2(u^2)', \tag{7.4.14}$$

and then integrating both sides of (7.4.14) with respect to $p$, we obtain

$$u'' = -2k^2u^3 + \beta_1 u. \tag{7.4.15}$$

where $\beta_1$ is a constant. Multiplying (7.4.15) by $u'$ and rewriting gives

$$\frac{1}{2}[(u')^2]' = -\frac{1}{2}k^2(u^4)' + \frac{1}{2}\beta_1(u^2)', \tag{7.4.16}$$

so that

$$(u')^2 = -k^2u^4 + \beta_1u^2 + \gamma_1. \tag{7.4.17}$$

where $\gamma_1$ is a constant.

We get similar equations when we integrate the second term in (7.4.13) with respect to $q$. After the first and second integrations, respectively, we obtain

$$v'' = 2k^2v^3 + \beta_2 v, \tag{7.4.18}$$

$$(v')^2 = k^2v^4 + \beta_2v^2 + \gamma_2. \tag{7.4.19}$$

where $\beta_2$ and $\gamma_2$ are constants.

Note that since differentiation was required to get to equation (7.4.13), we would expect that there should be some relationship between the constants in (7.4.15) and (7.4.17) - (7.4.19) (Lamb, 1980). To find this, we insert these equations into (7.4.13), which gives

$$(-2k^2u^2 + \beta_1 + 2k^2v^2 + \beta_2)(u^2 + v^2) + 2k^2u^4 - 2\beta_1 u^2 - 2\gamma_1 \\ - 2k^2v^4 - 2\beta_2 v^2 - 2\gamma_2 - v^2 + u^2 = 0, \tag{7.4.20}$$

which simplifies to

$$(\beta_1 - \beta_2)(v^2 - u^2) - (v^2 - u^2) - 2\gamma_1 - 2\gamma_2 = 0. \tag{7.4.21}$$

The coefficients in (7.4.21) may be equated to get

$$\beta_1 = 1 + \beta_2, \\ \gamma_1 = -\gamma_2. \tag{7.4.22}$$

Let $\beta_1 = m^2$ and $\gamma_1 = n^2$. Then $\beta_2 = m^2 - 1$ and $\gamma_2 = -n^2$. Then (7.4.17) and (7.4.19) may be written as

$$(u')^2 = -k^2u^4 + m^2u^2 + n^2, \tag{7.4.23}$$

$$(v')^2 = k^2v^4 + (m^2 - 1)v^2 - n^2. \tag{7.4.24}$$

We may manipulate the constants $k, u,$ and $m$ in (7.4.23) and (7.4.24) in order to generate various solutions to the sine-Gordon equation. For example,

if we set $k = 0, \quad m > 1, \quad n = 0,$ we obtain (Lamb, 1980)

$$u' = \pm mu,$$
$$v' = \pm\sqrt{m^2 - 1}\, v, \tag{7.4.25}$$

which leads to

$$u = b_1 \exp(\pm mp),$$
$$v = b_2 \exp(\pm\sqrt{m^2 - 1}\, q). \tag{7.4.26}$$

This implies that

$$\phi(p,q) = 4\tan^{-1}\left[\frac{b_1}{b_2}\exp(\pm mp \mp \sqrt{m^2 - 1}\, q)\right]. \tag{7.4.27}$$

If we choose the signs appropriately, and let $\rho = \sqrt{m^2 - 1}/m$, then we may rewrite one of the above solutions as (letting $\gamma = b_1/b_2$)

$$\phi(p,q) = 4\tan^{-1}\left[\gamma\exp\left(\frac{p - \rho q}{\sqrt{1 - \rho^2}}\right)\right]. \tag{7.4.28}$$

If we substitute back for $p$ and $q$ in terms of $\xi$ and $\tau$ using equation (7.4.1), we find

$$\begin{aligned}\phi(\xi,\tau) &= 4\tan^{-1}\left[\gamma\exp\left(\frac{\xi b(1+\rho) + (\tau/b)(1-\rho)}{\sqrt{1-\rho^2}}\right)\right] \\ &= 4\tan^{-1}[\gamma\exp(\tilde{b}\xi + \tau/\tilde{b})],\end{aligned} \tag{7.4.29}$$

where we have let $\tilde{b} = b(1+\rho)/\sqrt{1-\rho^2}$. This is exactly the solitary wave solution found by simpler means as presented in (7.3.6), if $\gamma = \exp(\nu)$ and $\tilde{b} = a$.

The 2-soliton solution is obtained if we let $k = 0, \quad m > 1, \quad n \neq 0$ (Lamb, 1980). Then the $u(p)$ equation becomes

$$(u')^2 = m^2 u^2 + n^2. \tag{7.4.30}$$

This may be rewritten as

$$\frac{du}{\sqrt{u^2 + (n/m)^2}} = m dp. \tag{7.4.31}$$

Upon integration of both sides of (7.4.31), we find

$$\sinh^{-1}(mu/n) = mp + c_1, \tag{7.4.32}$$

where $c_1$ is a constant. Thus we obtain

$$u(p) = (n/m)\sinh(mp + c_1). \tag{7.4.33}$$

Similarly, the $v(q)$ equation is integrated to give

$$v(q) = \frac{n\cosh(\sqrt{m^2 - 1}\, q + c_2)}{\sqrt{m^2 - 1}}, \tag{7.4.34}$$

and so the solution is

$$\phi(p, q) = 4\tan^{-1}\left[\frac{\sqrt{m^2 - 1}}{m}\frac{\sinh(mp + c_1)}{\cosh(\sqrt{m^2 - 1}\, q + c_2)}\right]. \tag{7.4.35}$$

Note that the solution is independent of $n$, which is due to the fact that $u/v$ turns out to be a ratio of exponentials (Lamb, 1980). Equation (7.4.35) represents the collision of two solitons, which can be more easily seen if we rewrite this

equation as

$$\phi(\xi,\tau) = 4\tan^{-1}\left[\left(\frac{a_1-a_2}{a_1+a_2}\right)\frac{\sinh\{\frac{1}{2}(\theta_1+\theta_2)+c_1\}}{\cosh\{\frac{1}{2}(\theta_1-\theta_2)+c_2\}}\right], \tag{7.4.36}$$

where we have used $m = (a_1+a_2)/2\sqrt{a_1a_2}$ and $b = \sqrt{a_1a_2}$, and where $\theta_i = a_i\xi + \tau/a_i$, $i = 1,2$ (Lamb, 1980). Using the transform (7.3.8) we may write $\phi$ in terms of $(X,T)$ as follows

$$\phi(X,T) = 4\tan^{-1}\left[\left(\frac{a_1-a_2}{a_1+a_2}\right)\frac{\sinh\{\frac{1}{2}[\kappa_1(X-v_1T)+\kappa_2(X-v_2T)]+c_1\}}{\cosh\{\frac{1}{2}[\kappa_1(X-v_1T)-\kappa_2(X-v_2T)]+c_2\}}\right]. \tag{7.4.37}$$

A plot of (7.4.37) with $a_1 = 2.0$, $a_2 = 0.4$, $\mu = 2.0$, $k = 0.5$, and $c_1 = c_2 = 0$ is shown in Figure 13a (see Program 5 in the Appendix for the *Mathematica* program used to calculate this figure and Figure 13b). We now find the solution for R is

$$\phi_\xi = R = 2\gamma\frac{(a_1+a_2)\frac{\cosh[\frac{1}{2}(\theta_1+\theta_2)]}{\cosh[\frac{1}{2}(\theta_1-\theta_2)]} - (a_1-a_2)\tanh[\frac{1}{2}(\theta_1-\theta_2)]\frac{\sinh[\frac{1}{2}(\theta_1+\theta_2)]}{\cosh[\frac{1}{2}(\theta_1-\theta_2)]}}{1+\gamma^2\mathrm{sech}^2[\frac{1}{2}(\theta_1-\theta_2)\sinh^2[\frac{1}{2}(\theta_1+\theta_2)]}. \tag{7.4.38}$$

where $\gamma = (a_1-a_2)/(a_1+a_2)$. A plot of this equation with the same parameters as used for (7.4.37) (and using $(X,T)$ coordinates) is shown in Figure 13b. We see in this plot that we have a collision between a faster moving small soliton, and a slower moving larger soliton, and that the constants $a_1$ and $a_2$ are representative of the amplitudes of the solitons. We see that the solitons retain their form after the collision process, as expected.

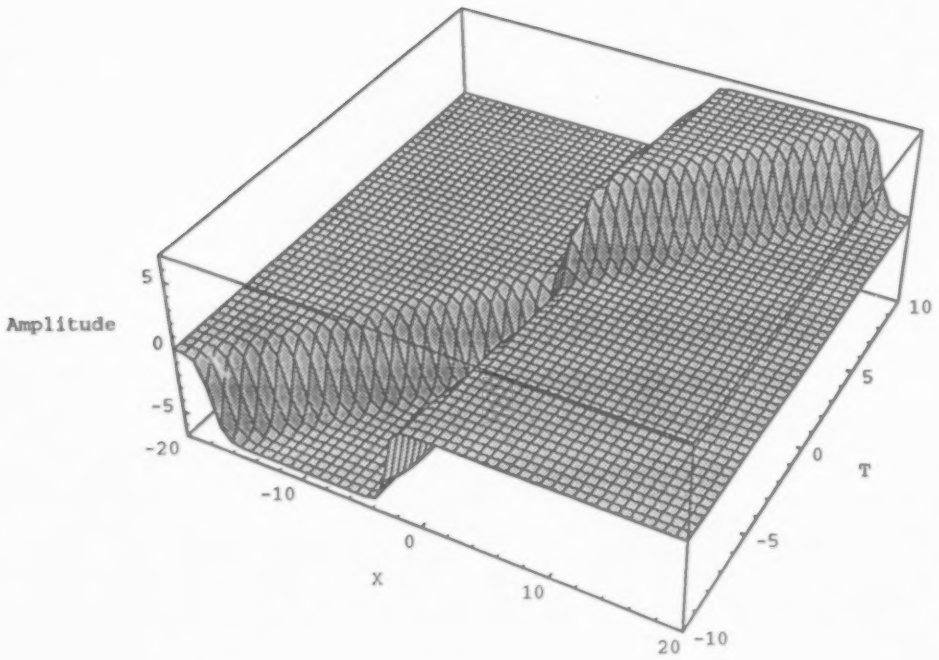


Figure 13a. Plot of the 2-soliton arctan solution (from equation (7.4.37)) for the sine-Gordon equation where $a_1 = 2.0$, $a_2 = 0.4$, $k = 0.5$, $l = 0.866$ and $\mu = 2.0$.

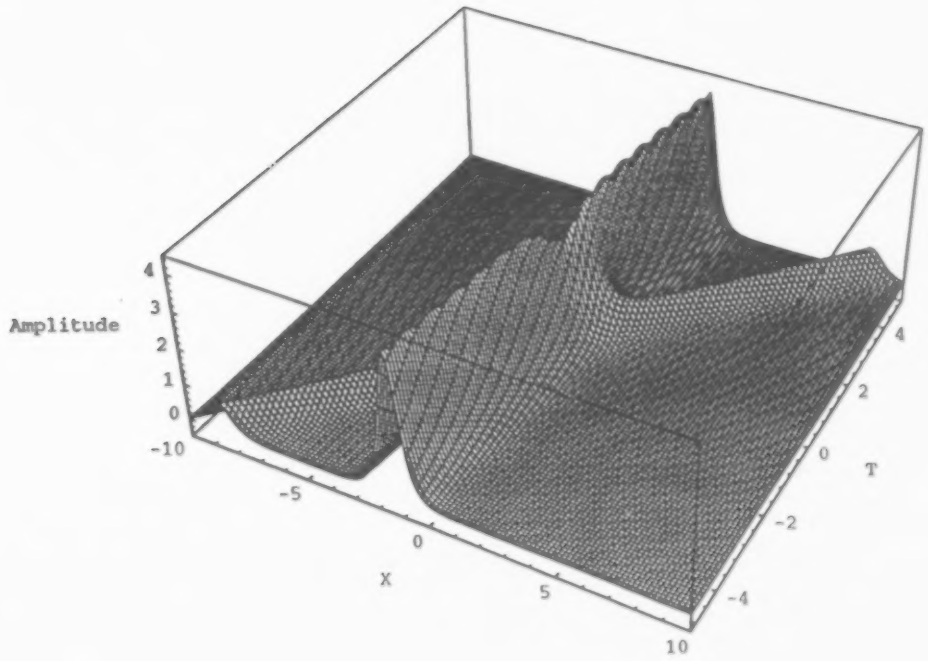


Figure 13b. Plot of the 2-soliton "hump" solution (from equation (7.4.38)) for the sine-Gordon equation where $a_1 = 2.0$, $a_2 = 0.4$, $k = 0.5$, $l = 0.866$ and $\mu = 2.0$.

*7.5 A Kink-Antikink Solution*

Another kind of solution is obtained if we set $k \neq 0, \quad n = 0, \quad m^2 > 1$ in the equation set (7.4.23) - (7.4.24), so that (Lamb, 1980)

$$(u')^2 = -k^2u^4 + m^2u^2, \tag{7.5.1}$$

$$(v')^2 = k^2v^4 + (m^2 - 1)v^2. \tag{7.5.2}$$

We look at the $u$ equation first. We may rewrite (7.5.1) as

$$u' = ku\sqrt{\Gamma^2 - u^2}, \tag{7.5.3}$$

where $\Gamma = m/k$. Upon separation of the variables and integrating, we obtain

$$-\frac{1}{\Gamma}\ln\left(\frac{\Gamma + \sqrt{\Gamma^2 - u^2}}{u}\right) = kp + C, \tag{7.5.4}$$

where $C$ is a constant. Taking exponentials and rearranging, we have

$$\frac{\Gamma + \sqrt{\Gamma^2 - u^2}}{u} = \exp[-(mp + c_1)], \tag{7.5.5}$$

where $c_1$ is a constant. If we add the inverse of (7.5.5) to each side of this equation, we obtain

$$\frac{\Gamma + \sqrt{\Gamma^2 - u^2}}{u} + \frac{u}{\Gamma + \sqrt{\Gamma^2 - u^2}} = 2\cosh(mp + c_1). \tag{7.5.6}$$

After some algebra, we find the solution for $u$ to be

$$u(p) = \frac{\Gamma}{\cosh(mp + c_1)}. \tag{7.5.7}$$

In an exactly analogous manner, we find the solution for $v$ to be

$$v(q) = -\frac{\Gamma_1}{\sinh(\Gamma_1 kq + c_2)}, \tag{7.5.8}$$

where $\Gamma_1 = \sqrt{m^2 - 1}/k$. Inserting (7.5.7) and (7.5.8) into the arctan solution (7.4.3), we find that

$$\phi(p,q) = -4\tan^{-1}\left[\frac{m}{\sqrt{m^2-1}}\frac{\sinh(\sqrt{m^2-1}q + c_2)}{\cosh(mp + c_1)}\right], \tag{7.5.9}$$

where we have used the fact that $\tan^{-1}(-x) = -\tan^{-1}(x)$. In the same way as was done in Section 7.4, (7.5.9) may be rewritten in terms of $(X,T)$ coordinates, which gives

$$\phi(X,T) = -4\tan^{-1}\left[\left(\frac{a_1+a_2}{a_1-a_2}\right)\frac{\sinh\{\frac{1}{2}[\kappa_1(X-v_1T) - \kappa_2(X-v_2T)] + c_2\}}{\cosh\{\frac{1}{2}[\kappa_1(X-v_1T) + \kappa_2(X-v_2T)] + c_1\}}\right]. \tag{7.5.10}$$

A plot of this equation, with the same parameters as was used in Section 7.4, is found in Figure 14a (this figure and Figure 14b were plotted on a *Mathematica* program in the same manner as Figures 13a and b - see Program 5 in the Appendix). The derivative with respect to $\xi$ gives the soliton solution, as in Section 7.4, which is

$$\phi_\xi = R = \\ -2\gamma\frac{(a_1-a_2)\frac{\cosh[\frac{1}{2}(\theta_1-\theta_2)]}{\cosh[\frac{1}{2}(\theta_1+\theta_2)]} - (a_1+a_2)\tanh[\frac{1}{2}(\theta_1+\theta_2)]\frac{\sinh[\frac{1}{2}(\theta_1-\theta_2)]}{\cosh[\frac{1}{2}(\theta_1+\theta_2)]}}{1+\gamma^2\sinh^2[\frac{1}{2}(\theta_1-\theta_2)]\mathrm{sech}^2[\frac{1}{2}(\theta_1+\theta_2)]}, \tag{7.5.11}$$

where $\gamma = (a_1+a_2)/(a_1-a_2)$ in this case, and where we have set $c_1 = c_2 = 0$, (and recalling that $\theta_i = \kappa_i(X - v_iT)$). A plot of this solution may be found in Figure 14b, where we see that we have a soliton and an anti-soliton (a soliton with

a negative amplitude) colliding, and again retaining their form after the collision process.

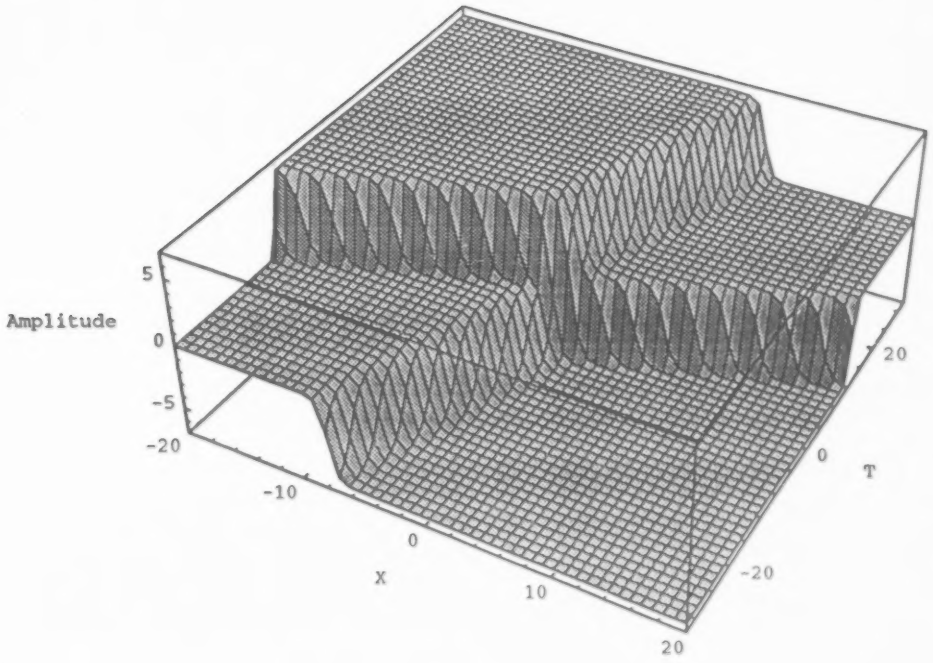


Figure 14a. Plot of the kink-antikink arctan solution (from equation (7.5.10)) for the sine-Gordon equation where $a_1 = 2.0$, $a_2 = 0.4$, $k = 0.5$, $l = 0.866$ and $\mu = 2.0$.

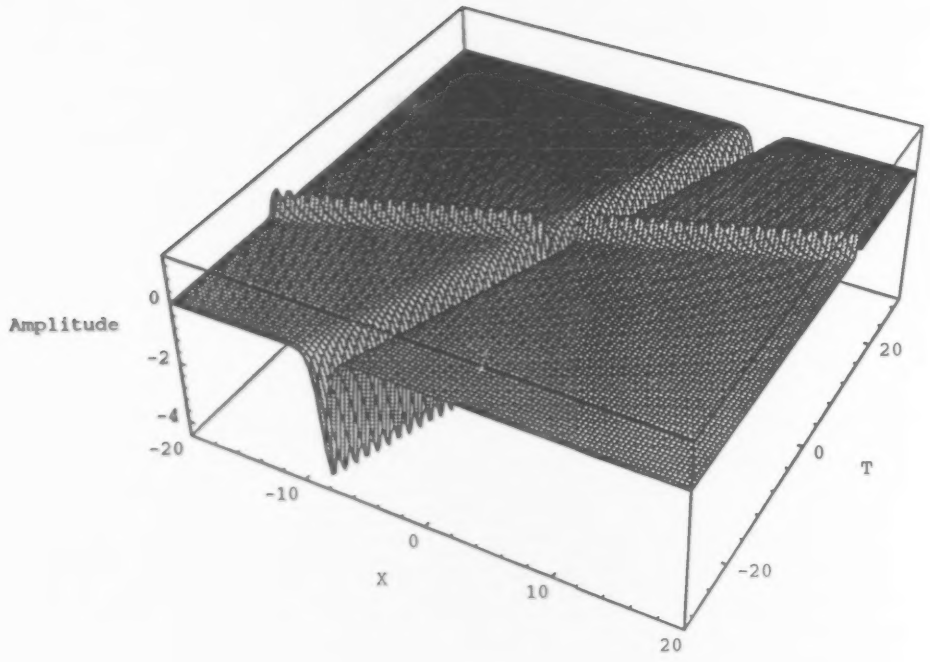


Figure 14b. Plot of the kink-antikink "hump" solution (from equation (7.5.11)) for the sine-Gordon equation where $a_1 = 2.0$, $a_2 = 0.4$, $k = 0.5$, $l = 0.866$ and $\mu = 2.0$.

*7.6 Breather Solutions*

If we take the kink-antikink solution of Section 7.5, but require that $m^2 < 1$, then we obtain breather solutions, which are essentially stationary solitons (Lamb, 1980). We see that we may rewrite $\sqrt{m^2-1} = i\sqrt{1-m^2}$, and along with the identity $\sinh(ix) = i\sin(x)$, equation (7.5.9) becomes

$$\phi(p,q) = -4\tan^{-1}\left[\frac{m}{\sqrt{1-m^2}}\frac{\sin(\sqrt{1-m^2}\,q + c_2)}{\cosh(mp + c_1)}\right]. \tag{7.6.1}$$

This is the breather solution in $(p,q)$ coordinates. If we now write this in terms of $(\xi,\tau)$ coordinates, we have

$$\phi(\xi,\tau) = -4\tan^{-1}\left[\frac{m}{\sqrt{1-m^2}}\frac{\sin[\sqrt{1-m^2}(b\xi - \tau/b) + c_2]}{\cosh[m(b\xi + \tau/b) + c_1]}\right]. \tag{7.6.2}$$

This leads to, in $(X,T)$ coordinates

$$\phi(X,T) = -4\tan^{-1}\left[\frac{m}{\sqrt{1-m^2}}\frac{\sin[\sqrt{1-m^2}\kappa_1^*(X - v_1^*T) + c_2]}{\cosh[m\kappa_1(X - v_1T) + c_1]}\right], \tag{7.6.3}$$

where $v_1$ and $\kappa_1$ depend on the choice of $b$, and where

$$\begin{aligned} v_1^* &= c_1 - (c_1 - c_2)[Nb^2\sigma^{-2} + 1]^{-1}, \\ \kappa_1^* &= -(\sigma^2 + b^2N)[bN^{\frac{1}{2}}(c_1 - c_2)]^{-1}. \end{aligned} \tag{7.6.4}$$

We show a plot of (7.6.3) in Figure 15 (calculated using *Mathematica* - see Program 6 in the Appendix), where we have set $m = 0.5$, $b = 2.0$, and $c_1 = c_2 = 0$. This is a plot of a *moving* breather, and so we see that the change in coordinate system transforms a stationary breather into one which is propagating.

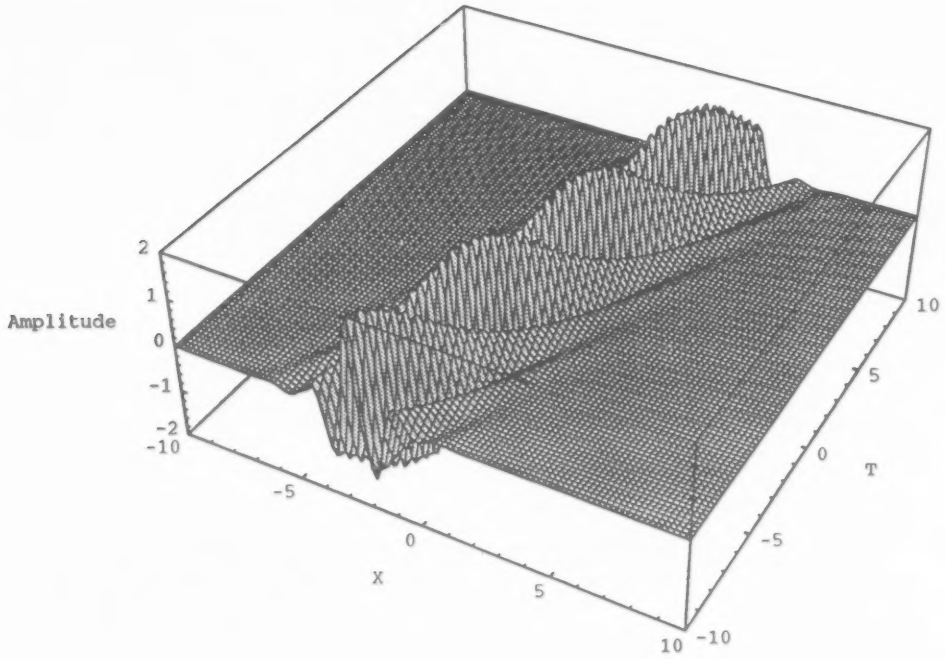


Figure 15. Plot of a moving breather solution (from equation (7.6.3)) for the sine-Gordon equation where $m = 0.5$, $k = 0.5$, $l = 0.866$ and $\mu = 2.0$.

# Chapter 8

## Summary and Conclusions

In this thesis, a theory has been developed to describe the weakly nonlinear stability characteristics of a baroclinic mesoscale gravity current in a channel with a sloping bottom. The model assumes that the gravity current evolves geostrophically but not quasigeostrophically, because the interface deflections are not small compared to the scale depth of the current. The ambient channel water dynamics are quasigeostrophic, however, which leads to strong interaction between the geostrophic pressure and the height of the front.

It is shown, with the use of a hamiltonian formulation of the governing equations, that there exists the possibility of linear and nonlinear instability when small perturbations are applied to a simple steady solution to the channel model. Linear stability theory was then applied to the model in order to generate a marginal stability curve which relates the rate of change of gravity current thickness to the horizontal wavenumber. We then utilized weakly nonlinear stability theory to derive finite-amplitude equations which follow the evolution of an unstable mode after application of a small supercriticality to the gravity current thickness slope. It was found that if the wavenumber was not at the bottom of the marginal stability curve, then the amplitude of the wave is periodic in time and it takes the form of a Jacobi dnoidal function.

If the supercriticality is centred on the mode at the bottom of the marginal stability curve, then an infinite set of nonlinear partial differential equations, in slow space and time, are required to describe the finite-amplitude evolution of the flow. These equations link the perturbation pressure amplitude to an infinite number of modes for the amplitude of the frontal thickness and the mean flow

adjustment. If the truncation of this set is applied so that only the perturbation pressure and the first mode for the mean flow adjustment are included, then solitary wave solutions are possible. It is also shown that a sine-Gordon equation may be derived from this set, which opens up the possibility for multisoliton solutions, among others. If more modes are included then numerical integrations of the spatially-independent equations suggest that the solutions are oscilliatory, and that if enough equations are included, a constriction of the oscillation also becomes apparent.

The theory shows that the retention of the nonlinear interaction terms in the stability equations sets up a balance between the tendency of the wave to extract potential energy and grow, and the adjustment to the mean flow which necessarily results from this, which *reduces* the available potential energy and so slows the growth. This balance produces an oscillation between states of maximum amplitude and minimum available potential energy, and vice versa. The "saturation" and eventual reversal of the initially exponential growth rate of the disturbance makes it possible to think of this as a mechanism for the breakup of the gravity current into coherent cold eddies.

There are weaknesses in the weakly nonlinear analysis which has been done in this thesis. The timescale over which the nonlinear disturbance evolves is unphysically long, because of the very small supercriticality which is applied. As well, the physical configuration upon which the model equations are applied is quite simplistic. However, the analysis did answer the main questions asked of it; the disturbances do indeed saturate with the inclusion of the nonlinear interactions, and a form for these disturbances was elucidated.

Addressing the concerns forms the basis for further research. Numerical schemes may be used to overcome the need for a small initial instability. The

model itself may be applied to more complicated physical situations, such as an arbitrarily-shaped gravity current on a sloping continental shelf, or a channel with more complex bottom topography. It would be interesting to see whether the fundamental nature of the instabilities in such cases would change from what was found in this thesis.

## References


Ablowitz, M.J. and Segur, H., *Solitons and the Inverse Scattering Transform*, SIAM Studies in Applied Mathematics 4, Society for Industrial and Applied Mathematics (1981).

Abramowitz, M. and Stegun, I.A., *Handbook of Mathematical Functions*, National Bureau of Standards, Applied Mathematics Series 55 (1964).

Armi, L. and D'Asaro, E., "Flow structures in the benthic ocean," *J. Geophys. Res.* **85**, 469-483 (1980).

Benjamin, T.B., "The stability of solitary waves," *Proc. R. Soc. Lond. A* **328**, 153-183 (1972).

Benjamin, T.B., "Impulse, force flow and variational principles," *IMA J. Appl. Math.* **32**, 3-68 (1984).

Boville, B.A., "Amplitude vacillation on a $\beta$ – plane," *J. Atmos. Sci.* **38**, 609-618 (1981).

Boyce, W.E. and DiPrima, R.C., *Elementary Differential Equations and Boundary Value Problems*, John Wiley and Sons (1986).

Chandrasekhar, S., *Hydrodynamic and Hydromagnetic Stability*, Dover Publications, Inc. (1961).

Dixon, A.C., *The Elementary Properties of Elliptic Functions, with Examples*, Macmillan (1894).

Drazin, P.G., *Solitons*, Cambridge University Press (1983).

Drazin, P.G. and Johnson, R.S., *Solitons: An Introduction*, Cambridge University Press (1989).

Drazin, P.G. and Reid, W.H., *Hydrodynamic Stability*, Cambridge University Press (1981).

Ebin, D.G. and Marsden, J., "Groups of diffeomorphisms and motion of an incompressible fluid," *Ann. Math.* **92**, 102-163 (1970).

Gibbon, J.D., James, I.N. and Moroz, I.M., "An example of soliton behaviour in a rotating baroclinic fluid," *Proc. R. Soc. Lond.* **A 367**, 219-237 (1979).

Griffiths, R.W., Killworth, P.D., and Stern, M.E., "Ageostrophic instability of ocean currents," *J. Fluid Mech.* **117**, 343-377 (1982).

Holm, D.D., Marsden, J.E., Ratiu, T. and Weinstein, A., "Nonlinear stability of fluids and plasma equilibria," *Phys. Rep.* **123**, 1-116 (1985).

Houghton, R.W., Schlitz, R., Beardsley, R.C., Butman, B. and Chamberlin, J.C., "The middle Atlantic bight pool: evolution of the temperature structure during 1979," *J. Phys. Oceanogr.* **12**, 1019-1029 (1982).

Kundu, P.K., *Fluid Mechanics*, Academic Press, Inc. (1990).

Lamb, G.L., *Elements of Soliton Theory*, John Wiley and Sons (1980).

Leblond, P.H., Ma, H., Doherty, F. and Pond, S., "Deep and intermediate water replacement in the Strait of Georgia," *Atmosphere-Ocean* **29**, 288-312 (1991).

Leblond, P.H. and Mysak, L.A., *Waves in the Ocean*, Elsevier (1978).

McIntyre, M.E. and Shepherd, T.G., "An exact local conservation theorem for finite amplitude disturbances to non-parallel shear flow, with remarks on Hamiltonian structure and on Arnol'd's stability theorems," *J. Fluid Mech.* **181**, 527-565 (1987).

Milne-Thomson, L.M., *Jacobian Elliptic Function Tables*, Dover (1950).

Mory, M., Stern, M.E. and Griffiths, R.W., "Coherent baroclinic eddies on a sloping bottom," *J. Fluid Mech.* **183**, 45-62 (1987).

Newell, A.C., *Solitons in Mathematics and Physics*, Society for Industrial and Applied Mathematics (1985).

Nof, D., "The translation of isolated cold eddies on a sloping bottom," *Deep Sea Res.* **30**, 171-182 (1983).

Olver, P.J., "A nonlinear Hamiltonian structure for the Euler equation," *J. appl. math. Analysis* **89**, 233-250 (1982).

Paldor, N. and Killworth, P.D., "Instabilities of a two-layer coupled front," *Deep Sea Res.* **34**, 1525-1539 (1987).

Pedlosky, J., "Finite-amplitude baroclinic waves," *J. Atmos. Sci.* **27**, 15-30 (1970).

Pedlosky, J., "Finite-amplitude baroclinic wave packets," *J. Atmos. Sci.* **29**, 680-686 (1972).

Pedlosky, J., "Finite-amplitude baroclinic waves at minimum shear," *J. Atmos. Sci.* **39**, 555-562 (1982a).

Pedlosky, J., "A simple model for nonlinear critical layers in an unstable baroclinic wave," *J. Atmos. Sci.* **39**, 2119-2127 (1982b).

Pedlosky, J., *Geophysical Fluid Dynamics*, 2nd Edition, Springer (1987).

Scinocca, J.F. and Shepherd, T.G., "Nonlinear wave-activity conservation laws and Hamiltonian structure for two-dimensional anelastic equations," *J. Atmos. Sci.* **49**, 5-27 (1992).

Shen, S.S., *A Course on Nonlinear Waves*, Kluwer Academic Publishers (1993).

Shepherd, T.G., "Symmetries, conservation laws and Hamiltonian structure in geophysical fluid dynamics," *Adv. Geophys.* **32**, 287-338 (1990).

Smith, P.C., "Baroclinic instability in the Denmark Strait overflow," *J. Phys. Oceanogr.* **6**, 355-371 (1976).

Swaters, G.E. and Flierl, G.R., "Dynamics of ventilated coherent cold eddies on a sloping bottom," *J. Fluid Mech.* **223**, 565-587 (1991).

Swaters, G.E., "On the baroclinic instability of cold-core coupled density fronts on a sloping continental shelf," *J. Fluid Mech.* **224**, 361-382 (1991).

Swaters, G.E., "Nonlinear stability of intermediate baroclinic flow on a sloping bottom," *Proc. R. Soc. Lond. A* **442**, 249-272 (1993).

Warn, T. and Gauthier, P. "Potential vorticity mixing by marginally unstable waves at minimum shear," *Tellus* **41A**, 115-131 (1989).

Whitehead, J.A. and Worthington, L.U., "The flux and mixing rates of Antarctic Bottom Water within the North Atlantic," *J. Geophys. Res.* **87**, 7903-7924 (1982).

Zoccolotti, L. and Salusti, E., "Observations on a very dense marine water in the Southern Adriatic Sea," *Continent. Shelf Res.* **7**, 535-551 (1987).

# Appendix

```
(*************************************************************)
(*                                                           *)
(*     PROGRAM 1                                             *)
(*                                                           *)
(*                                                           *)
(*     NAME: PLOTDNOIDAL.M                                   *)
(*                                                           *)
(*     PURPOSE:  THIS IS A MATHEMATICA PROGRAM TO PLOT       *)
(*               THE DNOIDAL SOLUTION TO THE TEMPORAL        *)
(*               AMPLITUDE EQUATION FOR MODES NOT AT         *)
(*               THE BOTTOM OF THE MARGINAL STABILITY        *)
(*               CURVE                                       *)
(*                                                           *)
(*                                                           *)
(*                                                           *)
(*     PROGRAMMED BY: C. J. MOONEY                           *)
(*                                                           *)
(*************************************************************)

ao=0.1
mu=2.0

sigma=Sqrt[(mu*k^2)/(k^2+l^2)]
rmaxsqd=ao^2+((sigma^2)/(mu^2*l^2*k^2))*
        (1+Sqrt[1+(2*mu^2*k^2*l^2*ao^2)/(sigma^2)])
rminsqd=ao^2+((sigma^2)/(mu^2*l^2*k^2))*
        (1-Sqrt[1+(2*mu^2*k^2*l^2*ao^2)/(sigma^2)])
kappa=1-rminsqd/rmaxsqd
tpfactor=Sqrt[2/(mu^2*l^2*k^2*rmaxsqd)]
taunot=InverseJacobiDN[ao/Sqrt[rmaxsqd],kappa]

dn=Sqrt[rmaxsqd]*JacobiDN[((1/tpfactor)*t-taunot),kappa]

Plot[dn,{t,0,100},AxesLabel->{"T","R"}]
```

```
CCCCCCCCCCCCCCCCCCCCCCCCCCCCCCCCCCCCCCCCCCCCCCCCCCCCCCCCCCCCCCCCCC
C                                                                     C
C     PROGRAM 2                                                       C
C                                                                     C
C                                                                     C
C     NAME: SECHTANHMF.F                                              C
C                                                                     C
C     PURPOSE:  THIS PROGRAM GENERATES DATA FOR THE                   C
C               SECHTANH CONTOUR PLOT (PERTURBATION                   C
C               THICKNESS IN THE CHANNEL) FOR                         C
C               SPYGLASS                                              C
C                                                                     C
C               2 CASES - FOR THICKNESS PERTURBATION                  C
C                         ONLY, USE h_0 ONLY;  FOR                    C
C                         LEADING ORDER VARIABLE THICK-               C
C                         NESS, USE -Y+h_0                            C
C                                                                     C
C     PROGRAMMED BY: C. J. MOONEY                                     C
C                                                                     C
CCCCCCCCCCCCCCCCCCCCCCCCCCCCCCCCCCCCCCCCCCCCCCCCCCCCCCCCCCCCCCCCCC
```

```
      REAL*8 X,Y,Z,EPSLN,AO,KAPPA,SIGMA,K,L,MU
      REAL*8 MU2,K2,L2,AO2,V
      INTEGER I,J
C
      X=-18.0                0
      Y=0.0
      AO=0.5
      AO2=AO*AO
      EPSLN=0.1
      K=0.5
      K2=K*K
      L=SQRT(1-K*K)
      L2=L*L
      MU=2.0
      MU2=MU*MU
C
C           NOW CALCULATE KAPPA FOR THE SECH ARGUMENT
C
      KAPPA=SQRT((AO2*MU2*L2*K2)/2)*((2*K2*MU-AO2*MU2*L2*K2)/
     &            (2*AO2*MU2*L2*K**4))
C
C            NOW CALCULATE V FOR THE COEFFICIENT
C
      V=(2*K2*MU-AO2*MU2*L2*K2*(1-2*K2))/(2*K2*MU-
     &             AO2*MU2*L2*K2)
      WRITE(7,50)KAPPA,V
50    FORMAT(F9.5,F9.5)
```

```
C
C              CALCULATE THE THICKNESS AT EACH POINT
C
         DO 200 I=1,248
          DO 300 J=1,248
            Z=-Y-(MU*L/2)*((1-2*K2-V)/(1-V))*AO2*
     &           ((1/COSH(KAPPA*EPSLN*X))**2)*2*SIN(2*L*Y) +
     &         2*((AO*KAPPA*(V-1+2*K2))/K)*(1/COSH(KAPPA*EPSLN*X))
     &              *TANH(KAPPA*EPSLN*X)
     &              *COS(K*X+3.141592/2.0)*SIN(L*Y)
            WRITE(8,100)X,Y,Z
100         FORMAT(F7.2,F7.2,F9.4)
            Y=Y+.0146274

300       CONTINUE
          Y=0.0
          X=X+0.15
200       CONTINUE
C
         END
```

```
CCCCCCCCCCCCCCCCCCCCCCCCCCCCCCCCCCCCCCCCCCCCCCCCCCCCCCCCCCCCCCCCCCCC
C                                                                     C
C     PROGRAM 3                                                       C
C                                                                     C
C                                                                     C
C     NAME:  RK4_4EQN.F                                               C
C                                                                     C
C     PURPOSE:  THIS PROGRAM USES THE NSWC                            C
C               4TH ORDER RUNGE-KUTTA SCHEME                          C
C               TO SOLVE THE 4 EQUATION SYSTEM                        C
C               FOR THE CHANNEL MODEL - TO                            C
C               PLOT B, USE PSI/K                                     C
C                                                                     C
C                                                                     C
C                                                                     C
C     PROGRAMMED BY: C. J. MOONEY                                     C
C                                                                     C
CCCCCCCCCCCCCCCCCCCCCCCCCCCCCCCCCCCCCCCCCCCCCCCCCCCCCCCCCCCCCCCCCCCC


      REAL*4 A(15),AMP(5000),PSI(5000),PHI(5000),F,Z(5)
      REAL*4 B13(5000),ALPHA4(5000),T,H
      REAL*4 K,L,MU,AO
      EXTERNAL F
      INTEGER I



      T = 0.0
      H = 0.1
      K = 0.5
      L = SQRT(1.0-K**2)
      MU = 2.0
      AO = 0.01


      A(1) = AO
      A(2) = AO*SQRT(MU*K*K)
      A(3) = -AO*AO
      A(4) = 0.0
      A(5) = 0.0
      CALL RK(5,T,0.0,A,F)

       DO 10 I = 1,2000
       CALL RK(5,T,H,A,F)
        AMP(I) = A(1)
        PSI(I) = A(2)
        PHI(I) = A(3)
        B13(I) = A(4)
        ALPHA4(I) = A(5)
```

```
      WRITE(7,100) T,PSI(I)/K
100   FORMAT(F6.2,F10.6)
10    CONTINUE


      STOP
      END


      SUBROUTINE F(T,Z)

      REAL*4 Z(5),AMP,PHI,PSI,B13,ALPHA4,T
      REAL*4 K,L,MU

      K = 0.5
      L = SQRT(1.0-K**2)
      MU = 2.0

      AMP = Z(1)
      PSI = Z(2)
      PHI = Z(3)
      B13 = Z(4)
      ALPHA4 = Z(5)

      Z(1) = PSI
      Z(2) = MU*K*K*AMP - MU*MU*K*K*L*L*AMP*(PHI + AMP**2)
      Z(3) = 2.0*K*AMP*B13
      Z(4) = -(MU*MU*L*L*K*AMP/4.0)*(4.0*(PHI + AMP**2)
     &            - 16.0*ALPHA4)
      Z(5) = -2.0*K*AMP*B13


      RETURN
      END
```

```
CCCCCCCCCCCCCCCCCCCCCCCCCCCCCCCCCCCCCCCCCCCCCCCCCCCCCCCCCCCCCCCCCCCC
C                                                                     C
C     PROGRAM 4                                                       C
C                                                                     C
C                                                                     C
C     NAME:  RK8_56EQN.F                                              C
C                                                                     C
C     PURPOSE:  THIS PROGRAM USES THE NSWC                            C
C               8TH ORDER RUNGE-KUTTA SCHEME                          C
C               TO SOLVE THE 56 EQUATION SYSTEM                       C
C               FOR THE CHANNEL MODEL - TO                            C
C               PLOT B, USE PSI/K                                     C
C                                                                     C
C                                                                     C
C                                                                     C
C     PROGRAMMED BY: C. J. MOONEY                                     C
C                                                                     C
CCCCCCCCCCCCCCCCCCCCCCCCCCCCCCCCCCCCCCCCCCCCCCCCCCCCCCCCCCCCCCCCCCCC


      REAL*4 Y(56),DY(56),WK(560),AMP,PSI,PHI,F,Z(56),T,H,K
      REAL*4 B13,ALPHA4,B22,B24,B15,B31,B33,B35,ALPHA6,MU,L
      REAL*4 B17,B19,B26,B28,B37,B39,B42,B44,B46,B48,B51
      REAL*4 B53,B55,B57,B59,B62,B64,B66,B68,B71,B73,B75,B77
      REAL*4 B79,ALPHA8,ALPHA10
      REAL*4 B82,B84,B86,B88,B810,B91,B93,B95,B97,B99
      REAL*4 B210,B410,B610
      REAL*4 P,Q,AO
      EXTERNAL F
      INTEGER I

      K = 0.5
      L = SQRT(1-K**2)
      MU = 2.0
      P = (MU*K*L*AMP)/2.0
      Q = (MU*MU*L*L*K*AMP)/4.0
      AO = 0.01

      T = 0.0
      H = 0.1


C     INITIAL CONDITIONS

      Y(1) = AO
      Y(2) = AO*SQRT(MU*K*K)
      Y(3) = -AO*AO
      Y(4) = 0.0
      Y(5) = 0.0
      Y(6) = 0.0
      Y(7) = 0.0
      Y(8) = 0.0
```

```
      Y(9) = 0.0
      Y(10) = 0.0
      Y(11) = 0.0
      Y(12) = 0.0
      Y(13) = 0.0
      Y(14) = 0.0
      Y(15) = 0.0
      Y(16) = 0.0
      Y(17) = 0.0
      Y(18) = 0.0
      Y(19) = 0.0
      Y(20) = 0.0
      Y(21) = 0.0
      Y(22) = 0.0
      Y(23) = 0.0
      Y(24) = 0.0
      Y(25) = 0.0
      Y(26) = 0.0
      Y(27) = 0.0
      Y(28) = 0.0
      Y(29) = 0.0
      Y(30) = 0.0
      Y(31) = 0.0
      Y(32) = 0.0
      Y(33) = 0.0
      Y(34) = 0.0
      Y(35) = 0.0
      Y(36) = 0.0
      Y(37) = 0.0
      Y(38) = 0.0
      Y(39) = 0.0
      Y(40) = 0.0
      Y(41) = 0.0
      Y(42) = 0.0
      Y(43) = 0.0
      Y(44) = 0.0
      Y(45) = 0.0
      Y(46) = 0.0
      Y(47) = 0.0
      Y(48) = 0.0
      Y(49) = 0.0
      Y(50) = 0.0
      Y(51) = 0.0
      Y(52) = 0.0
      Y(53) = 0.0
      Y(54) = 0.0
      Y(55) = 0.0
      Y(56) = 0.0

C     CARRY OUT THE INTEGRATIONS

      CALL RK8(56,T,0.0,Y,DY,WK,F)
```

```
DO 10 I = 1,4000
  CALL RK8(56,T,H,Y,DY,WK,F)
  AMP = Y(1)
  PSI = Y(2)
  PHI = Y(3)
  B13 = Y(4)
  ALPHA4 = Y(5)
  B22 = Y(6)
  B24 = Y(7)
  B15 = Y(8)
  B31 = Y(9)
  B33 = Y(10)
  B35 = Y(11)
  ALPHA6 = Y(12)
  B17 = Y(13)
  B19 = Y(14)
  B26 = Y(15)
  B28 = Y(16)
  B37 = Y(17)
  B39 = Y(18)
  B42 = Y(19)
  B44 = Y(20)
  B46 = Y(21)
  B48 = Y(22)
  B51 = Y(23)
  B53 = Y(24)
  B55 = Y(25)
  B57 = Y(26)
  B59 = Y(27)
  B62 = Y(28)
  B64 = Y(29)
  B66 = Y(30)
  B68 = Y(31)
  B71 = Y(32)
  B73 = Y(33)
  B75 = Y(34)
  B77 = Y(35)
  B79 = Y(36)
  ALPHA8 = Y(37)
  ALPHA10 = Y(38)
  B210 = Y(39)
  B410 = Y(40)
  B610 = Y(41)
  B810 = Y(42)
  B82 = Y(43)
  B84 = Y(44)
  B86 = Y(45)
  B88 = Y(46)
  B91 = Y(47)
  B93 = Y(48)
  B95 = Y(49)
  B97 = Y(50)
```

```
      B99 = Y(51)
      B102 = Y(52)
      B104 = Y(53)
      B106 = Y(54)
      B108 = Y(55)
      B1010 = Y(56)


            WRITE(7,100) T,AMP
  100       FORMAT(F10.2,F10.6)
  10        CONTINUE


      STOP
      END


C     SUBROUTINE TO DEFINE THE EQUATIONS

      SUBROUTINE F(T,Z)

      REAL*4 Z(56),AMP,PHI,PSI,B13,ALPHA4,B22,B24
      REAL*4 B15,B31,B33,B35,ALPHA6,T
      REAL*4 B17,B19,B26,B28,B37,B39,B42,B44,B46
      REAL*4 B48,B51,B53,B55,B57,B59,B62,B64,B66
      REAL*4 B68,B71,B73,B75,B77,B79,ALPHA8
      REAL*4 ALPHA10,B82,B84,B86,B88,B91,B93
      REAL*4 B95,B97,B99,B210,B410,B610,B810
      REAL*4 B1010,B102,B104,B106,B108
      REAL*4 K,L,MU,P,Q

      K=0.5
      L=SQRT(1.0-K**2)
      MU=2.0
      P = (MU*K*L*AMP)/2.0
      Q = (MU*MU*L*L*K*AMP)/4.0

      AMP = Z(1)
      PSI = Z(2)
      PHI = Z(3)
      B13 = Z(4)
      ALPHA4 = Z(5)
      B22 = Z(6)
      B24 = Z(7)
      B15 = Z(8)
      B31 = Z(9)
      B33 = Z(10)
      B35 = Z(11)
      ALPHA6 = Z(12)
      B17 = Z(13)
      B19 = Z(14)
      B26 = Z(15)
      B28 = Z(16)
```

```
      B37 = Z(17)
      B39 = Z(18)
      B42 = Z(19)
      B44 = Z(20)
      B46 = Z(21)
      B48 = Z(22)
      B51 = Z(23)
      B53 = Z(24)
      B55 = Z(25)
      B57 = Z(26)
      B59 = Z(27)
      B62 = Z(28)
      B64 = Z(29)
      B66 = Z(30)
      B68 = Z(31)
      B71 = Z(32)
      B73 = Z(33)
      B75 = Z(34)
      B77 = Z(35)
      B79 = Z(36)
      ALPHA8 = Z(37)
      ALPHA10 = Z(38)
      B210 = Z(39)
      B410 = Z(40)
      B610 = Z(41)
      B810 = Z(42)
      B82 = Z(43)
      B84 = Z(44)
      B86 = Z(45)
      B88 = Z(46)
      B91 = Z(47)
      B93 = Z(48)
      B95 = Z(49)
      B97 = Z(50)
      B99 = Z(51)
      B102 = Z(52)
      B104 = Z(53)
      B106 = Z(54)
      B108 = Z(55)
      B1010 = Z(56)

      Z(1) = PSI
      Z(2) = MU*K*K*AMP - MU*MU*K*K*L*L*AMP*(PHI + AMP**2)
      Z(3) = 2*K*AMP*B13
      Z(4) = -Q*(4*(PHI+AMP**2)-16*ALPHA4)+
     &           P*(4*B22-2*B24)
      Z(5) = 2*K*AMP*(B15-B13)
      Z(6) = -P*(4*B31 + 4*B13)
      Z(7) = -P*(6*B33 - 2*B35 - 2*B13 + 6*B15)
      Z(8) = -Q*(16*ALPHA4 - 36*ALPHA6) +
     &            P*(6*B24-4*B26)
      Z(9) = P*(4*B22+2*B42)
      Z(10) = P*(6*B24+6*B42)
```

```
Z(11) = P*(8*B44-2*B46-2*B24+8*B26)
Z(12) = 2*K*AMP*(B17-B15)
Z(13) = -Q*(36*ALPHA6-64*ALPHA8)+P*(8*B26-6*B28)
Z(14) = -Q*(64*ALPHA8-100*ALPHA10)+P*(10*B28-8*B210)
Z(15) = -P*(8*B35-4*B37-4*B15+8*B17)
Z(16) = -P*(10*B37-6*B39-6*B17+10*B19)
Z(17) = P*(10*B46-4*B48-4*B26+10*B28)
Z(18) = P*(12*B48-6*B410-6*B28+12*B210)
Z(19) = -P*(6*B51+2*B53+2*B31+6*B33)
Z(20) = -P*(8*B53+8*B35)
Z(21) = -P*(10*B55-2*B57-2*B35+10*B37)
Z(22) = -P*(12*B57-4*B59-4*B37+12*B39)
Z(23) = P*(4*B62+6*B42)
Z(24) = P*(8*B62+4*B64+4*B42+8*B44)
Z(25) = P*(10*B64+10*B46)
Z(26) = P*(12*B66-2*B68-2*B46+12*B48)
Z(27) = P*(14*B68-4*B610-4*B48+14*B410)
Z(28) = -P*(8*B71+4*B73+4*B51+8*B53)
Z(29) = -P*(10*B73+2*B75+2*B53+10*B55)
Z(30) = -P*(12*B75+12*B57)
Z(31) = -P*(14*B77-2*B79-2*B57+14*B59)
Z(32) = P*(6*B82+8*B62)
Z(33) = P*(10*B82+4*B84+4*B62+10*B64)
Z(34) = P*(12*B84+2*B86+2*B64+12*B66)
Z(35) = P*(14*B86+14*B68)
Z(36) = P*(16*B88-2*B810-2*B68+16*B610)
Z(37) = 2*K*AMP*(B19-B17)
Z(38) = 2*K*AMP*(-B19)
Z(39) = -P*(12*B39-8*B19)
Z(40) = -P*(14*B59-6*B39)
Z(41) = -P*(16*B79-4*B59)
Z(42) = -P*(18*B99-2*B79)
Z(43) = -P*(10*B91+6*B93+6*B71+10*B73)
Z(44) = -P*(12*B93+4*B95+4*B73+12*B75)
Z(45) = -P*(14*B95+2*B97+2*B75+14*B77)
Z(46) = -P*(16*B97+16*B79)
Z(47) = P*(8*B102+10*B82)
Z(48) = P*(12*B102+6*B104+6*B82+12*B84)
Z(49) = P*(14*B104+4*B106+4*B84+14*B86)
Z(50) = P*(16*B106+2*B108+2*B86+16*B88)
Z(51) = P*(18*B108+18*B810)
Z(52) = -P*(8*B91+12*B93)
Z(53) = -P*(6*B93+14*B95)
Z(54) = -P*(4*B95+16*B97)
Z(55) = -P*(2*B97+18*B99)
Z(56) = 0.0


RETURN
END
```

```
(*************************************************************)
(*                                                           *)
(*     PROGRAM 5                                             *)
(*                                                           *)
(*                                                           *)
(*     NAME: ARCTAN1.M                                       *)
(*                                                           *)
(*     PURPOSE:  THIS IS A MATHEMATICA PROGRAM TO PLOT       *)
(*               THE 2-SOLITON SOLUTION TO THE SINE-         *)
(*               GORDON EQUATION                             *)
(*                                                           *)
(*                                                           *)
(*     PROGRAMMED BY: C. J. MOONEY                           *)
(*                                                           *)
(*************************************************************)



k=0.5
l=Sqrt[1-k^2]
mu=2.0
sigma2=mu*k^2
c1=1.0-2*k^2
c2=1.0
a1=2.0
a2=0.4
n=mu^2*k^2*l^2
kappa1=(sigma2-a1^2*n)/(a1*n^0.5*(c1-c2))
kappa2=(sigma2-a2^2*n)/(a2*n^0.5*(c1-c2))
v1=c1+(c1-c2)/((n*a1/sigma2)-1)
v2=c1+(c1-c2)/((n*a2/sigma2)-1)
gamma=(a1-a2)/(a1+a2)

phi=4*ArcTan[((a1-a2)*Sinh[(1/2)*(kappa1*(x-v1*t)+kappa2*
    (x-v2*t))])/((a1+a2)*Cosh[(1/2)*(kappa1*(x-v1*t)-kappa2*
    (x-v2*t))])]


dphi=2*gamma*((-(a1-a2)*Tanh[(1/2)*(kappa1*(x-v1*t)-kappa2*
    (x-v2*t))]*Sech[(1/2)*(kappa1*(x-v1*t)-kappa2*(x-v2*t))]*
    Sinh[(1/2)*(kappa1*(x-v1*t)+kappa2*(x-v2*t))]
    +(a1+a2)*Sech[(1/2)*(kappa1*(x-v1*t)-kappa2*(x-v2*t))]*
    Cosh[(1/2)*(kappa1*(x-v1*t)+kappa2*(x-v2*t))])/
    (1+gamma^2*Sech[(1/2)*(kappa1*(x-v1*t)-kappa2*(x-v2*t))]^2
    *Sinh[(1/2)*(kappa1*(x-v1*t)+kappa2*(x-v2*t))]^2))

Plot3D[phi,{x,-20,20},{t,-10,10},PlotPoints->50,PlotRange->
      {-7.0,7.0},AxesLabel->{"X","T","Amplitude"}]

(* Plot3D[dphi,{x,-10,10},{t,-5,5},PlotPoints->120,          *)
(*   PlotRange->{-0.5,4.5},AxesLabel->{"X","T","Amplitude"}] *)

(*  Plot[phi,{x,-10,10}]                                     *)
```

```
(*************************************************************)
(*                                                           *)
(*     PROGRAM 6                                             *)
(*                                                           *)
(*                                                           *)
(*     NAME: BREATHER1.M                                     *)
(*                                                           *)
(*     PURPOSE:  THIS IS A MATHEMATICA PROGRAM TO PLOT       *)
(*               THE MOVING BREATHER SOLUTION TO THE         *)
(*               SINE-GORDON EQUATION                        *)
(*                                                           *)
(*               PHI - (X,T) COORDINATES                     *)
(*               PHIXITAU - (XI,TAU) COORDINATES             *)
(*               PHIPQ - (P,Q) COORDINATES  (STAT-           *)
(*                           IONARY SOLUTION)                *)
(*                                                           *)
(*                                                           *)
(*     PROGRAMMED BY: C. J. MOONEY                           *)
(*                                                           *)
(*************************************************************)


k=0.5
l=Sqrt[1-k^2]
mu=2.0
sigma2=mu*k^2
c1=1.0-2*k^2
c2=1.0
a1=2.0
n=mu^2*k^2*l^2
kappa1=(sigma2-a1^2*n)/(a1*n^0.5*(c1-c2))
v1=c1+(c1-c2)/((n*a1/sigma2)-1)
kappa1star=-(sigma2+a1^2*n)/(a1*n^0.5*(c1-c2))
v1star=c1-(c1-c2)/((a1^2*n/sigma2)+1)
m=0.5

phi=-4*ArcTan[((m/Sqrt[1-m^2])*Sin[Sqrt[1-m^2]*
        kappa1star*(x-v1star*t)])/(Cosh[m*kappa1*(x-v1*t)])]

phixitau=-4*ArcTan[((m/Sqrt[1-m^2])*Sin[Sqrt[1-m^2]*(a1*xi-
        tau/a1)])/(Cosh[m*(a1*xi+tau/a1)])]

phipq=-4*ArcTan[((m/Sqrt[1-m^2])*Sin[Sqrt[1-m^2]*q])/
     (Cosh[m*p])]

Plot3D[phi,{x,-10,10},{t,-10,10},PlotPoints->100,PlotRange->
      {-2.0,2.0},AxesLabel->{"X","T","Amplitude"}]

(* Plot3D[phixitau,{xi,-10,10},{tau,-10,10},PlotPoints->50,   *)
(*               PlotRange->{-6.2,6.2}]                       *)

(* Plot3D[phipq,{p,-20,20},{q,-20,20},PlotPoints->50,         *)
(*               PlotRange->{-6.2,6.2}]                       *)
```